Living Radical Polymerization in Aqueous Dispersed Systems with Water-Soluble Catalysts

by

Elijah Baruch Bultz

A thesis submitted to the Department of Chemical Engineering

In conformity with the requirements for

the degree of Doctor of Philosophy

Queen's University

Kingston, Ontario, Canada

September, 2015

Abstract

Living radical polymerization is an important technique for synthesizing advanced macromolecules including block copolymers. Since its discovery in the early 1990s the capability of the field has expanded with new types of chemistry and techniques. One of the most widely used chemistries is atom transfer radical polymerization (ATRP) also known as "metal mediated living radical polymerization" (Mt-LRP). Mt-LRP has also expanded its use to aqueous dispersed systems including emulsion, miniemulsion and microemulsion, with the biggest advancements seen in miniemulsion where the droplets act as nanosized reactors. Extremely hydrophobic catalyst complexes are typically used in miniemulsion. While effective in controlling the polymerization, these hydrophobic catalyst complexes also get trapped in the final polymer particles and are difficult to remove. Herein I report the progress made using thermoresponsive polymer bound catalysts for Mt-LRP reactions in miniemulsion, which allow the successful LRP in miniemulsion with facile catalyst removal. Polymers could be prepared with less than 10 ppm of ruthenium in the final polymer compared to >500 ppm in the reaction mixture. The polymerizations were improved by the addition of ferrocene (FeCp2) in miniemulsion, to give almost complete conversion in significantly shorter times. The addition of ferrocene adds a second catalytic cycle that is ionic in nature and requires excess halogens present for a successful polymerization to occur. The ionic species in this catalytic cycle meant that the use of cationic surfactants with halogen counter-ions could directly affect the polymerization chemistry, which was shown by increasing rates with the addition of a bromine counter-ion versus a chlorine counter ion in the cationic surfactant used. Water-soluble $FeCp_2$ derivative cocatalysts were also used to improve the rates and conversions of Mt-LRP of ruthenium catalyzed polymerizations while also allowing colourless polymers to be synthesized. Finally, the ligand EHA_6TREN, was found to be active in bulk or solution (anisole) when complexed to iron (III) bromide with reverse ATRP, or to iron (II) bromide with AGET ATRP, yielding an iron-mediated living radical polymerization.

Co-Authorship

Chapter 3 has been accepted and published as *ACS Macro Lett*, **2015**, 4 (6), 628–631 (DOI: 10.1021/acsmacrolett.5b00286), co-authored by Michael F. Cunningham, Mitsuo Sawamoto, Keita Nishizawa and Makoto Ouchi. I performed the laboratory experiments and analysis and writing. Keita Nishizawa taught the laboratory techniques for air free techniques. Guidance was provided by Prof. Ouchi, Prof. Sawamoto and Prof. Cunningham.

Chapter 4 is being prepared for submission and will be co-authored by Michael F. Cunningham, Kojiro Fujimura, Mitsuo Sawamoto and Makoto Ouchi. I performed the laboratory experiments. Guidance was provided by Prof. Ouchi, Prof. Sawamoto and Prof. Cunningham and Kojiro Fujimura.

Chapter 5 is being for submission and will be co-authored by Michael F. Cunningham, Mitsuo Sawamoto and Makoto Ouchi. I performed the laboratory experiments. Guidance was provided by Prof. Ouchi, Prof. Sawamoto and Prof. Cunningham.

Chapter 6 is being for submission and will be co-authored by Michael F. Cunningham. I performed the laboratory experiments and analysis and writing. Guidance was provided by Prof. Cunningham.

Acknowledgements

I would like to thank Prof. Michael Cunningham for his support over the past 4 years and allowing me the opportunity to be set free abroad for significant portions of my PhD research. His support has provided opportunities in research and life I did not imagine when beginning this project. I would also like to thank everyone in the Chemical Engineering Department at Queen's and in the Cunningham lab for the good conversation, banter and discussions.

皆さん、京都大学の澤本研でありがとうございました。

To everyone in Kyoto University at the Sawamoto lab I too would like to thank you for your warm hospitality over the past 2 years and your help in teaching me Japanese. Prof. Takaya Terashima and Prof. Makoto Ouchi, thank you for your support and discussions on research over the past 2 years in your lab. I could not have done this research without your help. Prof. Mitsuo Sawamoto, thank you for accepting me into your lab and providing endless questions during seminars and even more opportunities in the world of chemistry.

Last but not least, to my parents, family and friends, thank you for your endless moral support from around the world. It has always made me feel more at home when so far away!

"Pain is just knowledge rushing in to fill a gap. When you stub your toe on the edge of a bed that was a gap in knowledge. And the pain is just a lot of information, very quick!" - Jerry Seinfeld

Statement of Originality

I hereby certify that all of the work described within this thesis is the original work of the author. Any published or unpublished ideas and/or techniques from the work of others are fully acknowledged in accordance with the standard referencing practices.

Elijah Bultz

September 2015

Table of Contents

Abstract ii
Co-Authorship iii
Acknowledgements iv
Statement of Originality v
List of Figures ix
List of Tables xii
List of Abbreviations xiii
Chapter 1 Introduction 1
Chapter 2 Literature Review 5
Aqueous Dispersed Polymerization 5
2.1 5
2.1.1 Emulsion Polymerization 5
2.1.2 Miniemulsion Polymerization 6
2.1.3 Living Radical Polymerization in Aqueous Dispersions (Reversible-Deactivation Radical Polymerization) 8
2.2 Transition Metal Mediated Polymerization (TMMP)/ Atom Transfer Radical Polymerization (ATRP) 9
2.2.1.1 Catalyst and Ligands 10
2.2.2 ATRP in dispersed systems 12
2.2.2.1 ATRP in miniemulsion 12
2.2.2.2 ATRP in Microemulsion and Seeded Emulsion 15
2.3 Thermoresponsive phase regulated catalysis 17
2.3.1 Thermoresponsive polymers 17
2.3.2 Thermoresponsive phase regulated catalysis 19
Chapter 3 24
3.1 Preface 24
3.2 Abstract 24
3.3 Introduction 25
3.4 Experimental 27
3.4.1 Materials 27
3.4.2 Characterization 28
3.4.3 PEG-5000 Phosphine synthesis 28

3.4.4 Catalyst synthesis 29
3.4.5 Miniemulsion polymerization 29
3.4.6 Toluene free miniemulsion polymerization 29
3.4.7 Catalyst removal 30
3.4.8 Reproducibility 30
3.5 Results and Discussion 30
3.6 Conclusions 35
3.7 References 35
Chapter 4 38
4.1 Preface 38
4.2 Abstract 38
4.3 Introduction 39
4.4 Experimental 42
4.4.1 Materials 42
4.4.2 PPEG Synthesis 43
4.4.3 Miniemulsion polymerization 43
4.4.4 Characterization 44
4.5 Results and Discussion 44
Addition of FeCp2 44
4.5.1 44
4.5.2 Surfactant and counter-ion effect 47
4.5.3 Surfactant Counter-ion Effects on Polymerization 49
4.6 Conclusions 55
4.7 References 56
Chapter 5 58
5.1 Preface 58
5.2 Abstract 58
5.3 Introduction 59
5.4 Experimental 62
5.4.1 Materials 62
5.4.2 Synthesis of PPEG45 and PPEG113 63
5.4.3 Synthesis of FcPEG2000 (3) 64
5.4.4 Synthesis of FcPEG5000 (4) 64
5.4.5 Miniemulsion polymerization 64

5.4.6 Characterization 65
5.5 Results and Discussion 65
5.5.1 Amine Cocatalysts 66
5.5.2 FcPEG co-catalysts 68
5.5.3 Ferrocene Surfactant 72
5.6 Conclusions 75
5.7 References 76
Chapter 6 78
6.1 Preface 78
6.2 Abstract 78
6.3 Introduction 79
Experimental 82
6.4 82
6.4.1 Materials 82
6.4.2 General polymerization procedures 82
6.4.2.1 Bulk polymerization of BMA 82
6.4.3 Characterization 83
Results and Discussion 83
6.5 83
6.5.1 Reverse ATRP 83
6.5.1.1 Bulk Polymerization 83
6.5.1.2 Solution Polymerizations 85
AGET ATRP 87
6.5.2 87
6.6 Conclusions 90
6.7 References 91
Chapter 7 93
Chapter 8 95
Appendix A 99
Appendix B 103

List of Figures

Figure 1. The proposed equilibrium reaction in ATRP/TMMP. The metal catalyst abstracts a halogen atom from the dormant alkyl bromide to produce a propagating radical species. 10
Figure 2. Example of ruthenium, iron and copper catalysts used in ATRP processes. 11
Figure 3. Hydrophobic ligands for ATRP in miniemulsion. 13
Figure 4. The temperature vs volume fraction of polymer showing the UCST and the LCST for a given polymer.[29] 18
Figure 5. The reaction process for a thermoresponsive phase regulated catalysis reaction. Here the catalyst, C, can easily transfer from the aqueous layer to the organic layer once the cloud point is reached, catalyzing the reaction in the organic phase. After the reaction is completed, the temperature is dropped and the catalyst transfers back to the organic phase allowing for easy separation and ideally recycling. [48] 20
Figure 6. (A) Pictures for phase transfer of the thermoresponsive catalyst on heating (from r.t. to 95˚C) and cooling (from 95˚C to r.t.). (B) Normal ^{1}H NMR and the NOE spectrum at 25˚C (1, 2) and 80˚C (3, 4), respectively. The PEG peak was chosen for irradiation at both temperatures with a strong NOE observed at 80°C between the BMA proton and the PEG proton while no NOE was observed after cooling to 25°C. 32
Figure 7. Conversion versus time plots of miniemulsion polymerizations of BMA with RuCp*Cl(PPEG) or RuCp*Cl$(PPh_3)_2$ at 80°C: $[BMA]_0$:$[ECPA]_0$:$[Ru\ Catalyst]_0$ = 100/1/0.05 with [CTAB]/[hexadecane] = 4.3/5.2 wt% vs BMA; [CTAB]/[hexadecane] = 4.3/5.2 wt% vs BMA. RuCp*Cl(PPEG) was prepared through aging of $[Ru(Cp^*)Cl]_4$ with PEG-ligand ($[[Ru(Cp^*)Cl]_4]$:[PEG-ligand] = 1:2) before polymerization, followed by use as it was. For the miniemulsion polymerizations in the presence of toluene, the solution was prepared for the volume ratio of organic/water to be 1/5 v/v%. Curves on the conversion plot are used to guide the eye. (B) The GPC traces for the "toluene free" miniemulsion polymerization with RuCp*Cl(PPEG): just dried latex (as they are: top) and after washing in MeOH (bottom). 33
Figure 8. Conversion data on the left for the miniemulsion polymerizations of BMA catalyzed by RuCp*Cl$(PPEG_{113})$ with or without $FeCp_2$: $[BMA]_0$:$[ECPA]_0$:$[Ru\ Catalyst]_0$ /$[FeCp_2]_0$ = 100/1/0.05/0.5 or 0 with [CTAB]/[hexadecane] = 4.3/5.2 wt% vs BMA at 80 °C or 60 °C. Lines are shown to guide the eye. On the right are the GPC traces for the polymerization containing $FeCp_2$ polymerized at 80 °C. 46
Figure 9. Conversion data for the miniemulsion polymerizations of BzMA catalyzed by RuCp*Cl$(PPEG_{45})$ with $FeCp_2$ stabilized by Brij 98 with or without the addition of NaCl in the water

phase: $[BzMA]_0$:$[Dimer\text{-}Br]_0$:[Ru Catalyst]$_0$ /$[FeCp_2]_0$/[NaCl] = 100/1/0.05/0.5/1.6 or 0 with [surfactant]/[hexadecane] = 8.6/5.2 wt% vs BMA at 80 °C. Lines are shown to guide the eye. On the right are the GPC traces for the same polymerizations. 49
Figure 10. The molecular structures of the surfactants and initiators used in these polymerizations 50
Figure 11. Conversion data for the miniemulsion polymerizations of BzMA catalyzed by RuCp*Cl($PPEG_{45}$) with $FeCp_2$ stabilized by either CTAB or CTAC: $[BzMA]_0$:$[ECPA]_0$:[Ru Catalyst]$_0$ /$[FeCp_2]_0$/[surfactant] = 100/1/0.05/0.5/1.6 or 0 with [surfactant]/[hexadecane] = 4.3/5.2 wt% vs BMA at 80 °C. Lines are shown to guide the eye. On the right is the GPC data for the same polymerizations. 52
Figure 12. Molecular weight distributions for the miniemulsion polymerizations of BzMA catalyzed by RuCp*Cl($PPEG_{45}$) with $FeCp_2$ stabilized by either CTAB or CTAC: $[BzMA]_0$:$[ECPA]_0$:[Ru Catalyst]$_0$ /$[FeCp_2]_0$/[surfactant] = 100/1/0.05/0.5/1.6 or 0 with [surfactant]/[hexadecane] = 4.3/5.2 wt% vs BMA at 80 °C. 52
Figure 13. Conversion data for the miniemulsion polymerizations of BzMA catalyzed by RuCp*Cl($PPEG_{45}$) with $FeCp_2$ stabilized by either CTAB or CTAC: $[BzMA]_0$:$[Dimer\text{-}Br]_0$:[Ru Catalyst]$_0$ /$[FeCp_2]_0$/[surfactant] = 100/1/0.05/0.5/1.6 or 0 with [surfactant]/[hexadecane] = 4.3/5.2 wt% vs BMA at 80 °C. Lines are shown to guide the eye. On the right is the GPC data for the same polymerizations. 53
Figure 14. Molecular weight distributions for the miniemulsion polymerizations of BzMA catalyzed by RuCp*Cl($PPEG_{45}$) with $FeCp_2$ stabilized by either CTAB or CTAC: $[BzMA]_0$:$[Dimer\text{-}Br]_0$:[Ru Catalyst]$_0$ /$[FeCp_2]_0$/[surfactant] = 100/1/0.05/0.5/1.6 or 0 with [surfactant]/[hexadecane] = 4.3/5.2 wt% vs BMA at 80 °C. 53
Figure 15. MALDI-TOF of polymer samples synthesized by miniemulsion stabilized by chloride surfactant CTAC initiated by brominated alkyl halide initiator MMA_2-Br (top) and chlorine alkyl halide initiator ECPA (bottom) showing fully chlorinated end groups at the low end of the molecular weight distribution. 55
Figure 16. Conversion data for the miniemulsion polymerizations of BMA catalyzed by RuCp*Cl($PPEG_{113}$) with amine cocatalyst 1 or 2 stabilized by either CTAB: $[BMA]_0$:$[ECPA]_0$:[Ru Catalyst]$_0$ /[amine]$_0$/[surfactant] = 100/1/0.05/0. 5/1.6 with [surfactant]/[hexadecane] = 4.3/5.2 wt% vs BMA at 80 °C. On the right is the GPC data for the same polymerizations. 68
Figure 17. GPC traces for the BMA polymerizations in Figure 16 cocatalyzed with amine coactalyst 1 or 2. 68
Figure 18. Conversion data for the miniemulsion polymerizations of BMA catalyzed by RuCp*Cl($PPEG_{113}$) with FcPEG cocatalyst 3 or 4 stabilized by CTAB: $[BMA]_0$:$[ECPA]_0$:[Ru Catalyst]$_0$ /$[FcPEG]_0$/[surfactant] = 100/1/0.05/0. 05/1.6 with [surfactant]/[hexadecane] = 4.3/5.2 wt% vs BMA at 80 °C. Lines are shown to guide the eye. On the right is the GPC data for the same polymerizations. 70

Figure 19 GPC traces for the BMA polymerizations in Figure 18 cocatalyzed with FcPEG cocatalyst 3 or 4. 71
Figure 20 Conversion data for the miniemulsion polymerizations of BzMA catalyzed by RuCp*Cl($PPEG_{45}$) with FcPEG cocatalyst 3 or 4 stabilized by CTAB: $[BzMA]_0$:$[ECPA]_0$:$[Ru\ Catalyst]_0$ /$[FcPEG]_0$/[surfactant] = 100/1/0.05/0. 05/1.6 with [surfactant]/[hexadecane] = 4.3/5.2 wt% vs BMA at 80 °C. Lines are shown to guide the eye. On the right is the GPC data for the same polymerizations. 72
Figure 21 GPC traces for the BzMA polymerizations in Figure 20 cocatalyzed either amine coactalyst 3 or 4. 72
Figure 22. Conversion data for the miniemulsion polymerizations of various monomers catalyzed by RuCp*Cl($PPEG_{45}$) with FcTMA surfactant cocatalyst, 5, stabilized by CTAB: $[monomer]_0$:$[ECPA]_0$:$[Ru\ Catalyst]_0$ /$[FcPEG]_0$/[surfactant] = 100/1/0.05/0. 05/1.6 with [surfactant]/[hexadecane] = 4.3/5.2 wt% vs BMA at 80 °C. On the right is the GPC data for the same polymerizations. 75
Figure 23. The normalized conversion and M_n vs Conversion plot for the reverse ATRP polymerization of BMA in bulk mediated by EHA_6TREN. 84
Figure 24. Normalized GPC traces for polymerization 1 of bulk BMA. 85
Figure 25. GPC traces from polymerization entry 2 and 3 in A and B respectively. The final molecular weight data is shown in Table 1. 86
Figure 26. AGET ATRP initiated by EBib with Fe(III) reduced by either tin(II) ethylhexanoate, iron powder or ascorbic acid. 90
Figure 27. GPC traces for the ab initio emulsion polymerization with RuCp*$PPEG_{45}$ initiated by ECPA with FcTMA surfactant cocatalyst, 5, stabilized by CTAB: $[monomer]_0$:$[ECPA]_0$:$[Ru\ Catalyst]_0$ /$[FcPEG]_0$/[surfactant] = 100/1/0.05/0. 05/1.6 with [surfactant] 4.3 wt% vs BzMA at 80 °C. Polymerizations were run at solids content of 15 wt%. 97

List of Tables

Table 1. Results for the reverse ATRP polymerization of BMA run at 50% wt anisole 85

List of Abbreviations

AA	Ascorbic acid
AIBN	Azobisisobutyronitrile
ATRP	Atom transfer radical polymerization
AGET	Activators generated by electron transfer
ARGET	Activators regenerated by electron transfer
BMA	Butyl methacrylate
BzMA	Benzyl methacrylate
CTAB	Cetyl trimethylammonium bromide
CTAC	Cetyl trimethylammonium chloride
Cp*	pentamethylcyclopentadienyl
Đ	Dispersity (M_w/M_n)
DLS	Dynamic light scattering
DMAE	Dimethylamino ethanol
EBiB	Ethyl α-bromoisobutyrate
ECPA	Ethyl α-chlorophenylacetate
EHA_6TREN	Tris(2-bis(3-(2-ethylhexoxy)-3-oxopropyl)aminoethyl)amine
EHMA	2-ethylhexylmethacrylate
$FeCp_2$	Ferrocene
FcPEG	poly(ethylene glycol)-ferrocenecarboxylate
FcTMA	11-Ferrocenyltrimethylundecylammonium bromide
HD	Hexadecane
ICP-AES	Inductively coupled plasma atomic emission spectroscopy
LCST	Lower critical solution temperature
LRP	Living radical polymerization
MALDI-TOF	Matrix-aided laser desorption/ionization time-of-flight mass spectroscopy
MMA	Methyl methacrylate
MMA_2-Br	Dimethyl 2-bromo-2,4,4-trimethylgiutarate
M_n	Number averaged molecular weight
M_w	Weight averaged molecular weight
Mt-LRP	Metal mediated living radical polymerization
NOE	Nuclear overhauser effect (NMR)
NMR	Nuclear magnetic resonance
PEG	Poly(ethylene glycol)
PPEG	Poly(ethylene glycol) di-(4-hydroxyphenyl)diphenylphosphin
TBA	Tributylamine
TPMA	Tris(2-pirydylmethyl)amine
VOC	Volatile organic compound

Chapter 1

Introduction

Living radical polymerization and specifically atom transfer radical polymerization (ATRP) is an important synthetic tool allowing one to produce polymers with precise molecular weights, narrow molecular weight distributions, and ideally high chain end fidelity allowing for the synthesis of more complex architectures such as block, gradient, graft and star polymers. These polymers allow a chemist or engineer to produce materials that have significantly different properties than they can make with free radical polymerizations. Examples are polymeric compatibilizers for polymer blends, new thermoplastic elastomers and more complex vehicles for carrying catalysts.

Performing these polymerizations in aqueous settings such as emulsion or miniemulsion is also important step towards industrializing this technology as one can eliminate VOCs as solvents from the reaction mixture as well as produce nanosized particles, which may be useful in coatings or other specialized functions.

ATRP has been performed in miniemulsion but requires extremely hydrophobic ligands to keep the catalyst in the droplets and particles so they can effectively catalyze the polymerizations without significant partitioning into the aqueous phase. One major drawback of this system is the catalysts are effectively trapped in the polymer particles at the end of the reaction and to obtain clear and colourless final products requires significant processing to strip the particle of its residual metal.

The purpose of this thesis is to examine ATRP polymerizations in aqueous dispersed systems where the final products could be easily freed of the residual heavy metals that are used in the polymerization. This was done using a water-soluble/ thermoresponsive ruthenium catalyst that at low temperatures is water-soluble and at high temperatures becomes oil-soluble allowing it to diffuse into the monomer droplets to catalyze the living radical polymerization. At the end of the polymerization, the reaction mixture could be cooled, causing the catalyst to become water-soluble again allowing for its easy removal from the hydrophobic polymer particles. The presented findings are novel and important, as traditionally aqueous dispersed ATRP has required the catalyst to reside in the oil-phase while in this work it starts in aqueous phase. This is the first reported instance of thermoresponsive catalysts being used in an aqueous dispersed phase polymerization, where post polymerization the catalyst can easily be removed.

Chapter 2 of this thesis provides a short review of aqueous dispersed phase polymerizations (including emulsion and miniemulsion), metal mediated living radical polymerization in homogenous and heterogeneous systems, and the use of thermoresponsive phase transfer catalysis as a method of efficient catalyst transfer to the reaction medium and easy catalyst removal.

In Chapter 3, the first report using thermoresponsive catalyst for miniemulsion living radical polymerization in miniemulsion is presented. Here, triphenylphosphine derivatives containing a PEG chain were synthesized to form shuttling catalysts in conjunction with a ruthenium half-metallocene precursor. The shuttling behavior could be seen visually on the macro scale by photographs and the nanoscale by 1D NOE NMR. This shuttling catalyst successfully polymerized a BMA living radical polymerization in miniemulsion shown by increasing M_n with conversion and a shift of the entire molecular weight distribution to higher molecular weights. Post-polymerization the catalyst could be easily removed by washing with methanol.

In Chapter 4, I used a ferrocene cocatalyst in miniemulsion that showed significant rate enhancement compared to using the Ru catalyst alone, allowing nearly quantitative conversions to be reached. Ferrocene has been previously shown to add a second catalytic cycle to the standard LRP equilibrium where ferrocene acts to reduce the ruthenium catalyst and form an ionic species, which rapidly degrades and deactivates an active, growing radical. In miniemulsion we found that the addition of this co-cocatalyst would only work in the presence of excess aqueous halogen ions, otherwise a living radical polymerization would not occur. Because of these results we varied the initiator (alkyl halide and alkyl bromine) and the cationic surfactants (bromide or chloride counter ions), observing changes in the polymerization rate. The presence of chloride counter ion slowed the polymerization with respect to the bromide containing surfactant. Furthermore completely chlorine end capped polymers were seen by MALDI-TOF mass spectroscopy.

In Chapter 5 the use of cocatalysts with thermoresponsive ruthenium catalysts was investigated for the purposes of increasing the rate and the conversions seen in Chapter 4 but allowing for facile clear and colourless final products to be produced. This was done using either amine cocatalysts of varying hydrophobicity, water-soluble ferrocene derivatives containing a PEG chain like the ruthenium main catalyst, or a ferrocene containing cationic surfactant. In this chapter much lower metal cocatalyst loading was used with similar results in Chapter 4 but because the metal catalysts are likely located at, or near the surface they could easily be removed by washing or precipitation.

Chapter 6 presents work using an iron cocatalyst with a very hydrophobic ligand (EHA_6TREN), which has been used in copper based miniemulsion polymerizations. The original intent was to

find iron catalysts suitable for miniemulsion polymerization. Although this iron/ligand complex could not polymerize in miniemulsion due to its water instability, in small amounts (non dried solvents and monomer, hydroscopic metal salt) it did allow a living radical polymerization to proceed in solution. This ligand was not expected to have any activity in iron ATRP but showed reasonable speeds and livingness for iron-mediated ATRP.

Chapter 2

Literature Review

2.1 Aqueous Dispersed Polymerization

2.1.1 Emulsion Polymerization

Emulsion polymerizations are heterogeneous processes used at both the laboratory and industrial scale for the synthesis of commodity and/or high value products. Emulsion polymerizations have numerous benefits over the homogenous bulk and solution polymerizations, including reducing the use of volatile organic compounds (VOCs) as solvents, increased heat transfer and heat capacity and reduced viscosity.

Like bulk polymerizations, emulsion polymerization recipes include monomer, initiators and other can incorporate other components such as chain transfer agents, while in emulsion polymerization water and a surfactant are also present. The surfactant acts to reduce the interfacial tension between the oil phase and water phase, and is present in concentrations above the critical micelle concentrations (CMC) to allow for the presence of micelles at the start of the polymerization. Before the polymerization begins, during stirring, a coarse emulsion is formed of micron-sized droplets (1 – 10 μm, 10^{11} - 10^{14} droplets/L), monomer-swollen micelles (0.1 – 1 nm, 10^{19} – 10^{20} micelles/L) and dissolved surfactant.

In emulsion polymerization, the water-soluble initiator produces radicals that enter, almost exclusively, the micelles due their overwhelmingly large number compared to droplets. This drives the diffusion of the slightly water-soluble monomer from the droplets to the micelles, which become the primary loci of polymerization. The droplets act as a monomer reservoir for

the ensuing polymerization, diffusing to the micelles and particles throughout the reaction. At the end of the polymerization, a stabilized colloidal dispersion of polymer particles suspended in water with an average particle size ranging from 50 – 500 nm[1] is produced. Because of the segregation of growing chains into micelles/particles, free radical emulsion polymerization has the unique ability to allow for a fast rate of reaction with a high molecular weight. This is generally not possible in bulk or solution because the increase in radical concentration also increases the rate of bimolecular termination. As the growing radicals are physically segregated in aqueous dispersed phase polymerizations (known as radical compartmentalization), a high radical concentration can exist without increasing the rate of bimolecular termination. This effect is more pronounced with decreasing particle sizes. Initial work on the mechanism of free radical polymerization in emulsion systems was done by Harkins[2] and Smith and Ewart.[3] The kinetics for free radical polymerization in emulsion is shown below, which include the compartmentalization effects. This equation contains the number of particles per liter of aqueous phase N_p, and the average number of radicals per particle $\bar{n}$ while N_A represents Avogadro's number and $[M]_p$ is the monomer concentration in the particles where R_p is measuring in M/s and k_p is the polymer rate coefficient for free radical polymerization measuring in L/mol-s.

$$R_p = k_p \frac{N_p \bar{n}}{N_A} [\mathrm{M}]_p$$

2.1.2 Miniemulsion Polymerization

Like emulsion polymerization, miniemulsion polymerization contains a dispersion of oil soluble materials in water stabilized by a surfactant, but differs from traditional emulsion polymerization in a few important aspects. A miniemulsion polymerization consists of a stabilized oil-in-water

dispersion, where the droplets are sub-micron sized (100 – 500 nm) and are the loci of polymerization. A normal recipe includes water, surfactant (concentration - below the CMC, to prevent any micellar nucleation), monomer, and initiator as in emulsion polymerizations, but also requires a costabilizer (explained below) to allow for submicron droplets to be stabilized. To form droplets on the nanometer scale, a strong input of energy needed. This is done through ultrasonication or microfludizers to obtain the shear forces required.

In a miniemulsion polymerization, unlike emulsion polymerizations, the concentration of surfactant is below the critical micelle concentration, so there no micelles present. The absence of micelles inhibits or prevents secondary nucleation during the polymerization process to ensure that the droplets are the only loci of polymerization. Because no micelles are present and the droplets are sufficiently small, a radical can easily nucleate a droplet and initiate polymerization. Since the droplets are the loci of the polymerization, there is no monomer transfer through the water phase and ideally the final number of polymer particles should be the same as the initial number of monomer droplets present, although this is not generally the case because of any Ostwald ripening that still may occur, even with the use of from any aggregation during the polymerization process.

Miniemulsions, before the polymerization begins, are not thermodynamically stable, and require the use of a costabilizer to obtain kinetically stable droplets to prevent monomer diffusion long enough for the miniemulsion polymerization process to proceed under the expected mechanism. The shearing process will produce a population of droplet sizes. Droplets surfaces are subject to pressure differences between the inside and outside of the droplet, known as Laplace pressure. The Laplace pressure increases with increasing curvature of the surface (decreasing droplet size) and the miniemulsion will experience a Laplace pressure differential from droplets of different

sizes since the size distribution is not perfectly monodisperse. The smaller droplets exert a larger Laplace pressure from the increased curvature of the droplet, and this increased pressure causes an increase in chemical potential, which drives the diffusion of monomer from smaller droplets to larger droplets. This effect is known as Ostwald ripening; costabilizer is used to counter these effects. Common costabilizers are cetyl alcohol and hexadecane, and they should be completely soluble in the monomer and possess an extremely low solubility in water. When droplets are formed the costabilizer is in equal concentrations in all droplets, regardless of size. The costabilizer effectively stops or severely inhibits Ostwald ripening due to the costabilizer's insolubility in water. If monomer in a smaller droplet were to diffuse into the larger droplet then the concentration of the costabilizer in the smaller droplet would be increased and the concentration in the larger droplet would be decreased, causing a concentration gradient, and thereby causing the monomer to diffuse back into the small droplet to minimize the chemical potential difference.

2.1.3 Living Radical Polymerization in Aqueous Dispersions (Reversible-Deactivation Radical Polymerization)

Unlike free radical polymerizations, reversible-deactivation radical polymerization, commonly called living radical polymerizations are a class of radical polymerizations with additional components that either: decrease the radical concentration in a polymerization (atom transfer radical polymerization, ATRP, or nitroxide mediated polymerization, NMP) or includes a transfer agent that reacts significantly quicker than the monomer propagation step (reversible addition-fragmentation chain transfer polymerization, RAFT), allowing for polymerization systems with decreased bimolecular termination and high end group functionality. Applying living radical polymerization to aqueous dispersed polymerizations has been investigated in depth as the

economic benefits are similar to that of free radical polymerization in emulsion: better heat transfer, lower viscosity and ease of processing (e.g. in semibatch polymerizations).

Initial studies with LRP attempted to use emulsion polymerization but because of differences in the polymer chain-growth and phase transfer of components to the water layer (NMP or RAFT) or lack of catalyst diffusion through the aqueous layer to the micelles, the polymerizations were generally not successful and suffered from poor colloidal stability. In free radical polymerization, even at early stages of the polymerization high molecular weight polymer is quickly produced. In living radical polymerization a different process occurs with, ideally, all the chains initiated at the beginning of the reaction. Since all chains ideally grow at the same rate, at the beginning of the polymerization only oligomers are present. These oligomers act as swelling agents and have been identified as one of the main problem areas in emulsion LRP, causing the 'superswelling effect' where at low conversions the particles swell to many time larger than sizes expected in free radical polymerizations due to the presence of large amount of oligomers.[4] Various solutions to this have been found with seeded emulsions being used to reduce the amount of monomer present at the earliest stages of the polymerization, thereby minimizing the effects of superswelling. The use of miniemulsion living radical polymerization largely circumvents superswelling. Much of the current understanding of living radical polymerization in aqueous dispersions comes from the research started in miniemulsion.

2.2 Transition Metal Mediated Polymerization (TMMP)/ Atom Transfer Radical Polymerization (ATRP)

In 1995 Sawamoto and Matyjaszewski[5,6] independently developed a technique that allows for the synthesis of polymers with molecular weight distribution dispersity Đ that is much lower (~ 1.1 –

1.4) than the theoretical minimum for free radical polymerizations (1.5), called either Atom Transfer Radical Polymerization (ATRP) or transition metal mediated polymerization (TMMP). Sawamoto used a ruthenium catalyst while Matyjaszewski discovered this process using a copper catalyst, which has proven to be the most commonly used catalysts to date[7] to mediate an ATRP polymerization. Figure 1 shows the main reaction mechanism in ATRP that allows the polymerization to proceed in a controlled or living manner. A transition metal – ligand complex (catalyst), Mt^m/L_n can abstract the halogen from an alkyl halide (R-X), increasing the oxidation state of the metal catalyst by +1 ($X\text{-}Mt^{m+1}/L_n$) and forming an active radical center that can propagate as in free radical polymerization. The reverse, deactivation reaction occurs when the active radical is capped by the formation of an alkyl halide and a reduction in the oxidation state of the metal centered catalyst (forming Mt^m/L_n). This deactivated state is highly preferred at equilibrium, which keeps the active radical population low, suppressing the rate of bimolecular termination. As termination is suppressed, the livingness of the polymer samples is increased, allowing for more complex molecular architectures, including specific molecular weights targets with low dispersity, and block copolymers, which are not possible to synthesize using free radical polymerization due to the short lifetime of the active radicals.[8]

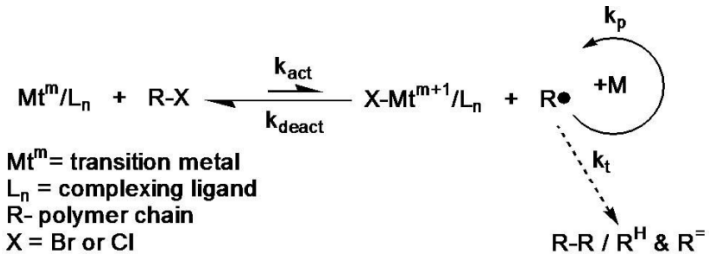

Figure 1. The proposed equilibrium reaction in ATRP/TMMP. The metal catalyst abstracts a halogen atom from the dormant alkyl bromide to produce a propagating radical species.

2.2.1.1 Catalyst and Ligands

The transition metal catalyst in ATRP is paramount for running a successful living radical polymerization. The catalyst choice affects the ATRP equilibrium through the dynamic activation/deactivation reactions shown in Figure 1. For a catalyst to be effective in ATRP, the equilibrium should be driven towards the deactivated state to keep the radical concentration low. The catalyst should have an affinity for a halogen, and the catalyst must be able to expand its coordination sphere upon abstraction of the halogen atom from the alkyl halide. Also, the catalyst must be able to effectively switch between two oxidation states separated by a single electron.[9] The ligand in an ATRP polymerization should improve the solubility of the transition metal salt in the monomer or solution being used and tune the electronic properties of the metal catalyst. Depending on the electronic structure of the ligands and how it complexes with the metal center, the redox potential of the catalyst complex[10] can be changed. Using ligands with different electron donating ability or withdrawing power, or ligands with multidentate binding, the final redox potential of the catalyst can be tailored to yield effective polymerizations for different monomer classes. The measured redox potential of a catalyst complex can be directly related to the catalyst activity[11] since the ATRP process is essentially driven by a one electron redox reaction of the catalyst. The most commonly researched catalysts include ruthenium, iron and copper catalysts[12] and are seen in Figure 2.

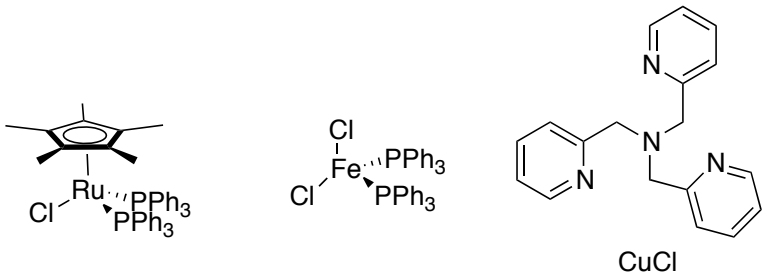

Figure 2. Example of ruthenium, iron and copper catalysts used in ATRP processes.

2.2.2 ATRP in dispersed systems

Living radical polymerization is believed to be most economically viable if used in dispersed systems. The most successful results using ATRP in dispersed systems have been in miniemulsion[13] as the loci of polymerization is in the droplet and there is ideally no mass transfer through the organic phase as in traditional emulsion polymerization, where the droplets act as a monomer reservoir. The difficulty in transferring the catalyst from the droplet to the micelle or particle is a major issue in unseeded emulsion ATRP.

2.2.2.1 ATRP in miniemulsion

Initial attempts using a catalyst in the lower oxidation state (activator) in miniemulsion ATRP were found to be successful but the experimental setup was difficult due the air sensitivity of the catalyst during the sonication process and preventing the oxidation of the catalyst.[14] It is believed that the use of sonication or a microfluidizer can more easily expose the catalyst to oxidation, deactivating the catalyst.

The use of ATRP processes with the catalyst starting in the deactivator state (Cu(II)) allowed for successful miniemulsion ATRP to be conducted, as the Cu(II) is generally much more oxygen tolerant than Cu(I). Working with Cu(II) catalysts allows for facile preparation. For miniemulsion ATRP to be successful it is imperative for the catalyst to stay almost exclusively in the droplets/particles. In the initial work, 2,2-bipyridine was compared to polymerizations using a much more hydrophobic catalyst 4,4-di(5-nonyl)-2,2-bipyridyl (dNbpy), which showed better control throughout the polymerization as the catalyst would preferentially reside in the droplets.[14]

The synthesis of highly hydrophobic ligands producing high activity catalysts including tris(2-bis(3-(2-ethylhexoxy)-3-oxopropyl)aminoethyl)amine (EHA_6TREN),[15] and bis(2-pyridylmethyl)octadecylamine (BPMODA)[16] allowed for better control over the polymerization. More recently, bis[2-(4-methoxy-3,5-dimethyl)pyridylmethyl]octadecylamine (BPMODA*)[17] has been developed with a much higher activity than BPMODA, which has allowed for the polymerization with much lower concentrations of catalyst compared to the BPMODA. These ligands can be seen in Figure 3.

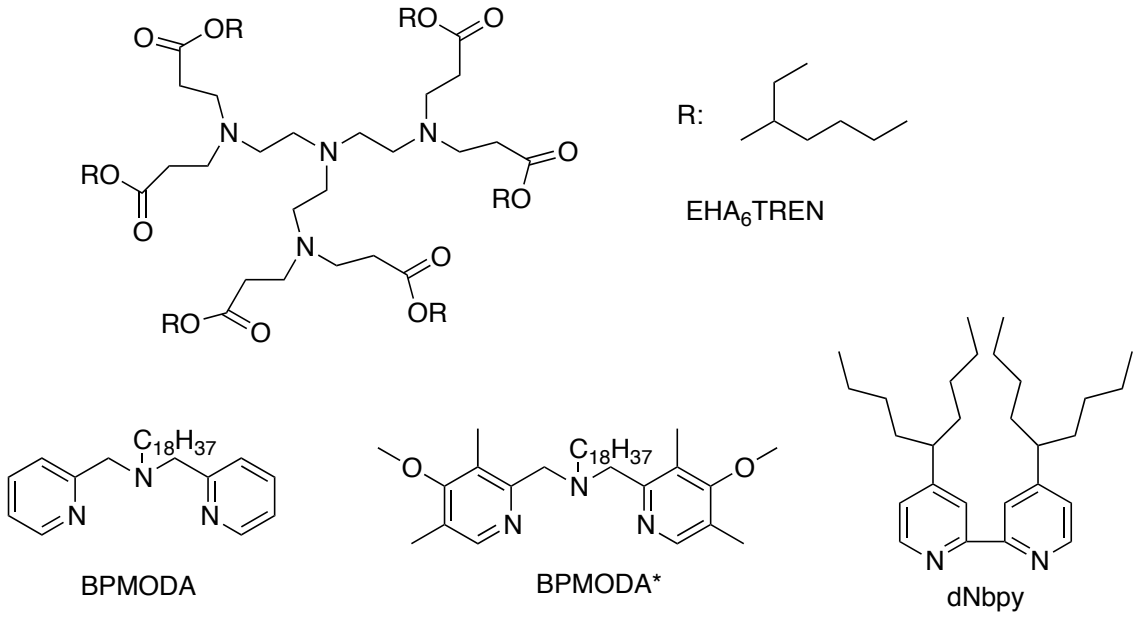

Figure 3. Hydrophobic ligands for ATRP in miniemulsion.

The first report of using a cationic surfactant of hexadecyltrimethylammonium bromide or cetyltrimethylammonium bromide (CTAB) was demonstrated by Simms and Cunningham.[15] This was an important improvement for ATRP in aqueous dispersed systems because before this only nonionic surfactants such as Brij 98 (poly(ethylene glycol)-b-oleyl ether) had been used. Ionic surfactants generally provide better colloidal stability and also stability at significantly higher reaction temperatures. The work by Simms and Cunningham demonstrated that successful

reverse ATRP miniemulsion polymerizations could be run at temperatures 30°C higher than miniemulsions using a nonionic surfactant. In an attempt to increase the initiator efficiency of a reverse ATRP polymerization in miniemulsion, Simms and Cunningham used an initiating system of ascorbic acid and hydrogen peroxide.[18] The result of using this system was a low initiator efficiency, but polymerizations that occurred at a rapid rate, with high conversion occurring within 8 h. The most noteworthy result was the extremely high molecular weights (~10^6 Da) and very low dispersities (~1.2) of the synthesized polymer. It was proposed that the observed polymerization rate as well as the molecular weights could occur through compartmentalization effects or a complex redox reaction from using the ascorbic acid/hydrogen peroxide initiating system. A traditional reverse ATRP using a water-soluble thermal initiator would generally have molecular weights in $10^3 – 10^4$ Da range for a similar system.

ATRP in miniemulsion can also be initiated through an 'activators generated by electron transfer' AGET process with the Cu(II) reduced to Cu(I) using a water-soluble reducing agent.[16] Ideally this process allows pure diblock copolymers to be synthesized, as there are no thermal radical initiators present that could initiate new chains when synthesizing the second block. AGET ATRP also allows the polymerization to take place in the presence of air (oxygen)[19] as the reducing agent present will reduce any remaining oxygen in the system. Ascorbic acid is the common reducing agent used in miniemulsion as it is highly water-soluble and can be added post shearing. As ascorbic acid is water-soluble and the catalysts reside in the droplets it is likely that the reduction of catalyst occurs at the interface of the droplets and the water phase. AGET ATRP in miniemulsion shows a linear increase in M_n with respect to conversion and the polymers have dispersities (~1.2-1.3). One of the major advantages of miniemulsions is the ability to produce hybrid materials as one can stabilize a hydrophobic material in the droplets and perform a polymerization around this material. Bomblanski et al.[20] reported a polymerizations in

miniemulsion initiated from nanosized silica particles that were modified with initiator functionalities. The segregation of silica initiators into different droplets provided improved results with respect to the onset of gelation when the polymerization occurred in solution and bulk.

ATRP has also been performed in inverse miniemulsions. Inverse miniemulsions are important tools for synthesizing potential medical products including cross-linked nanogels for drug delivery systems. Oh et al.[21] synthesized linear polymers in inverse miniemulsion with the continuous phase composed of cyclohexane and catalyzed by copper complexed to tris(2-pirydylmethyl)amine (TPMA). They were also able to synthesize biodegradable cross-linked polymers from PEG containing acrylates including disulfide crosslinkers. These polymerizations were all reported to have low dispersities (1.2 - 1.3) and actual M_n followed the theoretical molecular weight (M_n) curve closely. ATRP in inverse miniemulsion has also been used for synthesizing protein-containing nanogels as shown by Averick et al..[22] They show that living radical polymerization in an inverse miniemulsion does not affect the structure of a green fluorescent protein as the nanoparticles fluoresce under irradiation, indicating that the nanogels have potential use in medical imaging. Other hybrid materials have also been prepared using inverse miniemulsion including the use of gold nanoparticles.[23] These gold nanoparticle containing nanogels were taken up by cells, showing their potential for drug delivery devices.

2.2.2.2 ATRP in Microemulsion and Seeded Emulsion

ATRP in microemulsion has been employed using copper catalysts to make transparent or translucent latexes of small particle diameters (d < 100nm). Initial attempts at ATRP in microemulsion used either forward ATRP,[24] using the hydrophobic ligand dNbpy or reverse ATRP[25] using the bpy ligand. Both produced polymerizations that showed a linear increase of

polymer molecular weight with conversion although the reverse ATRP showed a much higher dispersity (M_w/M_n = 1.6) compared to the forward ATRP, which had lower dispersity (as low as M_w/M_n =1.15) and lower M_n values. In a reverse ATRP, it is possible that a radical can enter a droplet which does not contain a deactivating catalyst due to the large number of droplets in a microemulsion, likely leading to this large difference in molecular weights and distributions. AGET ATRP was first demonstrated in microemulsion by Min and Matyjaszewski[26] and was found to proceed more smoothly compared to forward or reverse ATRP, since the catalyst in the a deactivator state and the initiator were both initially present in the droplets compared with normal or reverse ATRP. The reducing agent used was ascorbic acid, a water-soluble reducing agent. The nucleation time was found to be extremely fast, leading to narrow molecular weight distributions. This work expanded into a seeded emulsion polymerization,[27] first developed by Matyjaszewski. Initially an AGET ATRP microemulsion was used with a small fraction of the total monomer charged to the reaction. Ten minutes after initiation the remainder of monomer was added to the reaction forming droplets, which act as the monomer reservoir for the polymerization occurring in the initial seed particles. This system allows larger, emulsion-sized particles to be formed without the use of high shearing devices as in miniemulsion polymerizations while still allowed for an route to decrease the amount of surfactant used compared to a miniemulsion polymerization.

ATRP inverse microemulsions have been reported for synthesizing small (particle diameter ≈ 40 – 200 nm) polymer particles and crosslinked nanogels.[28] The particle size was tuned by the choice of reducing agent and the amount used. These polymers showed low dispersities (< 1.5) and the gel permeation chromatography (GPC) traces show the distribution moving to higher molecular weights, indicating a living polymerization was taking place, although the molecular weights did not closely follow the theoretical M_n vs conversion curve.

2.3 Thermoresponsive phase regulated catalysis

2.3.1 Thermoresponsive polymers

Thermoresponsive polymers are a subset of polymers that respond to changes in temperature and have been investigated for a variety of uses including biomedical materials, drug delivery and green chemistry/ catalysis.[29,30] These polymers go through a volume phase transition at critical temperature, depending on the polymer structure.[31] Polymers solutions that when heated display immiscibility or insolubility exhibit a lower critical solution temperature (LCST, Figure 4, left side - lowest point on the curve) while polymer solutions that become soluble/miscible upon heating have an upper critical solution temperature (UCST, Figure 4, right side - highest point on the curve). Depending on the polymer used, molecular weight, and concentration in solvent the cloud point temperature (T_{cp}), which represents the transition temperature at any composition (Figure 4, black curve). The cloud point temperature can be very similar to the LCST/UCST or can differ significantly depending on this system used. There are many classes of polymers which display these sorts of behaviours.[30]

The most studied thermoresponsive polymer, poly(N-isopropylacrylamide) (PNIPAM) was first discovered in 1963 by Heskins et al.,[32] to have cloud point, where the insolubility becomes macroscopically visible in water, at approximately 32 °C. The T_{cp}/LCST can also be tuned by copolymerizing with monomers of differing hydrophobicity/hydrophilicity.[33,34] Increasing relative amounts of hydrophobic sections on a polymer can decrease the T_{cp}/LCST while increasing the amount of hydrophilic co-monomer increases the T_{cp}/LCST value as the polymer increases its solubility in water by the addition of these hydrophilic units.

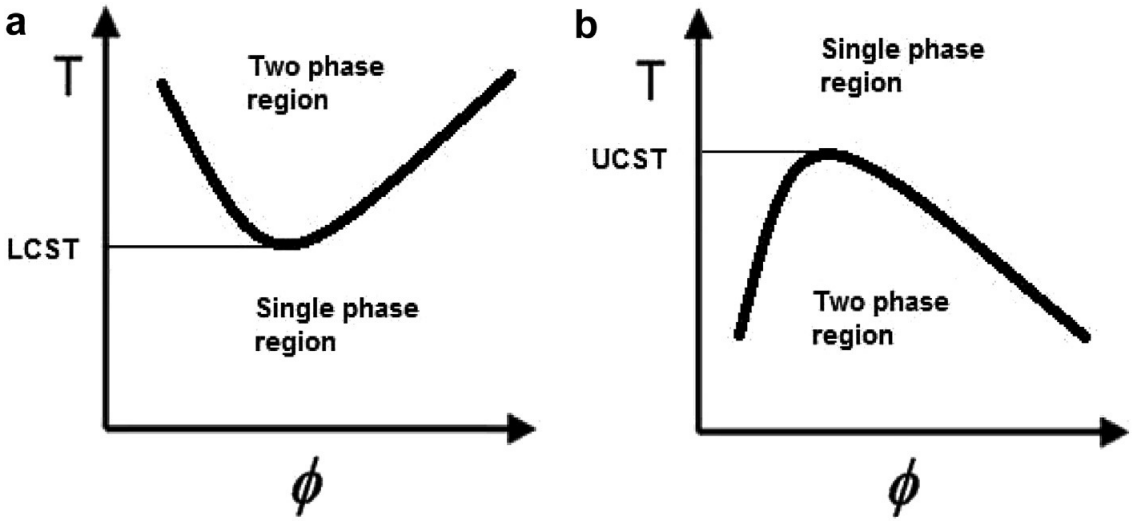

Figure 4. The temperature vs volume fraction of polymer showing the UCST and the LCST for a given polymer.[29]

Poly(ethylene glycol) (PEG), also known as poly(ethylene oxide) (PEO), is another water-soluble/ thermoresponsive polymer that has been investigated intensively as it has been identified for its use in green chemistry, and its biocompatibility.[35] Low molecular weight PEG is a liquid at room temperature and has no discernable vapor pressure, and is fairly tolerant to temperature, acidity levels, and various reactions adding to its use in green chemistry. PEG and its derivatives have also been identified as a thermoresponsive polymer, which has been used for various purposes including phase transfer catalysis,[36] temperature responsive surfactants[37] and biomedical purposes including drug delivery.[38]

The thermoresponsive characteristics of PEG have been extensively studied. PEG obtains its thermoresponsive properties from the unique spacing of the methylene groups and the regularly placed ether linkages. At low temperatures hydrogen bonding between the ether linkages and

water allow for effective solvation of the polymer. As the polymer solution is heated the thermal energy disrupts this network of hydrogen bonding, which provides an enthalpic driving force for PEG's solubility in water.[39,40] In addition there is an entropic force of hydrophobic bonding which causes the methylene units to aggregate as the driving force for solubility has been decreased. There are many parameters which can determine the cloud point transition temperature of PEG in an aqueous solution including the molecular weight, which is known to decrease the transition temperature as the MW increases, and the effects of additives in an aqueous solution including salts and other polymers in solution, which also decreases the cloud point temperature.[41]

2.3.2 Thermoresponsive phase regulated catalysis

Thermoresponsive phase regulated catalysis (TPRC) is a technique that uses a catalyst bound to a thermoresponsive polymer, and takes advantage of the LCST/USCT properties and uses the changing solubility as a means to successfully remove a catalyst from the final products provided the products are significantly hydrophobic. It is an important development, as it allows for similar characteristics of high activity in homogenous catalysis with the benefit of easy removal as in heterogeneous catalysis. In Figure 5 we can see an example of a two-phase reaction system with the starting material or substrate in the organic phase and the catalyst in the aqueous phase. The catalyst can be a thermoresponsive polymer like PEG or PNIPAM. When the reaction mixture is mixed and heated to the cloud point, polymer bound catalyst will transfer from the water to the organic phase due to the changing solubility. With the catalyst and the substrate now present in the same phase the catalyzed reaction can proceed at reasonable rates at the given reaction temperature. At the end of the reaction the reaction is cooled down significantly below the cloud point so the catalyst can easily transfer back to the water phase. If the product formed during this

reaction is sufficiently hydrophobic, it will be retained in the organic layer and the two layers can be separated from each other allowing for a catalyst free final product and aqueous layer containing the catalyst, which can be easily recycled for multiple runs. This has been shown for multiple types of reactions including reductions,[42] hydroformylations,[43] hydrogenations,[44] and even living radical polymerizations using either ruthenium[45,46] or copper.[47]

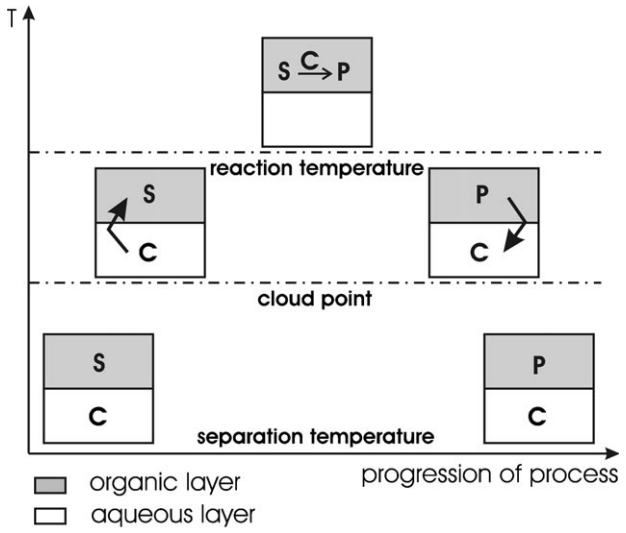

Figure 5. The reaction process for a thermoresponsive phase regulated catalysis reaction. Here the catalyst, C, can easily transfer from the aqueous layer to the organic layer once the cloud point is reached, catalyzing the reaction in the organic phase. After the reaction is completed, the temperature is dropped and the catalyst transfers back to the organic phase allowing for easy separation and ideally recycling. [48]

References

(1) Gilbert, R. G. *Emulsion Polymerization – A Mechanistic Approach*; Academic Press: London, 1995.

(2) Harkins, W. D. *J. Am. Chem. Soc.* **1947**, *69*, 1428–1444.

(3) Smith, W. V.; Ewart, R. H. *J. Chem. Phys.* **1948**, *16*, 592–599.

(4) Luo, Y.; Tsavalas, J.; Schork, F. J. *Macromolecules* **2001**, *34*, 5501–5507.

(5) Kato, M.; Kamigaito, M.; Sawamoto, M.; Higashimura, T. *Macromolecules* **1995**, *28*, 1721–1723.

(6) Wang, J.-S.; Matyjaszewski, K. *J. Am. Chem. Soc.* **1995**, *117*, 5614–5615.

(7) Tsarevsky, N. V; Braunecker, W. A.; Tang, W.; Brooks, S. J.; Matyjaszewski, K.; Weisman, G. R.; Wong, E. H. *J. Mol. Catal. A Chem.* **2006**, *257*, 132–140.

(8) Braunecker, W. a.; Matyjaszewski, K. *Prog. Polym. Sci.* **2007**, *32*, 93–146.

(9) Matyjaszewski, K.; Xia, J. *Chem. Rev.* **2001**, *101*, 2921–2990.

(10) Jianhui, X.; Xuan, Z.; Krzysztof, M. In *Transition Metal Catalysis in Macromolecular Design*; ACS Symposium Series; American Chemical Society, 2000; Vol. 760, pp. 13–207.

(11) Braunecker, W. a.; Tsarevsky, N. V.; Gennaro, A.; Matyjaszewski, K. *Macromolecules* **2009**, *42*, 6348–6360.

(12) Di Lena, F.; Matyjaszewski, K. *Prog. Polym. Sci.* **2010**, *35*, 959–1021.

(13) Cunningham, M. F. *Prog. Polym. Sci.* **2008**, *33*, 365–398.

(14) Matyjaszewski, K.; Qiu, J.; Tsarevsky, N. V.; Charleux, B. *J. Polym. Sci. Part A Polym. Chem.* **2000**, *38*, 4724–4734.

(15) Simms, R. W.; Cunningham, M. F. *J. Polym. Sci. Part A Polym. Chem.* **2006**, *44*, 1628–1634.

(16) Min, K.; Gao, H.; Matyjaszewski, K. *J. Am. Chem. Soc.* **2005**, *127*, 3825–3830.

(17) Elsen, A. M.; Burdyńska, J.; Park, S.; Matyjaszewski, K. *Macromolecules* **2012**, *45*, 7356–7363.

(18) Simms, R. W.; Cunningham, M. F. *Macromolecules* **2007**, *40*, 860–866.

(19) Smith, A. P.; Fraser, C. L. *Macromolecules* **2002**, *35*, 594–596.

(20) Bombalski, L.; Min, K.; Dong, H.; Tang, C.; Matyjaszewski, K. *Macromolecules* **2007**, *40*, 7429–7432.

(21) Oh, J. K.; Tang, C.; Gao, H.; Tsarevsky, N. V; Matyjaszewski, K. *J. Am. Chem. Soc.* **2006**, *128*, 5578–5584.

(22) Averick, S. E.; Magenau, A. J. D.; Simakova, A.; Woodman, B. F.; Seong, A.; Mehl, R. a.; Matyjaszewski, K. *Polym. Chem.* **2011**, *2*, 1476.

(23) Siegwart, D. J.; Srinivasan, A.; Bencherif, S. a; Karunanidhi, A.; Oh, J. K.; Vaidya, S.; Jin, R.; Hollinger, J. O.; Matyjaszewski, K. *Biomacromolecules* **2009**, *10*, 2300–2309.

(24) Kagawa, Y.; Kawasaki, M.; Zetterlund, P. B.; Minami, H.; Okubo, M. *Macromol. Rapid Commun.* **2007**, *28*, 2354–2360.

(25) Kai, P.; Yi, D. *J. Appl. Polym. Sci.* **2006**, *101*, 3670–3676.

(26) Min, K.; Matyjaszewski, K. *Macromolecules* **2005**, *38*, 8131–8134.

(27) Min, K.; Gao, H.; Matyjaszewski, K. *J. Am. Chem. Soc.* **2006**, *128*, 10521–10526.

(28) Li, W.; Matyjaszewski, K. *Polym. Chem.* **2012**, *3*, 1813.

(29) Gandhi, A.; Paul, A.; Sen, S. O.; Sen, K. K. *Asian J. Pharm. Sci.* **2015**, *10*, 99–107.

(30) Roy, D.; Brooks, W. L. a; Sumerlin, B. S. *Chem. Soc. Rev.* **2013**, *42*, 7214–7243.

(31) Fujishige, S.; Kubota, K.; Ando, I. *J. Phys. Chem.* **1989**, *93*, 3311–3313.

(32) Heskins, M.; Guillet, J. E. *J. Macromol. Sci. Part A - Chem.* **1968**, *2*, 1441–1455.

(33) Chen, G.; Hoffman, A. S. *Nature* **1995**, *373*, 49–52.

(34) Feil, H.; Bae, Y. H.; Feijen, J.; Kim, S. W. *Macromolecules* **1993**, *26*, 2496–2500.

(35) ChenCurrent address: Key Lab. of Ra, J.; Spear, S. K.; Huddleston, J. G.; Rogers, R. D. *Green Chem.* **2005**, *7*, 64.

(36) Sauvagnat, B.; Lamaty, F.; Lazaro, R.; Martinez, J. *Tetrahedron Lett.* **1998**, *39*, 821–824.

(37) Feng, H.; Verstappen, N. a. L.; Kuehne, A. J. C.; Sprakel, J. *Polym. Chem.* **2013**, *4*, 1842.

(38) Ward, M. a.; Georgiou, T. K. *Polymers (Basel).* **2011**, *3*, 1215–1242.

(39) Smith, G. D.; Bedrov, D. *J. Phys. Chem. B* **2003**, *107*, 3095–3097.

(40) Dormidontova, E. E. *Macromolecules* **2002**, *35*, 987–1001.

(41) Han, S. K.; Jhun, B. H. *Arch. Pharm. Res.* **1984**, *7*, 1–9.

(42) Jiang, J.; Mei, J.; Wang, Y.; Wen, F.; Jin, Z. *Appl. Catal. A Gen.* **2002**, *224*, 21–25.

(43) Jiang, J.; Wang, Y.; Liu, C.; Han, F.; Jin, Z. **1999**, 131–136.

(44) Terashima, T.; Ouchi, M.; Ando, T.; Sawamoto, M. *Polym. J.* **2011**, *43*, 770–777.

(45) Terashima, T.; Nomura, A.; Ouchi, M.; Sawamoto, M. *Macromol. Rapid Commun.* **2012**, *33*, 833–841.

(46) Toshihide, Y.; Yasuhiro, W.; Tsuyoshi, A.; Masami, K.; Mitsuo, S. *Control. Radic. Polym.* **2006**, *944*, 2–14.

(47) Bai, L.; Zhang, L.; Pan, J.; Zhu, J.; Cheng, Z.; Zhu, X. *Macromolecules* **2013**, *46*, 2060–2066.

(48) Behr, A.; Henze, G.; Schomäcker, R. *Adv. Synth. Catal.* **2006**, *348*, 1485–1495.

Chapter 3

Shuttling Catalyst for Living Radical Miniemulsion Polymerization: Thermoresponsive Ligand for Efficient Catalysis and Removal

3.1 Preface

The purpose of this project was to solve the problem of residual metal in the final product produced by metal mediated living radical polymerization, or ATRP in miniemulsion. Often the final product needs to be precipitated or dried and then dissolved in a solvent and run though a packed column of alumina to remove the metal residue, which reduces the viability of this process on an industrial scale. Previously the Sawamoto laboratory had synthesized PEG polymer-bound ligands for ruthenium half metallocene catalysts, which were shown to be effective in a toluene/MMA and water suspension in regards to catalysis and removability. In the summer of 2012, I visited the Sawamoto laboratory for the first time showing proof of concept that this system would work in miniemulsion and returned again in September 2013 for another stay where I completed the work showing the shuttling-capability of the water-soluble catalyst at elevated temperatures and its ability to successfully mediate an LRP in miniemulsion and its removal. This was the first time using solely a water-soluble catalyst in a miniemulsion polymerization. This work was accepted for publication in *ACS Macro Lett*, **2015**, 4 (6), 628–631 (DOI: 10.1021/acsmacrolett.5b00286)

3.2 Abstract

In this report we demonstrate the use of a thermoresponsive ligand for the ruthenium-catalyzed living radical polymerization of butyl methacrylate (BMA) in miniemulsion. A phosphine ligand-functionalized poly(ethylene glycol) chain (PPEG) in conjunction with Cp*-based ruthenium complex (Cp*: pentamethylcyclopentadienyl) provided thermoresponsive character as well as

catalysis for living polymerization: the complex migrated from the water phase to the oil phase for polymerization upon heating, and then migrated from oil to water phase when the temperature was decreased to quench polymerization. Consequently, simple treatment (i.e., water washing or methanol re-precipitation) yielded metal-free polymeric particles containing less than 10 μg/g (by ICP-AES) of ruthenium residue.

3.3 Introduction

Aqueous dispersed radical polymerizations have been practically used to produce latex or particles in industry. Using water as a continuous phase and adding surfactant allows polymerization of hydrophobic monomers in the dispersed oil phase. These processes are highly favorable for polymer production, because they generally have much lower viscosities and better heat transfer than comparable bulk or solution polymerizations. More importantly, they are environmentally benign: additional volatile organic compounds (VOCs) such as organic solvents are significantly reduced compared to solution polymerization.

Living radical polymerization (LRP), which allows precise control of polymer structures, has been adapted to aqueous dispersed systems.[1–3] Among LRP systems, metal-catalyzed living radical polymerization (Mt-LRP) or atom transfer radical polymerization (ATRP)[4,5] has been most widely employed due to the simple procedure and multiplicity of the initiator design. Ligands of the catalyst in Mt-LRP often play critical roles for catalyst solubility as well as the catalysis by controlling the electron passage to promote the catalytic cycle. Thus, various ligand designs have allowed emulsions,[6–13] miniemulsions[14–22] and microemulsions[23,24].

Despite the good usability, Mt-LRP incurs a serious issue: metal residue could contaminate the final product. The issue is especially serious with dispersed systems, since as-polymerized

polymers generally become products for particle or emulsion applications. One solution is extreme reduction of the catalyst concentration[25] through use of highly active catalysts[26] or in combination with reducing agents,[27,28] and extensive investigations on this subject have been done in homogeneous solution polymerization as well as in dispersed systems. However, there has been little real progress achieved in developing an ideal system satisfying all requirements such as controllability, reproducibility, production stability, and removability of metal.

With these objectives in mind, we focused on the development of thermoresponsive ligands for miniemulsion Mt-LRP to achieve "shuttling" of the catalyst in the dispersed system as follows (Scheme 1). Before polymerization at room temperature, the catalyst is soluble in the water phase because of the hydrophilicity of the ligand. However, upon heating to start the polymerization, the hydrophilicity of the ligand is significantly decreased, causing the complex to migrate into the oil phase, i.e., monomer droplet. Finally, through the cooling process to quench the polymerization, the catalyst is transferred back to the water phase. To realize such a shuttling process, we hypothesized poly(ethylene glycol) (PEG) chains might be promising candidates for the thermoresponsive feature,[29] since we have used designed PEG-decorated triphenyl phosphine for ruthenium[30] or iron[31] catalyst in solution Mt-LRP.

Scheme 1. Miniemulsion Mt-LRP with thermoresponsive shuttling catalysts

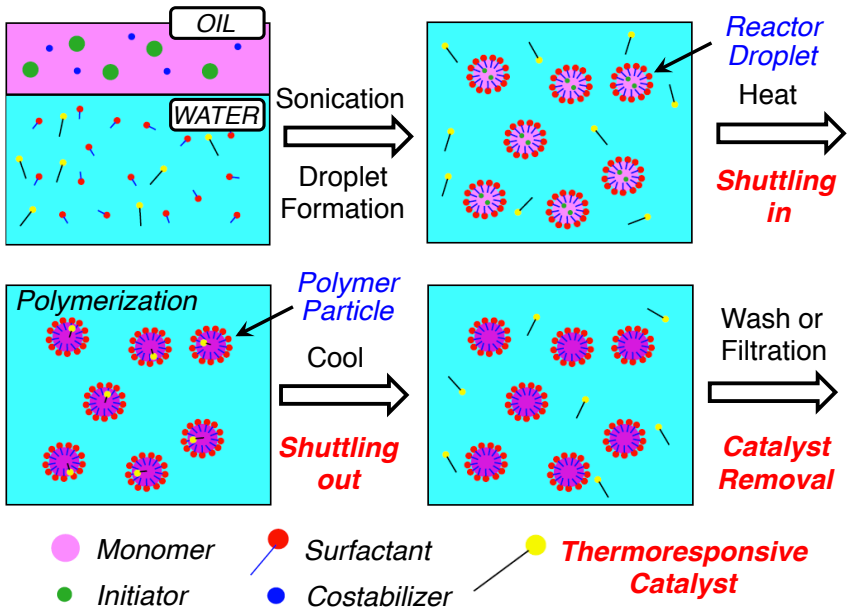

3.4 Experimental

3.4.1 Materials

Methyl methacrylate and butyl methacrylate (MMA and BMA, Tokyo Kasei; purity > 99%) were dried overnight over calcium chloride and purified by double distillation under reduced pressure over calcium hydride before use. Potassium carbonate (K_2CO_3, Wako, purity > 99.5%) was degassed by vacuum–argon purge cycles before use. Hexadecyltrimethylammonium bromide (CTAB, Sigma-Aldrich; BioXtra purity ≥99%,) and hexadecane (Sigma Aldrich, purity >99%,) were used without any purification. Ethyl-2-chloro-2-phenylacetate (ECPA, Aldrich; purity >97%) was distilled under reduced pressure before use. (4-hydroxyphenyl) diphenylphosphine (Sigma-Aldrich; purity > 98%), poly(ethylene glycol) methyl ether tosylate (PEG-tosylate, Sigma-Aldrich; average M_n 5000 Da) and $[RuCp^*Cl]_4$ [chloro(pentamethylcyclopentadienyl)

ruthenium(II) tetramer, Aldrich] were used as received, and were handled in a glove box under a moisture- and oxygen-free argon atmosphere (H_2O < 1 ppm, O_2 < 1 ppm). n-Octane (Wako; purity > 98%) and 1,2,3,4-tetrahydro-naphthalene (tetralin, Kisida Chemical; purity > 98%), internal standards in gas chromatography, respectively, were dried over calcium chloride overnight and distilled twice over calcium hydride. Water (Wako Chemicals; distilled) was bubbled with dry nitrogen for 15 mins before use.

3.4.2 Characterization

The molecular weight distributions of the polymers were measured by gel permeation chromatography (GPC) with THF as an eluent on three polystyrene gel columns (Shodex KF-803; pore size, 20-1000 A; 8.0 mm i.d. × 30 cm; flow rate, 1.0 mL min) connected to a DU-H2000 pump, a 74S-RI refractive index detector, and a 41-UV ultraviolet detector (all from Shodex). The columns were calibrated against 13 standard poly(MMA) samples (Polymer Laboratories; M_n = 500–3840000; M_w/M_n = 1.06–1.22) as well as the monomer. Reaction samples of p(BMA) samples were analyzed against the p(MMA) standards in this study.

^{1}H NMR spectra were recorded in $CDCl_3$ or CD_2Cl_2 at 25 °C on a JEOL JNM-LA500 spectrometer operating at 500.16 MHz. ^{31}P NMR spectra were recorded with $(C_2H_5O)_2POH$ (12 ppm) as an internal standard in $CDCl_3$ at 25°C on a JEOL JNM-LA500 spectrometer operating at 500.16 MHz.

Particle size was measured using dynamic light scattering (DLS) on an Otsuka Photal ELSZ-0 equipped with a semiconductor laser (wavelength: 658 nm) at 25 °C. The measurement angle was 165°, and the data were analyzed by the CONTIN fitting method.

3.4.3 PEG-5000 Phosphine synthesis

The PEG-phosphine ligand used for the temperature sensitive catalyst RuClCp*(PPEG) used in the solution and miniemulsion polymerizations was synthesized as follows: 0.200 g (0.719 mmol) (4-hydroxyphenyl)diphenylphosphine, 3.269 g (0.68 mmol) of poly(ethylene glycol) methyl ether

tosylate (average Mn 5,000 Da), and 0.136 g (0.965 mmol) of potassium carbonate were added to 10 mL of DMF and reacted at 80°C for 72 h. The solution was very viscous, and was therefore diluted with methanol prior to being precipitated by cooling and the addition of ether. The polymer was solubilized in chloroform to filter off the salt and was precipitated by cooling and the addition of ether and hexane.

3.4.4 Catalyst synthesis

The RuClCp*(PPEG) catalyst was synthesized by the addition of 2.7 mg (0.0025 mmol) of RuClCp* tetramer with 0.101 g (0.02 mmol) of the PEG-phosphine catalyst in 2.38 ml of toluene and heated at 80°C for 1 h to form the active catalyst.

3.4.5 Miniemulsion polymerization

1.91 mL (12 mmol) of BMA, 0.218 mL of tetraline as an internal standard for measuring conversion, 0.1406 mL of hexadecane (HD) were added to 62.2 mg (0.06 mmol) of catalyst in 0.52 mL of toluene. This solution was mixed and heated at 80°C for 15 min and then cooled to room temperature. 0.023 mg (0.12 mmol) of ECPA was then added and the reaction mixture was cooled to 0°C. 15 mL of deionized water containing 0.087 g (0.24 mmol) of CTAB were added to the organic phase and mixed at 0°C for 15 min at which point the solution was ultrasonicated for 10 mins at 50% output and 50% duty while under a flowing argon blanket. The polymerization took place in either sealed glass tubes or in an air free Schlenk flask. Aliquots were periodically taken and measured by GC conversion or NMR and GPC for molecular weight data. DLS measurements were taken for particle size analysis.

3.4.6 Toluene free miniemulsion polymerization

Thermoresponsive catalyst was synthesized using the same procedure as above. To prepare the toluene free miniemulsion polymerization the toluene was removed under vacuum and backfilled

with argon and vacuumed 3 times to ensure the catalyst was in an air free environment. The miniemulsion was then prepared using the procedure described above.

3.4.7 Catalyst removal

Post-polymerization the catalyst was removed by adding the resulting latex to a large volume of methanol (latex to methanol = 1 to 5 by volume). This mixture was then centrifuged at 4000 g for 10 minutes and the methanol was decanted. The polymer was resuspended by adding the same volume of methanol and this procedure was repeated two more times.

3.4.8 Reproducibility

The reproducibility of the results throughout this thesis, other than analytical precision, was expected to be within 5% of the reported values on an absolute scale.

3.5 Results and Discussion

Triphenylphosphine-terminated PEG (PPEG) was synthesized through the reaction of tosylated PEG and (4-hydroxyphenyl)diphenylphosphine (Appendix A - Figure A1). The thermoresponsive catalyst was synthesized through aging of Cp*-ruthenium complex precursor ($[Cp^*Ru(\mu_3\text{-}Cl)]_4$, Cp* = pentamethylcyclopentadienyl) with 2 equivalent of PPEG in toluene at 80 ˚C. ^{31}P NMR analyses indicated formation of one phosphine-ligated complex [RuCp*Cl(PPEG)], unlike with triphenylphosphine (PPh_3) giving two-ligated, probably due to the bulkiness of PEG (Appendix A Figure A2[30]). Such a coordinateively unsaturated complex (i.e., 16e) of RuCp*Cl(PPEG) might show higher catalytic activity than 18e saturated. The peak from the ligated phosphine was broad, promising high activity due to the dynamic coordination of the phosphine ligand.

The aged complex was perfectly soluble in water at r.t. to give yellow homogeneous solution, which also supported the PEG ligation to the ruthenium complex. Thus, the yellow solution in water was combined with toluene to prepare bilayer solution for simple demonstration of the thermoresponsive character (Figure 6A). Upon heating to 95˚C, the upper layer (i.e., toluene)

became yellow while the lower layer (i.e., water) became colorless, indicating the complex became hydrophobic and soluble in toluene rather than water. Afterwards, cooling to room temperature gave the original colored bilayer appearance. Thus, the PEG-ligated complex indeed showed temperature responsive property suitable for the concept in Scheme 1.

Furthermore, to confirm the expected thermoresponsive shuttling behavior on the colloidal scale, the interaction between PPEG and butyl methacrylate (BMA) under miniemulsion condition similar to the actual polymerization (see below) was observed with 1D Nuclear Overhauser effect (NOE) difference NMR. In general, the NOE spectrum can provide the location of chemical species from its interactions with nearby species (≤5Å) and has shown to be effective in providing insight on the chemical microenvironment within an emulsion,[32] allowing for the measurement of phase transfer on the colloidal scale.

The heterogeneous solution in D_2O containing PPEG, BMA, hexadecane (HD, stabilizer), and hexadecyltrimethylammonium bromide (CTAB, surfactant) was sonicated to make a milky NMR sample. For the NOE measurement, the peak from methylene PPEG at around 3.6 ppm was chosen as the "target." Figure 6-B shows the normal NMR and the NOE spectrum at 25˚C (**1, 2**) and 80˚C (**3, 4**), respectively. At 25˚C no correlation peak was observed between PPEG and BMA, indicating they do not exist close to each other in the dispersed medium. This would make sense since PPEG is rather hydrophilic at lower temperature but BMA is hydrophobic. On the other hand, upon heating to 80˚C, clear correlation peaks were observed between the two compounds, suggesting PPEG became hydrophobic and recognized by the BMA. Interestingly, peaks from methylene protons (*c*) neighboring the oxygen showed strong correlation peak, which may be due to the highest polarity of the protons among others in BMA. Since this model experiment was started at 80˚C and then cooled we believe the PPEG chain can be shuttled from the hydrophobic phase in the miniemulsion to the hydrophilic (water) phase simply by changing temperature.

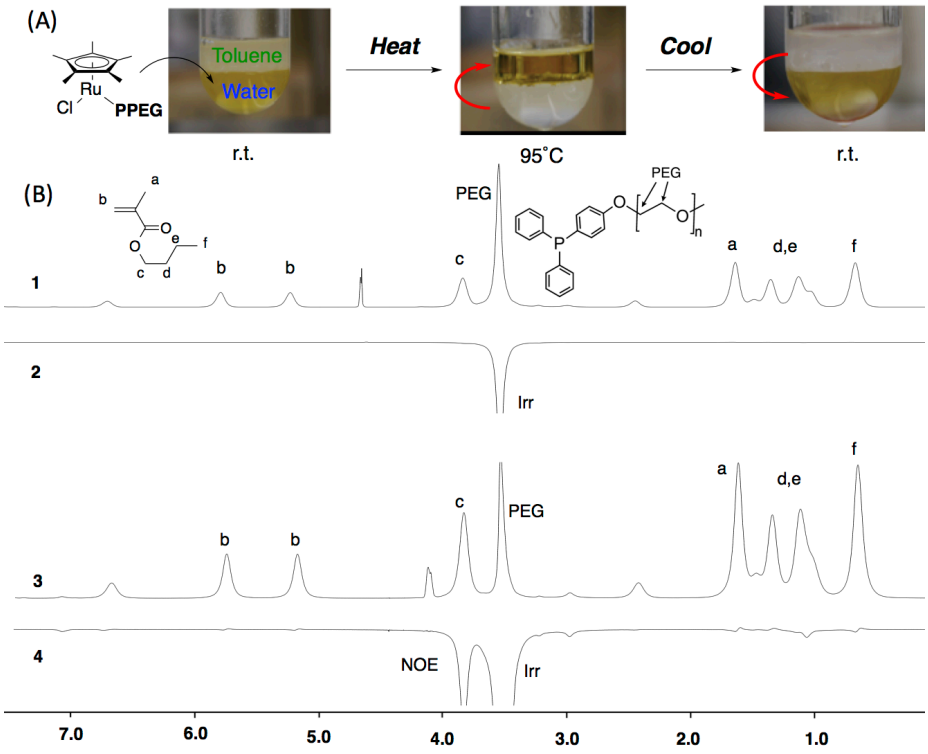

Figure 6. (A) Pictures for phase transfer of the thermoresponsive catalyst on heating (from r.t. to 95˚C) and cooling (from 95˚C to r.t.). (B) Normal ^{1}H NMR and the NOE spectrum at 25˚C (1, 2) and 80˚C (3, 4), respectively. The PEG peak was chosen for irradiation at both temperatures with a strong NOE observed at 80°C between the BMA proton and the PEG proton while no NOE was observed after cooling to 25°C.

I thus conducted living radical miniemulsion polymerizations of butyl methacrylate (BMA) with the PEG-ligated Ru catalyst [RuCp*Cl(PPEG)], in conjunction with ethyl-2-chloro-2-phenylacetate (ECPA, initiator), HD, and CTAB. These components were dispersed into water either in the presence or absence of toluene, followed by ultrasonication under argon to make highly dispersed solution. The system without toluene is more practical due to fewer amounts of VOCs. As the standard condition, RuCp*Cl(PPh_3)$_2$ was employed as the catalyst for the miniemulsion with toluene as it is not soluble in bulk monomer. Note that polymerization was

done without amine cocatalysts, which are commonly required for effective catalysis of ruthenium mediated polymerizations in solution,[33] though water may act as a activator or cocatalyst for this catalyst.[34]

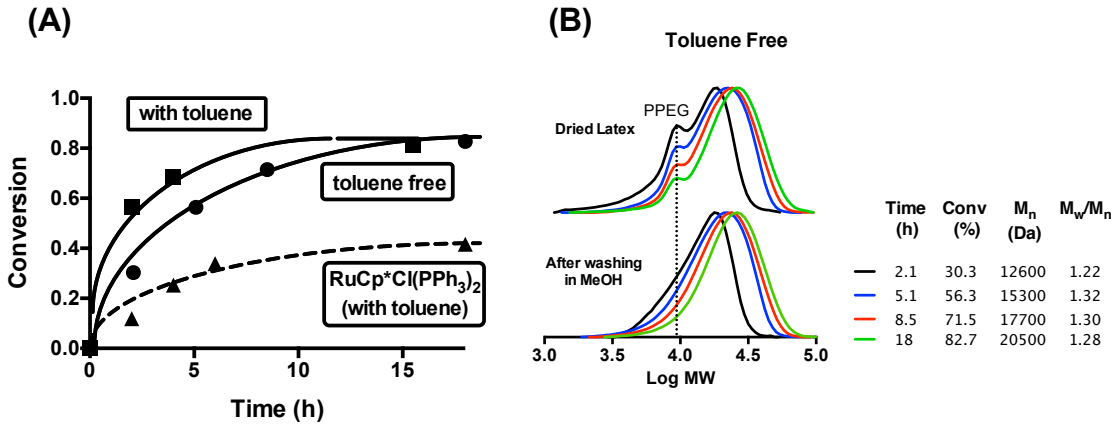

Figure 7. Conversion versus time plots of miniemulsion polymerizations of BMA with RuCp*Cl(PPEG) or RuCp*Cl(PPh$_3$)$_2$ at 80°C: [BMA]$_0$:[ECPA]$_0$:[Ru Catalyst]$_0$ = 100/1/0.05 with [CTAB]/[hexadecane] = 4.3/5.2 wt% vs BMA; [CTAB]/[hexadecane] = 4.3/5.2 wt% vs BMA. RuCp*Cl(PPEG) was prepared through aging of [Ru(Cp*)Cl]$_4$ with PEG-ligand ([[Ru(Cp*)Cl]$_4$]:[PEG-ligand] = 1:2) before polymerization, followed by use as it was. For the miniemulsion polymerizations in the presence of toluene, the solution was prepared for the volume ratio of organic/water to be 1/5 v/v%. Curves on the conversion plot are used to guide the eye. (B) The GPC traces for the "toluene free" miniemulsion polymerization with RuCp*Cl(PPEG): just dried latex (as they are: top) and after washing in MeOH (bottom).

The polymerizations were carried out at 80˚C. As shown in Figure 7-A, using the temperature-sensitive catalyst [RuCp*Cl(PPEG)] in the presence of toluene, the monomer was smoothly consumed to reach nearly 85% conversion at 15 h. The rate was much faster than that with RuCp*Cl(PPh$_3$)$_2$ resulting in limited conversion (~40%). A similar rate profile was also seen for the toluene free miniemulsion polymerization.

The RuCp*Cl(PPEG)-catalyzed polymerization exhibits a much faster polymerization rate than with RuCp*Cl(PPh$_3$)$_2$, which can be accounted for by the structure. The GPC data for the

polymerization catalyzed by RuCp*Cl(PPh_3)$_2$ is shown in Appendix A – Figure A3. The PEG containing triphenyl phosphine derivative has an electron-donating group in the para position that the triphenyl phosphine does not have. The introduction of the electron donating PEG group has been shown to produce a more active catalyst in reports investigating the effect of ligand (PEG and methoxy) substitutions.[26,29,35,36] In addition, the coordinateively unsaturated complex (i.e., 16e) of RuCp*Cl(PPEG) and the dynamic coordination would also contribute to the higher activity.

The upper portion of Figure 7-B shows the GPC traces of the latex samples with RuCp*Cl(PPEG) (without toluene). The main peaks shifted to higher molecular weight as the polymerization proceeded. These peaks were definitely from obtained poly(BMA)s and the peak shift would indicate controlled propagation in the miniemulsion polymerization. The M_n values from these samples increased linearly with respect to conversion, although they were above the theoretical values (Appendix A, Figure A5). Along with the peaks from the controlled polymers, motionless peaks, whose elution time was almost same as that of PPEG, were observed at lower molecular weight region. This would be reasonable, since the macromolecular ligand and the complex still exist in the latex.

The z-average diameter of obtained polymer particle (82% conversion, pre-washing) was 168 nm, as measured by dynamic light scattering. Interestingly, a polymerization was induced at a reaction temperature of 40°C, significantly below the cloud point, indicating that the catalyst may be surface bound or surface active while mediating the polymerization (Appendix A Figure A4)

The obtained latexes were cooled in an ice bath quickly stop the polymerizations before washing with methanol, leaving a colorless polymer. The unmoved peaks disappeared, indicating removal of the catalyst residue. The removal process allowed exact determination of the molecular weights and its molecular weight distributions, revealing the polymerization was certainly controlled: linear relationship between M_n and conversion; low PDI (M_w/M_n ~1.3).

Finally, the residual ruthenium concentration in the washed polymer (at 82% conversion) was measured with ICP-AES and compared with before the washing process (dried latex). It was less than 10 ppm, which was much lower than that for just dried sample (360 ppm). The rough estimation indicates that more than 98% of the ruthenium catalyst was removed from the product. Unfortunately at this time catalyst recovery using miniemulsion is not possible but will be explored in future studies. Further studies must also be done to determine the safety limit for residual ruthenium in final products.

3.6 Conclusions

In conclusion I have been able to successfully run metal mediated living radical polymerizations in miniemulsion by using solely a water-soluble/ thermoresponsive catalyst, which can shuttle into the monomer droplets and be easily removed to values below 10 ppm in the final polymer product.

3.7 References

(1) Monteiro, M.J.; Cunningham, M.F. *Macromolecules* **2012**, *45*, 4939–4957.

(2) Zetterlund, P.B.; Kagawa, Y.; Okubo, M. *Chem. Rev.* **2008**, *108*, 3747–3794.

(3) Cunningham, M. F. *Prog. Polym. Sci.* **2008**, *33*, 365–398.

(4) Kato, M.; Kamigaito, M.; Sawamoto, M.; Higashimura, T. *Macromolecules* **1995**, *28*, 1721–1723.

(5) Wang, J.-S.; Matyjaszewski, K. *J. Am. Chem. Soc.* **1995**, *117*, 5614–5615.

(6) Qiu, J.; Gaynor, S. G.; Matyjaszewski, K. *Macromolecules* **1999**, *32*, 2872–2875.

(7) Jousset, S.; Qiu, J.; Matyjaszewski, K.; Granel, C. *Macromolecules* **2001**, *34*, 6641–6648.

(8) Eslami, H.; Zhu, S. *Polymer.* **2005**, *46*, 5484–5493.

(9) Eslami, H.; Zhu, S. *J. Polym. Sci. Part A Polym. Chem.* **2006**, *44*, 1914–1925.

(10) Min, K.; Gao, H.; Yoon, J. A.; Wu, W.; Kowalewski, T.; Matyjaszewski, K. *Macromolecules* **2009**, *42*, 1597–1603.

(11) Okubo, M.; Minami, H.; Zhou, J. *Colloid Polym. Sci.* **2004**, *282*, 747–752.

(12) Kagawa, Y.; Minami, H.; Okubo, M.; Zhou, J. *Polymer.* **2005**, *46*, 1045–1049.

(13) Chan-Seng, D.; Georges, M. K. *J. Polym. Sci. Part A Polym. Chem.* **2006**, *44*, 4027–4038.

(14) Matyjaszewski, K.; Qiu, J.; Tsarevsky, N. V.; Charleux, B. *J. Polym. Sci. Part A Polym. Chem.* **2000**, *38*, 4724–4734.

(15) Simms, R. W.; Cunningham, M. F. *J. Polym. Sci. Part A Polym. Chem.* **2006**, *44*, 1628–1634.

(16) Elsen, A. M.; Burdyńska, J.; Park, S.; Matyjaszewski, K. *Macromolecules* **2012**, *45*, 7356–7363.

(17) Simms, R. W.; Cunningham, M. F. *Macromolecules* **2007**, *40*, 860–866.

(18) Min, K.; Gao, H.; Matyjaszewski, K. *J. Am. Chem. Soc.* **2005**, *127*, 3825–3830.

(19) Min, K.; Jakubowski, W.; Matyjaszewski, K. *Macromol. Rapid Commun.* **2006**, *27*, 594–598.

(20) Bombalski, L.; Min, K.; Dong, H.; Tang, C.; Matyjaszewski, K. *Macromolecules* **2007**, *40*, 7429–7432.

(21) Oh, J. K.; Tang, C.; Gao, H.; Tsarevsky, N. V; Matyjaszewski, K. *J. Am. Chem. Soc.* **2006**, *128*, 5578–5584.

(22) Averick, S. E.; Magenau, A. J. D.; Simakova, A.; Woodman, B. F.; Seong, A.; Mehl, R. a.; Matyjaszewski, K. *Polym. Chem.* **2011**, *2*, 1476.

(23) Kai, P.; Yi, D. *J. Appl. Polym. Sci.* **2006**, *101*, 3670–3676.

(24) Kagawa, Y.; Kawasaki, M.; Zetterlund, P. B.; Minami, H.; Okubo, M. *Macromol. Rapid Commun.* **2007**, *28*, 2354–2360.

(25) Ouchi, M.; Ito, M.; Kamemoto, S.; Sawamoto, M. *Chem. Asian J.* **2008**, *3*, 1358–1364.

(26) Magenau, A. J. D.; Kwak, Y.; Schröder, K.; Matyjaszewski, K. *ACS Macro Lett.* **2012**, *1*, 508–512.

(27) Zhang, H.; Schubert, U. S. *J. Polym. Sci. Part A Polym. Chem.* **2004**, *42*, 4882–4894.

(28) Matyjaszewski, K.; Jakubowski, W.; Min, K.; Tang, W.; Huang, J.; Braunecker, W. A.; Tsarevsky, N. V. *Proc. Natl. Acad. Sci. U. S. A.* **2006**, *103*, 15309–15314.

(29) Saeki, S.; Kuwahara, N.; Nakata, M.; Kaneko, M. *Polymer.* **1976**, *17*, 685–689.

(30) Yoshitani, T.; Watanabe, W.; Ando, T.; Kamigato, M.; Sawamoto, M. *Controlled/Living Radical Polymerization* **2006**, *944*, 2–14.

(31) Nishizawa, K.; Ouchi, M.; Sawamoto, M. *Macromolecules* **2013**, *46*, 3342–3349.

(32) Heins, A.; Sokolowski, T.; Stöckmann, H.; Schwarz, K. *Lipids* **2007**, *42*, 561–572.

(33) Hamasaki, S.; Kamigaito, M.; Sawamoto, M. *Macromolecules* **2002**, *35*, 2934–2940.

(34) Nishikawa, K.; Kamigaito, K.; Sawamoto, M. *Macromolecules.* **1999**, *32*, 2204–2209.

(35) Schröder, K.; Mathers, R. T.; Buback, J.; Konkolewicz, D.; Magenau, A. J. D.; Matyjaszewski, K. *ACS Macro Lett.* **2012**, *1*, 1037–1040.

(36) Wang, Y.; Kwak, Y.; Matyjaszewski, K. *Macromolecules* **2012**, *45*, 5911–5915.

Chapter 4

Iron-cocatalyzed living radical miniemulsion polymerization aided by surfactant selection

4.1 Preface

With the successful proof of concept shown of shuttling catalysts, further work was done to improve the performance of these water-soluble thermoresponsive catalysts in miniemulsion as high conversions could not be reached in prior work. Various monomers were polymerized using different ligands (see in Appendix B). Recently the Sawamoto laboratory found that the addition of an iron cocatalyst, ferrocene, added a secondary catalytic cycle to the main LRP cycle, where the cocatalyst could reduce the deactivator (Ru(III)) to Ru(II) and cap an active radical, allowing for both faster polymerizations, improved end group functionality, and polymerizations to be run at ppm levels of ruthenium catalyst. As iron catalysis in waterborne ATRP has been limited to this point, I wanted to see if this catalytic system would be stable in miniemulsion. Surprisingly the polymerizations were significantly faster than without the cocatalyst. The ferrocene catalytic cycle also included the formation of an ionic species, which prompted the study of the surfactant aided polymerization and it is described in this chapter. This chapter is currently being prepared for submission as a manuscript.

4.2 Abstract

I investigated the use of ferrocene ($FeCp_2$) as a cocatalyst for ruthenium mediated living radical polymerization (LRP) catalyzed by thermoresponsive PEG containing catalysts in miniemulsion.

$FeCp_2$ has been shown to effectively cocatalyze Ru-mediated LRP in solution by adding a secondary catalytic cycle that both reduces the Ru(III) deactivator to the Ru(II) activator species as well as increasing the rate of deactivation of the active radical by a halogen, thereby increasing the effectiveness of Ru LRP polymerizations. First the effectiveness of this iron cocatalyst in miniemulsion was investigated for its applicability with both faster rates and higher conversions reached (> 90 % conversion, < 10 h), compared to polymerizations without $FeCp_2$. Next, the effect of the halogen counter-ion on the cationic surfactant was investigated and shown to be a major factor in determining the polymerization rate and the end group fidelity. Ru-mediated polymerizations containing $FeCp_2$ in miniemulsion stabilized by nonionic surfactants require halogen to be present in the form of NaCl in order to obtain full conversion and control of the polymerization.

4.3 Introduction

Metal catalyzed living radical polymerizations[1] (Mt-LRP), also know as atom transfer radical polymerizations[2] (ATRP), have found success in various reaction media including organic solvents,[3] aqueous media,[4] and aqueous dispersions.[5–7] The most significant progress in Mt-LRP aqueous dispersions has been in miniemulsion, which uses water as the continuous phase with nanosized hydrophobic droplets being synthesized by use of a high shear device. Miniemulsion Mt-LRP is important for reducing the amount of volatile organic compounds such as solvents in the polymerization and has the added benefits of better heat transfer and lower reaction viscosities.[8] One of the major disadvantages of Mt-LRP in miniemulsion is the residual metal left in the final products due to the hydrophobic ligands used to keep the metal catalyst in the droplets and particles throughout the polymerization.[9] To solve this problem, I have developed the use of thermoresponsive ‘shuttling’ ruthenium catalysts, which at low temperature are water-soluble but

at reaction temperatures are oil-soluble and enter the particles and catalyze the LRP as seen in Scheme 2.[10] At the end of the polymerization the reaction can be cooled and the latex washed in methanol leaving a polymer with less than 10 ppm of residual ruthenium. This polymerization successfully showed signs of livingness and reached a maximum of 80% conversion at approximately 15 h.

Scheme 2. Metal mediated miniemulsion polymerization catalyzed by thermoresponsive catalysts made for easy removal from the final products.

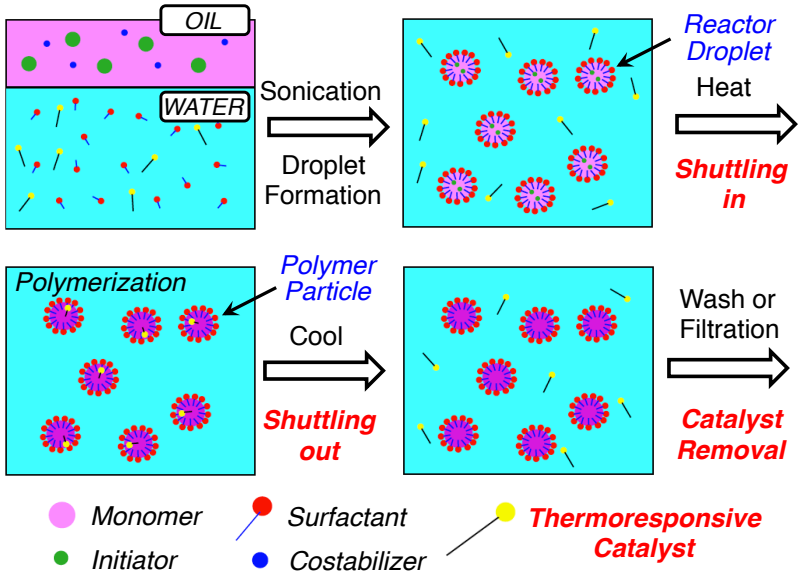

The use of co-catalysts or additives has been shown to increase the rate and the effectiveness of catalysts in ATRP, also allowing for a reduction in the catalyst concentration including for example the use of reducing agents in activators regenerated for electron transfer (ARGET) ATRP.[11] During the course of a polymerization there is generally accumulation of the deactivator form of the catalyst as a result of bimolecular termination. This increase of deactivator affects the ratio of deactivator to activator, and if this ratio becomes too large the polymerization can be

retarded or even stop at incomplete conversions. Reducing agents can reform the activator and allow higher to complete conversions to be realized. Recently the use of ferrocene ($FeCp_2$) as a co-catalyst for ruthenium catalyzed metal mediated polymerization showed increased rates of polymerization and better livingness through a concerted co-catalytic mechanism.[12] The rate of activation was increased by reducing the deactivating species, Ru(III), to the activator Ru(II) via a halogen abstraction by the $Fe(II)Cp_2$ to form an unstable ferrocenium salt complex $Fe(III)Cp_2^+Cl^-$. This complex quickly degrades through a redox process forming $Fe(II)Cp_2$ with the halogen capping an active radical, thereby increasing the rate of deactivation in $FeCp_2$ co-catalyzed polymerizations. The proposed mechanism for this concerted cocatalysis is shown in Scheme 3.

Scheme 3. The proposed mechanism for the concerted cocatalysis of ruthenium LRP by FeCp2.[12]

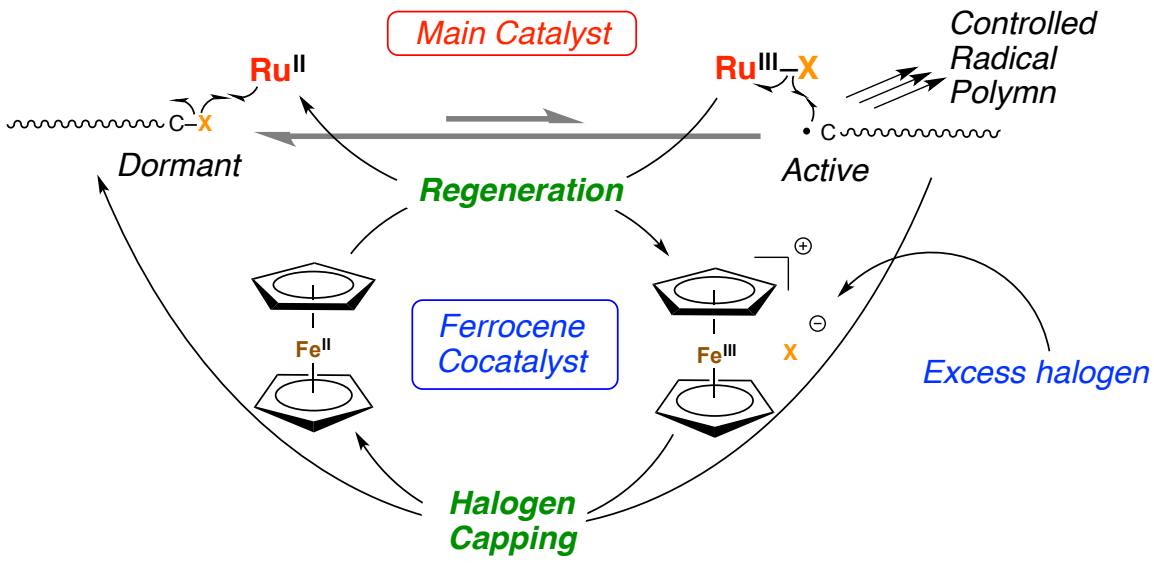

There is a drive in Mt-LRP research to find new iron based catalysts due to iron's lower biotoxicity compared to other Mt-LRP metals, its high availability and its low cost. Iron is generally less tolerant to functional monomers, which can easily deactivate the iron catalyst.

However improvements in ligand design[13] and 'all-iron' catalysis utilizing $FeCp_2$ derivatives[14] have resulted in improvements in catalyst stability toward functional monomers.. Furthermore, there are few reports of iron catalyzed Mt-LRP in reaction media containing large amounts of water.[15–17]

Herein I present a study using $FeCp_2$, an iron cocatalyst, in miniemulsion Mt-LRP, allowing thermoresponsive Ru catalysts to mediate a polymerization to conversions above 90% conversion in times under 8 h while still allowing for facile ruthenium removal from the final product. Furthermore, I explore the effect of the surfactant counter-ion on the rate and the polymer end-group functionality and demonstrate for the first time a surfactant aided Mt-LRP in miniemulsion. This work will ideally lead to improvements in catalysis in miniemulsion for the synthesis of living polymers and further reduce the amount of primary catalyst required.

4.4 Experimental

4.4.1 Materials

Butyl methacrylate and benzyl methacrylate (BMA and BzMA, Tokyo Kasei; purity > 99%) were dried overnight over calcium chloride and purified by double distillation under reduced pressure over calcium hydride before use. Potassium carbonate (K_2CO_3, Wako, purity > 99.5%) was degassed by vacuum–argon purge cycles before use. Hexadecyltrimethylammonium bromide (CTAB, Sigma-Aldrich; BioXtra purity ≥99%,), hexadecyltrimethylammonium chloride (CTAC, Sigma-Aldrich; BioXtra purity ≥99%), Polyoxyethylene (20) oleyl ether (Brij98, Sigma-Aldrich; average M_n 1150 Da), and hexadecane (Sigma Aldrich, purity >99%,) were used without any purification. Ethyl-2-chloro-2-phenylacetate (ECPA, Aldrich; purity >97%) was distilled under reduced pressure before use. (4-hydroxyphenyl) diphenylphosphine (Sigma-Aldrich; purity >

98%), poly(ethylene glycol) methyl ether tosylate (PEG-tosylate, Sigma-Aldrich; average M_n 5000 Da or M_n 2000 Da) and [RuCp*Cl]4 [chloro(pentamethylcyclopentadienyl) ruthenium(II) tetramer, Aldrich] were used as received, and were handled in a glove box under a moisture- and oxygen-free argon atmosphere (H_2O < 1 ppm, O_2 < 1 ppm). n-Octane (Wako; purity > 98%) and 1,2,3,4-tetrahydro-naphthalene (tetralin, Kisida Chemical; purity > 98%), internal standards in gas chromatography, respectively, were dried over calcium chloride overnight and distilled twice over calcium hydride. Water (Wako Chemicals; distilled) was bubbled with dry nitrogen for 30 mins before use. Dimethyl 2-bromo-2,4,4-trimethylglutarate (dimer-Br) was synthesized according to previous reports.[18] PEG-phosphine ligands (M_n 2000 and M_n 5000) were synthesized according to previous reports.[10]

4.4.2 PPEG Synthesis

The PEG_{113}-phosphine ligand used for the temperature sensitive catalyst RuClCp*(PPEG) used in the solution and miniemulsion polymerizations was synthesized as follows: 0.200 g (0.719 mmol) (4-hydroxyphenyl)diphenylphosphine, 3.269 g (0.68 mmol) of poly(ethylene glycol) methyl ether tosylate (average M_n 5,000 Da), and 0.136 g (0.965 mmol) of potassium carbonate were added to 10 mL of DMF and reacted at 80°C for 72 h. The solution was very viscous, and was therefore diluted with methanol prior to being precipitated by cooling and the addition of ether. The polymer was solubilized in chloroform to filter off the salt and was precipitated by cooling and the addition of ether and hexane. The same molar rations were used for the synthesis of $PPEG_{45}$ but used poly(ethylene glycol) methyl ether tosylate (average M_n 2,000 Da).

4.4.3 Miniemulsion polymerization

The RuCp*Cl(PPEG5000) catalyst was synthesized by the addition of 1.0 mg (0.0009 mmol) of RuClCp* tetramer with 14.5 mg (0.007 mmol) of the PEG-phosphine catalyst (M_n 5000) in 1.25

ml of toluene and heated at 80°C for 1 h to form the active catalyst. The toluene was removed under vacuum after this aging process and refilled with Ar. Under an inert atmosphere 7.5 mL of deionized water containing 0.0435 g (0.12 mmol) of CTAB was added 1.2 mL (7.1 mmol) of BMA, 0.1 mL of tetraline (internal standard for monomer conversion by ^{1}H NMR), 0.072 mL of hexadecane (HD), 6.6 mg (0.035 mmol) of ferrocene and 0.014 mg (0.078 mmol) of the initiator ECPA were mixed and then added to the water phase containing surfactant and catalyst at 0°C and was stirred vigorously. Under stirring at 0°C the mixture was ultrasonicated for 3 mins at 50% output and 50% duty while under a flowing argon blanket. The polymerization took place in either sealed glass tubes or in an air free Schlenk flask. Aliquots were periodically taken and measured by GC conversion and GPC for molecular weight data. DLS measurements were taken for particle size analysis.

4.4.4 Characterization

The molecular weight distributions of the polymers were measured by gel permeation chromatography (GPC) with THF as an eluent on three polystyrene gel columns (Shodex KF-803; pore size, 20-1000 A; 8.0 mm i.d. × 30 cm; flow rate, 1.0 mL min) connected to a DU-H2000 pump, a 74S-RI refractive index detector, and a 41-UV ultraviolet detector (all from Shodex). The columns were calibrated against 13 standard poly(MMA) samples (Polymer Laboratories; M_n = 500–3840000; M_w/M_n = 1.06–1.22) as well as the monomer.

^{1}H NMR spectra were recorded in $CDCl_3$ or CD_2Cl_2 or DMSO-d6 at 25 °C on a JEOL JNM-LA500 spectrometer operating at 500.16 MHz

4.5 Results and Discussion

4.5.1 Addition of FeCp2

Our previous work with thermoresponsive shuttling catalysts showed that RuCp*ClPPEG$_{113}$ could effectively mediate a BMA polymerization initiated by ECPA to approximately 80% conversion in 15 h before slowing significantly. The most important aspect of this system was that post-polymerization, washing or precipitating in methanol could effectively remove almost all metal residue leaving less than 10 ppm of residual ruthenium in the final product. In this work, $FeCp_2$ was tested to determine its tolerance in aqueous dispersions as there are very few iron catalysts that can tolerate large amounts of water that are applicable for LRP,[17,19,20] and the ability of $FeCp_2$ to cocatalyze a Ru Mt-LRP.

In Figure 8, one can see the rate data from the polymerizations cocatalyzed with $FeCp_2$ or no cocatalyst at 80 °C and a polymerization with $FeCp_2$ run at 60 °C. When $FeCp_2$ was added to the oil phase a significant rate enhancement was seen with over 90% conversion reached in 7 h as seen in Figure 1 (RuCp*/$FeCp_2$ 80 °C) compared to the polymerization run without any $FeCp_2$ present in our previous work (RuCp* 80 °C). The addition of $FeCp_2$ to the oil phase (water solubility = 4.25 x 10^{-5} mol/L @ 298K) clearly shows a large rate increase compared to the polymerizations just containing RuCp*ClPPEG$_{113}$. In addition, the polymerization run at 60 °C reached approximately 60% conversion in 7h (RuCp*/$FeCp_2$ 60 °C) following the rate curve of the previous work until it slowed significantly. Since this polymerization was run significantly below the cloud point for PEG, I believe that the conversion does not reach significantly higher values due to more of the catalyst partitioning into the water phase. It should be noted that the catalyst in pure water at 10 mg/ml (significantly higher than reaction conditions) did not show a cloud point up to 90 °C, though I have previously shown at 80 °C an NOE between the PEG chain and the monomer in miniemulsion indicating some solubility at this temperature. From the positive NOE results and the successful polymerization that occurred, one can assume that the partition coefficient changes enough to allow catalyst to preferentially enter the droplets in

miniemulsion at reaction temperatures. The GPC traces for the polymerization at 80 °C with RuCp*ClPPEG$_{113}$ and FeCp$_2$ show a clear shift to higher molecular weights with limited tailing indicating that a successful LRP occurred. A similar peak shift was noticed for the lower temperature polymerization. These results indicate that FeCp$_2$ can act as a suitable cocatalyst for Ru mediated living radical polymerization in miniemulsion. Ideally this will provide opportunities for synthesizing more complex architectures such as block copolymers in miniemulsion or for reducing the amount of Ru required for a successful miniemulsion LRP. After precipitation of this final polymer latex in MeOH, significant yellow color remained, likely the residual FeCp$_2$ trapped in the polymer. Although the Fe cannot be completely removed (120 ppm of residual iron in the final product), it can be considered significantly safer for many purposes compared to residual copper or ruthenium, and further research is being undertaken to use FeCp$_2$ derivatives that can easily be removed post-polymerization in a miniemulsion system.

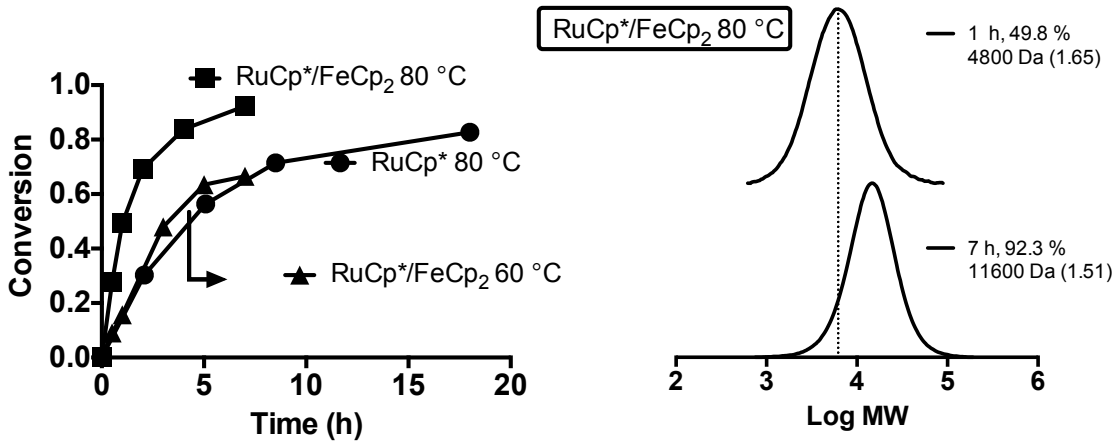

Figure 8. Conversion data on the left for the miniemulsion polymerizations of BMA catalyzed by RuCp*Cl(PPEG$_{113}$) with or without FeCp$_2$: [BMA]$_0$:[ECPA]$_0$:[Ru Catalyst]$_0$ /[FeCp$_2$]$_0$ = 100/1/0.05/0.5 or 0 with [CTAB]/[hexadecane] = 4.3/5.2 wt% vs BMA at 80 °C or 60 °C. Lines are shown to guide the eye. On the right are the GPC traces for the polymerization containing FeCp$_2$ polymerized at 80 °C.

4.5.2 Surfactant and counter-ion effect

The large rate enhancement by the addition of $FeCp_2$ to the miniemulsion polymerization was investigated further. Previously, addition of excess halide provided increased rates, higher final conversions and enhanced end group functionality[12] due to the active radical being capped more quickly by the ionic Fe(III) species (Scheme 2). We postulated that surfactant counter-ion present at the droplets and polymer particle interface likely had an enhancing effect on the polymerization rate. To test this theory I performed a polymerization of benzyl methacrylate catalyzed by $RuCp^*ClPPEG_{45}$ and co-catalyzed by $FeCp_2$ with a nonionic surfactant Polyoxyethylene(20) oleyl ether (Brij98). Benzyl methacrylate was in place of butyl methacrylate in following polymerizations to compare the thermoresponsive catalysts to $RuCp^*Cl(PPh_3)_2$ in miniemulsion polymerizations (Appendix B) since $RuCp^*Cl(PPh_3)_2$ was not soluble in BMA for direct comparisons between a thermoresponsive catalyst and the standard catalyst. In these polymerizations a shorter ligand, $PPEG_{45,}$ is used rather than $PPEG_{113}$, because the $RuCp^*ClPPEG_{45}$ was found to effectively mediate LRP for the BzMA monomer, while using the $PPEG_{113}$ displayed no livingness. (Appendix B – Figure B3).

This polymerization used approximately twice the amount of surfactant to stabilize the miniemulsion as the previous polymerizations required since nonionic surfactants can only stabilize emulsions by steric forces rather than ionic forces. Brij 98 also contains no halogen counter-ion, unlike the cationic surfactant CTAB. The polymerization of BzMA occurred very quickly for the first hour with almost 75% conversion reached but the conversion did not proceed much higher as seen in Figure 9. The GPC trace for this polymerization shows a very broad dispersity ($D > 8$) and bimodal molecular weight distribution, which did not shift to higher molecular weights throughout the polymerization. This indicated that the polymerization was not living, which was believed to be due to the ionic nature of the $Fe(III)Cp_2^+Cl^-$, formed when $FeCp_2$

reduces the Ru(III) deactivator, and the large amount of water present in the miniemulsion. The charged Fe(III) species may migrate to the droplet/particle surface, and the halogen may be lost to the water phase, removing the excess halogen present at the droplet interface as occurs when CTAB is used. To test this hypothesis I added a source of water-soluble Cl^- in the same molar ratio as the ionic surfactant used in the previous polymerizations (1.6 eq of Cl^- with respect to initiator) in a technique similar to that which allows ATRP to be run with anionic surfactants.[21] In Figure 9, one can see that this polymerization begins slightly slower although the conversion reached over 95% in 3 h and the GPC trace shows a clear distribution shift to higher molecular weights with increasing conversion, indicating that the presence of halogen in the water phase can promote a living radical polymerization in miniemulsion.

Although these miniemulsions latexes were not colloidally stable and showed significant coagulum formation (~ 30 -50 %), results shows the importance of excess halogen to promote the livingness of the polymerization in the presence of ferrocene. Even with NaCl in the water phase, the presence of excess halogen and ionic nature of the $Fe(III)Cp_2^+Cl^-$ promoted the halogen capping of the active radical to yield effective control of the polymerization.

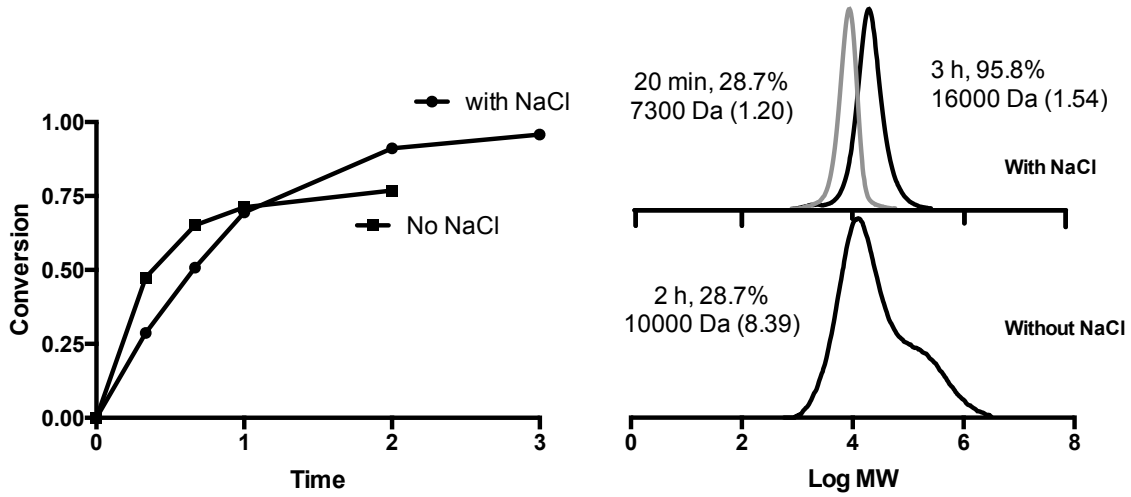

Figure 9. Conversion data for the miniemulsion polymerizations of BzMA catalyzed by RuCp*Cl($PPEG_{45}$) with $FeCp_2$ stabilized by Brij 98 with or without the addition of NaCl in the water phase: $[BzMA]_0$:$[Dimer\text{-}Br]_0$:$[Ru\ Catalyst]_0$ /$[FeCp_2]_0$/[NaCl] = 100/1/0.05/0.5/1.6 or 0 with [surfactant]/[hexadecane] = 8.6/5.2 wt% vs BMA at 80 °C. Lines are shown to guide the eye. On the right are the GPC traces for the same polymerizations.

4.5.3 Surfactant Counter-ion Effects on Polymerization

To further study the effect of the surfactant counter ion on ruthenium Mt-LRP in miniemulsion cocatalyzed by $FeCp_2$, I tested two different alkyl halide initiators with either chlorine (ECPA) or bromine (MMA_2-Br) as seen in Figure 10, with the cationic surfactants having either a chlorine (CTAC) or bromine (CTAB) counter ion. Since $FeCp_2$ co-catalyzed ruthenium Mt-LRP in solution demonstrated that the $FeCp_2$ reduction of the Ru(III) species would produce an ionic form of the halide (Scheme 2), and that excess halide was required for a living polymerization, I thought that there would be noticeable difference in the rates and end group functionality based on the surfactant counter-ion. To stabilize the miniemulsion, I chose the cationic surfactant cetyltrimethylammonium bromine (CTAB, Figure 10) in a polymerization initiated by ECPA, an

alkyl chloride initiator. This surfactant has previously been shown to effectively stabilize a miniemulsion at low surfactant loading levels[22] and in $FeCp_2$ co-catalyzed polymerizations can provide a source of Br^- ions which could displace the chlorine species on the $Fe(III)Cp_2^+Cl^-$ at the surface of the droplets and polymer particles, thereby acting as both a stabilizing agent for the miniemulsion, and a halide source for the ferrocene catalytic cycle. To test this hypothesis I compared the effects of changing the surfactant from CTAB to the analogous chlorine surfactant, cetyl trimethylammonium chloride (CTAC, Figure 10), to act as the stabilizer and halogen source in the $FeCp_2$ cocatalyzed polymerizations. This hypothesis was tested for the polymerization of benzyl methacrylate (BzMA) catalyzed with $RuCp^*ClPPEG_{45}$.

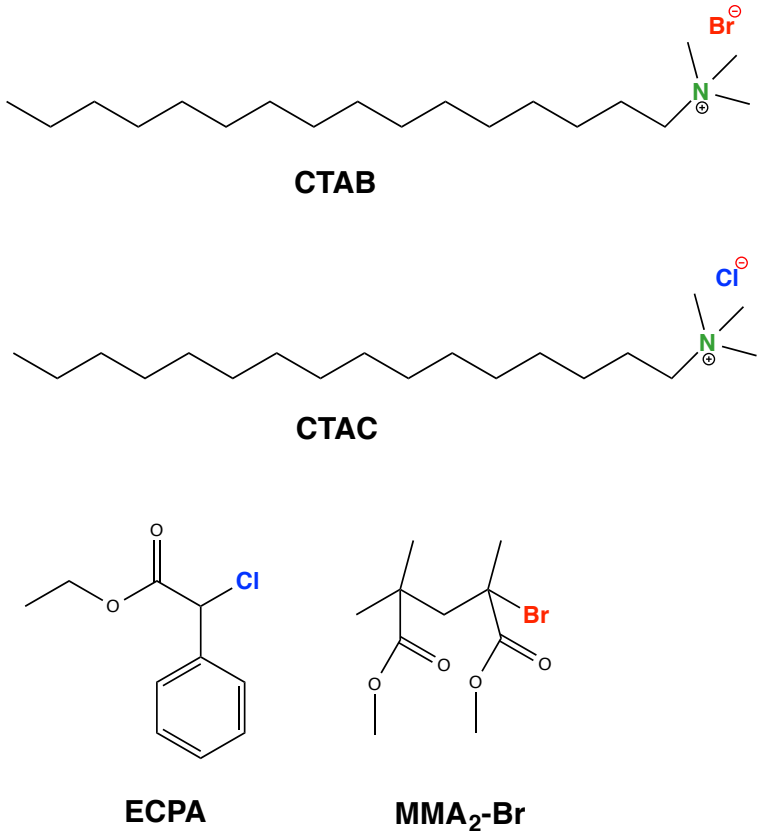

Figure 10. The molecular structures of the surfactants and initiators used in these polymerizations

In similar conditions as the BMA polymerizations, with respect to catalyst concentration (initiator:catalyst = 20:1), targeted degree of polymerization (DP = 100), surfactant concentration (80 mM on the organic basis) and volume of organic phase these polymerizations were run using either CTAB or CTAC. In Figure 11, it can be seen that using the bromine containing surfactant CTAB, a much faster polymerization occurred. In Figure 11, the conversion can be seen reaching over 95% in approximately 3 hours with a linear normalized conversion plot. With CTAC, a linear normalized conversion plot was also seen over 3 hours up to a conversion of approximately 80% conversion. The molecular weight evolution (Figure 12) for both CTAB and CTAC show that M_n increases linearly with conversion and follows the theoretical plot closely indicating that initiator efficiency is very high for the BzMA polymerizations with this catalyst. Interestingly the MWD was narrower for the polymerizations with CTAC compared to CTAB, with values of 1.2 vs 1.4 respectively. In the polymerization using CTAC, the slower rate and lower M_w/M_n could be due to the stronger C-Cl bond formed with the excess of chlorine present from the surfactant, compared to the excess bromide present when using CTAB, while the faster polymerization is likely due to the weaker C-Br bond that may formed by using CTAB. The C-Cl bond is stronger and therefore would be activated more slowly possibly leading to less bimolecular termination and a slower polymerization. The GPC traces (Figure 12) of the polymerizations using either surfactant show a clean shift to higher molecular weights, indicating that for either CTAB or CTAC the polymerization was living to high conversions and showing clear improvement compared to $FeCp_2$-free polymerizations.

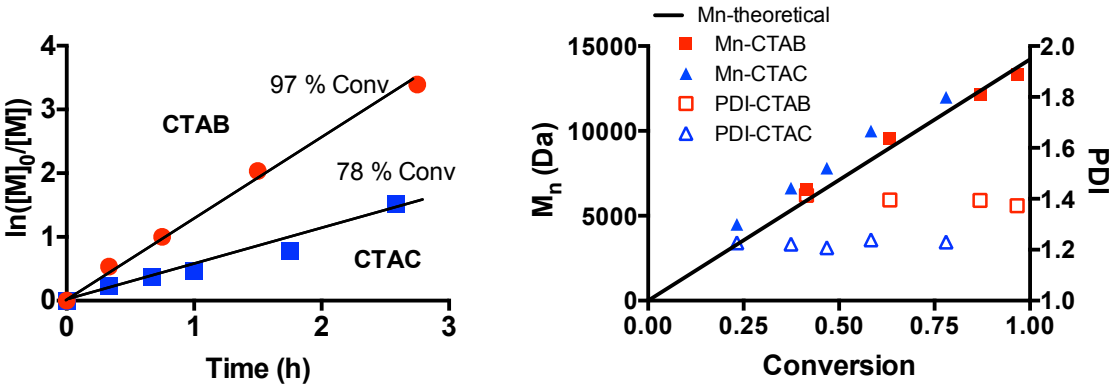

Figure 11. Conversion data for the miniemulsion polymerizations of BzMA catalyzed by RuCp*Cl(PPEG$_{45}$) with FeCp$_2$ stabilized by either CTAB or CTAC: [BzMA]$_0$:[ECPA]$_0$:[Ru Catalyst]$_0$ /[FeCp$_2$]$_0$/[surfactant] = 100/1/0.05/0.5/1.6 or 0 with [surfactant]/[hexadecane] = 4.3/5.2 wt% vs BMA at 80 °C. Lines are shown to guide the eye. On the right is the GPC data for the same polymerizations.

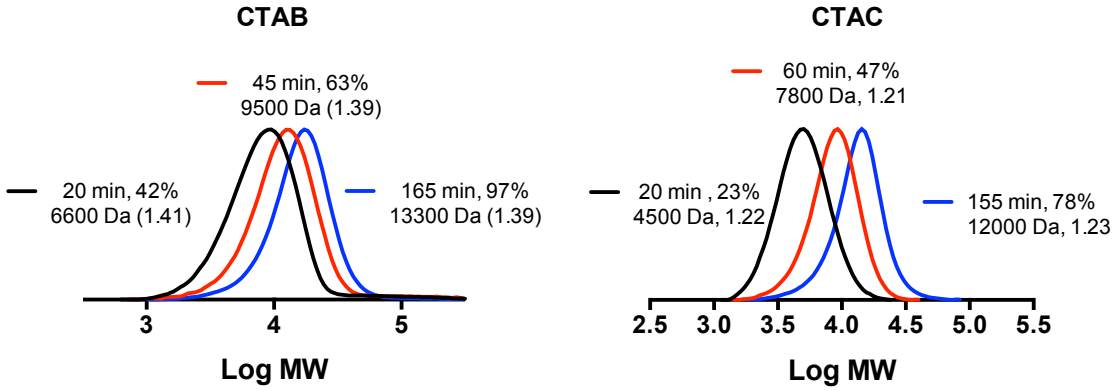

Figure 12. Molecular weight distributions for the miniemulsion polymerizations of BzMA catalyzed by RuCp*Cl(PPEG$_{45}$) with FeCp$_2$ stabilized by either CTAB or CTAC: [BzMA]$_0$:[ECPA]$_0$:[Ru Catalyst]$_0$ /[FeCp$_2$]$_0$/[surfactant] = 100/1/0.05/0.5/1.6 or 0 with [surfactant]/[hexadecane] = 4.3/5.2 wt% vs BMA at 80 °C.

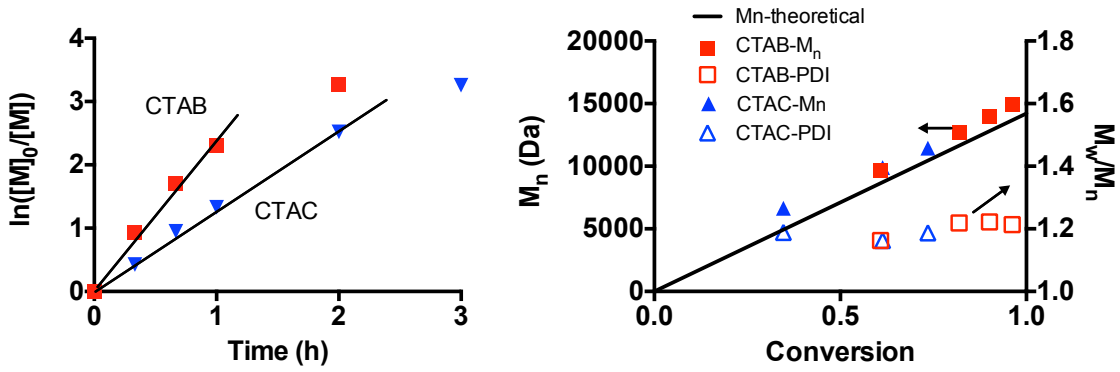

Figure 13. Conversion data for the miniemulsion polymerizations of BzMA catalyzed by RuCp*Cl(PPEG$_{45}$) with FeCp$_2$ stabilized by either CTAB or CTAC: [BzMA]$_0$:[Dimer-Br]$_0$:[Ru Catalyst]$_0$ /[FeCp$_2$]$_0$/[surfactant] = 100/1/0.05/0.5/1.6 or 0 with [surfactant]/[hexadecane] = 4.3/5.2 wt% vs BMA at 80 °C. Lines are shown to guide the eye. On the right is the GPC data for the same polymerizations.

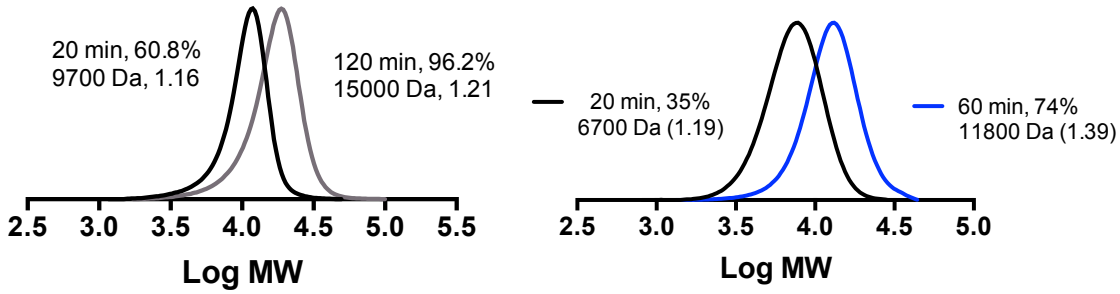

Figure 14. Molecular weight distributions for the miniemulsion polymerizations of BzMA catalyzed by RuCp*Cl(PPEG$_{45}$) with FeCp$_2$ stabilized by either CTAB or CTAC: [BzMA]$_0$:[Dimer-Br]$_0$:[Ru Catalyst]$_0$ /[FeCp$_2$]$_0$/[surfactant] = 100/1/0.05/0.5/1.6 or 0 with [surfactant]/[hexadecane] = 4.3/5.2 wt% vs BMA at 80 °C.

To further study the effect of the surfactant counter-ion on the polymerization, a bromine end capped initiator was used in the presence of CTAB or CTAC surfactants. In these runs a bromine end-capped MMA dimer[18] (MMA$_2$-Br) was used to initiate the polymerization of BzMA in the presence of RuCp*ClPPEG$_{45}$ and FeCp$_2$. The polymerization using an all bromine system (bromine initiator and surfactant) showed extremely fast rates of reactions reaching over 98%

conversion in 2 hours (Figure 13). The GPC evolution showed a linear increase of M_n vs conversion with low M_w/M_n values throughout the polymerization. In the CTAC stabilized polymerization initiated by MMA_2-Br, the polymerization reached high conversion (96% in 3 h). Similar to the ECPA initiated polymerizations, the miniemulsions stabilized with CTAC were slower than CTAB stabilized miniemulsions with slightly narrower molecular weight distributions (Figure 14) as seen in the molecular weight evolution plot. Interestingly the MMA_2-Br initiated polymerizations had lower dispersities than the chlorine initiated polymerizations, possibly due to faster activation during the initial steps of initiation.

To definitively observe the effects of the addition of chlorine surfactant in slowing the polymerization, MALDI mass spectrometry was performed on both miniemulsion polymerization samples stabilized by CTAC with either the bromine containing initiator (dimer-Br) or the chlorine containing initiator (ECPA). In both cases, the slower polymerization rate, likely from an excess of Cl^- present from the surfactant could be attributed to the stronger C-Cl bond formed from the excess of chlorine present from the CTAC surfactant compared to the CTAB stabilized polymerizations. In both of these polymerizations, exclusively chlorine end-capped polymers were observed when using either an alkyl bromide initiator or an alkyl chloride initiator (Figure 15). The upper MALDI spectrum shows complete conversion from an alkyl bromide initiator to a chlorine end capped polymer, while the lower spectrum shows in an all chlorine case a very clean spectrum can be seen with exclusively chlorine end-capped polymers as well, which agrees with previous studies that have shown a strong preference for chlorine end capped polymers in a mixed system.[23,24]

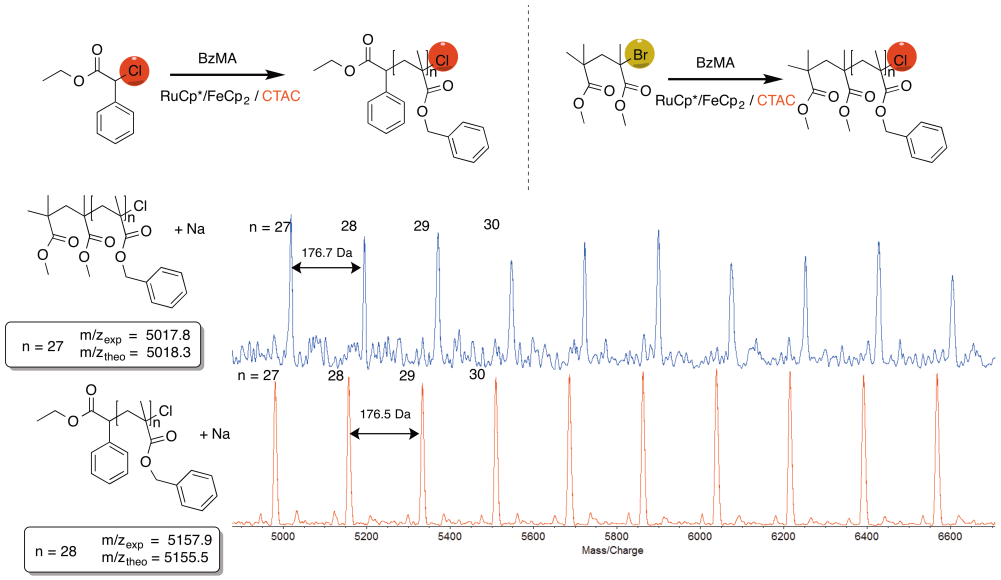

Figure 15. MALDI-TOF of polymer samples synthesized by miniemulsion stabilized by chloride surfactant CTAC initiated by brominated alkyl halide initiator MMA_2-Br (top) and chlorine alkyl halide initiator ECPA (bottom) showing fully chlorinated end groups at the low end of the molecular weight distribution.

4.6 Conclusions

In this study I have shown the effectiveness of $FeCp_2$ as cocatalyst for LRP in miniemulsion catalyzed by thermoresponsive RuCp*ClPPEG catalysts provided there is excess halogen present to prevent loss of the halogen to the water phase. Significant rate enhancement and final conversion improvements are seen in polymerizations with $FeCp_2$ present compared to those polymerizations without $FeCp_2$. The halogen on the cationic surfactants plays an important role in these miniemulsion polymerizations, with chlorine surfactants producing solely chlorine end capped polymers as shown by MALDI-TOF analysis.

4.7 References

(1) Kato, M.; Kamigaito, M.; Sawamoto, M.; Higashimura, T. *Macromolecules* **1995**, *28*, 1721–1723.

(2) Wang, J.-S.; Matyjaszewski, K. *J. Am. Chem. Soc.* **1995**, *117*, 5614–5615.

(3) Ouchi, M.; Terashima, T.; Sawamoto, M. *Chem. Rev.* **2009**, *109*, 4963–5050.

(4) Wang, X.-S.; Armes, S. P. *Macromolecules* **2000**, *33*, 6640–6647.

(5) Cunningham, M. F. *Prog. Polym. Sci.* **2008**, *33*, 365–398.

(6) Monteiro, M. J.; Cunningham, M. F. *Macromolecules* **2012**, *45*, 4939–4957.

(7) Zetterlund, P. B.; Kagawa, Y.; Okubo, M. *Chem. Rev.* **2008**, *108*, 3747–3794.

(8) Schork, F. J.; Luo, Y.; Smulders, W.; Russum, J.; Butté, A.; Fontenot, K. In *Polymer Particles SE - 2*; Okubo, M., Ed.; Advances in Polymer Science; Springer Berlin Heidelberg, 2005; Vol. 175, pp. 129–255.

(9) Li, M.; Matyjaszewski, K. *Macromolecules* **2003**, *36*, 6028–6035.

(10) Bultz, E.; Ouchi, M.; Nishizawa, K.; Cunningham, M. F.; Sawamoto, M. *ACS Macro Lett.* **2015**, 628–631.

(11) Jakubowski, W.; Matyjaszewski, K. *Angew. Chem. Int. Ed. Engl.* **2006**, *45*, 4482–4486.

(12) Fujimura, K.; Ouchi, M.; Sawamoto, M. *ACS Macro Lett.* **2012**, *1*, 321–323.

(13) Nishizawa, K.; Ouchi, M.; Sawamoto, M. *Macromolecules* **2013**, *46*, 3342–3349.

(14) Fujimura, K.; Ouchi, M.; Sawamoto, M. *Macromolecules* **2015**, 150616140133001.

(15) Fuji, Y.; Ando, T.; Kamigaito, M.; Sawamoto, M. *Macromolecules* **2002**, *35*, 2949–2954.

(16) He, W.; Zhang, L.; Miao, J.; Cheng, Z.; Zhu, X. *Macromol. Rapid Commun.* **2012**, *33*, 1067–1073.

(17) Simakova, A.; Mackenzie, M.; Averick, S. E.; Park, S.; Matyjaszewski, K. *Angew. Chem. Int. Ed. Engl.* **2013**, *52*, 12148–12151.

(18) Ando, T.; Kamigaito, M.; Sawamoto, M. *Tetrahedron* **1997**, *53*, 15445–15457.

(19) Wu, Y.; Wan, G.; Xu, J.; Cheng, S.; Fang, P. *Adv. Polym. Technol.* **2013**, *32*, n/a–n/a.

(20) Cao, J.; Zhang, L.; Jiang, X.; Tian, C.; Zhao, X.; Ke, Q.; Pan, X.; Cheng, Z.; Zhu, X. *Macromol. Rapid Commun.* **2013**, *34*, 1747–1754.

(21) Teo, V. L.; Davis, B. J.; Tsarevsky, N. V; Zetterlund, P. B. *Macromolecules* **2014**, *47*, 6230–6237.

(22) Simms, R. W.; Cunningham, M. F. *J. Polym. Sci. Part A Polym. Chem.* **2006**, *44*, 1628–1634.

(23) Ando, T.; Kamigaito, M.; Sawamoto, M. *Macromolecules* **2000**, *33*, 2819–2824.

(24) Peng, C.; Kong, J.; Seeliger, F.; Matyjaszewski, K. *Macromolecules* **2011**, *44*, 7546–7557.

Chapter 5

‘Smart’ catalysis with thermoresponsive ruthenium catalysts for miniemulsion living radical polymerization cocatalyzed by smart iron cocatalysts

5.1 Preface

The previous chapter dealt with improving the polymerization through adding a ferrocene cocatalyst, which improved the rates and the conversions that could be reached, and the counter-ion effect was explored in further detail. Because the polymerizations contained the organic soluble ferrocene, there was still significant residual iron in the final products. Therefore two amine catalysts and three ferrocene derivatives were investigated to obtain the benefits of cocatalyzed reaction rates and final products that had significant reductions in the residual metal concentration. In this chapter the effect of monomer hydrophobicity with respect to the thermoresponsive catalyst was explored to elucidate more information about catalyst partitioning between the water phase and the droplets/particles. Parts of this chapter are being prepared for submission as a manuscript

5.2 Abstract

In this work I report the use of cocatalysts in addition to ‘smart’ ruthenium catalysts for Ru-mediated living radical polymerization in miniemulsion, allowing for the synthesis of final products with significantly reduced residual metal. Using amine cocatalysts in miniemulsion allowed for the high conversions (> 90%) in under 10 hours. Two forms of ferrocene cocatalysts were also used, including ‘smart’ thermoresponsive PEGylated ferrocene derivatives (FcPEG)

and ferrocene containing surfactants (FcTMA). Using 'smart' thermoresponsive cocatalyst in low concentrations, rate enhancements in BMA and BzMA polymerizations were seen, with good catalyst removability. Using the FcTMA cocatalyst surfactant, increasing monomer hydrophobicity was clearly shown to increase the polymerization rate and initiator efficiency.

5.3 Introduction

Metal catalyzed living radical polymerization (Mt-LRP)[1] or atom radical transfer polymerization (ATRP)[2] is an effective technique capable of synthesizing advanced macromolecular architectures such as block copolymers, and graft copolymers. [3,4] Applying this chemistry to aqueous dispersions[5–8] such as emulsion, miniemulsion or microemulsion has been explored but there are very few reports of residual metal in the polymer products or methods for effective catalyst removal.

Catalyst removal is expected to be difficult as catalysts are generally designed to be extremely hydrophobic to keep them inside the droplets.[9,10] One method has been to reduce the overall catalyst concentration by using very active catalysts in miniemulsion.[10] The use of a microemulsion has been used to produce seed particles, which effectively trapped the catalyst and allowed for decreased surfactant and catalyst loading in the final product.[11]

Another route was to use amphiphilic[12,13] surfactant ligands in small amounts in conjunction with a hydrophobic complex residing in the oil phase. This work used an emulsion polymerization process, not requiring any sonication, with the surfactant ligand capturing copper in the water phase to prevent catalyst leakage. This allowed for lower catalyst and surfactant loading, although the work did not focus on catalyst removal.

Previously, I developed a thermoresponsive PEG phosphine ligand (DP =113, $PPEG_{113}$) that complexes to ruthenium to form a 'smart' shuttling complex ($RuCp^*ClPPEG_{113}$) which can effectively mediate an LRP of BMA in miniemulsion and easily then be removed to less than 10 ppm of residual Ru by precipitation into methanol,[14] but complete conversions (~80 %) could not be achieved and reaction times were relatively long (>15 h). Further improvements were seen using a $RuCp^*ClPPEG_{45}$ catalyst to mediate a benzyl methacrylate miniemulsion polymerization with ferrocene cocatalysts. These ligands were of significantly higher MW than in the work by Zhu et al.[12] The use of co-catalysts in Ru-LRP has often been required to allow polymerizations to occur at reasonable rates to high conversions, often employing aluminum compounds[1,15,16], amines,[17] or more recently ferrocene.[18] In miniemulsion, adding ferrocene to the oil phase allowed for significant improvements in the polymerizations, which included almost complete conversions and much shorter reaction times (conversion > 90%, reaction time < 8 h, Chapter 4). Very few iron catalysts for LRP have shown any stability in aqueous/aqueous dispersed media so it is important to improve emulsion LRP with the use of nontoxic and less expensive metals such as iron. Also, the significant improvements in conversion are important for reducing downstream processing costs for monomer removal.

$FeCp_2$ acts as a reducing agent for the Ru(III) species forming the activator Ru (II) by a halogen abstraction by the $Fe(II)Cp_2$ to form an unstable ferrocenium salt complex, $Fe(III)Cp_2^+Cl^-$ as seen in Scheme 4. This complex quickly degrades through a redox process forming $Fe(II)Cp_2$ with the halogen capping an active radical, increasing the rate of deactivation in $FeCp_2$ co-catalyzed polymerizations.

Unfortunately in miniemulsion, $FeCp_2$ gets trapped in polymer particles due to its hydrophobicity (water solubility = 4.25 x 10^{-5} mol/L).[19] This poses a problem for improving the catalysis of the main ruthenium catalysts while also allowing for easy removal of the co-catalysts for metal-free final products.

Herein I present a method for the synthesizing polymers through RuCp*ClPPEG mediated miniemulsion polymerizations with the added benefit of improved polymerizations with cocatalysts and low residual metal concentrations in the final products. Firstly I studied the use of two different amine cocatalysts, 2-dimethylaminoethanol (**1**) and tributylamine (**2**) (Scheme 4), which have been previously used in solution polymerization with ruthenium catalysts. Secondly I used $FeCp_2$ derivatives (Scheme 4) attached to either a thermoresponsive PEG chain or a surfactant molecule. The mechanism for the removable $FeCp_2$ derivatives is shown in Scheme 5. For PEGylated $FeCp_2$ derivatives, FcPEG (**3**, M_n = 2000 Da; **4**, M_n = 5000 Da) the FcPEG and the RuCp*ClPPEG catalysts likely reside in the water phase, upon heating to reaction temperature they can both enter the monomer droplets to catalyze the polymerization based on the ferrocene cocatalysis mechanism. Finally at the end of the polymerization the reaction mixture can be cooled and the polymer washed or precipitated in methanol allowing for efficient removal of the metal residue from the final product. A $FeCp_2$ surfactant derivative was also used (FcTMA, **5**) which would reside on the surface of the particle allowing cocatalysis to occur near the monomer-droplet interface. The washing or precipitation step with this cocatalyst should be easier than with $FeCp_2$ as the FcTMA is expected to reside at the surface of the droplets/particles. The mechanism is shown in Scheme 4.

Scheme 4. Miniemulsion polymerization catalyzed by smart thermoresponsive catalysts and removable cocatalysts allowing for almost metal free final poducts.

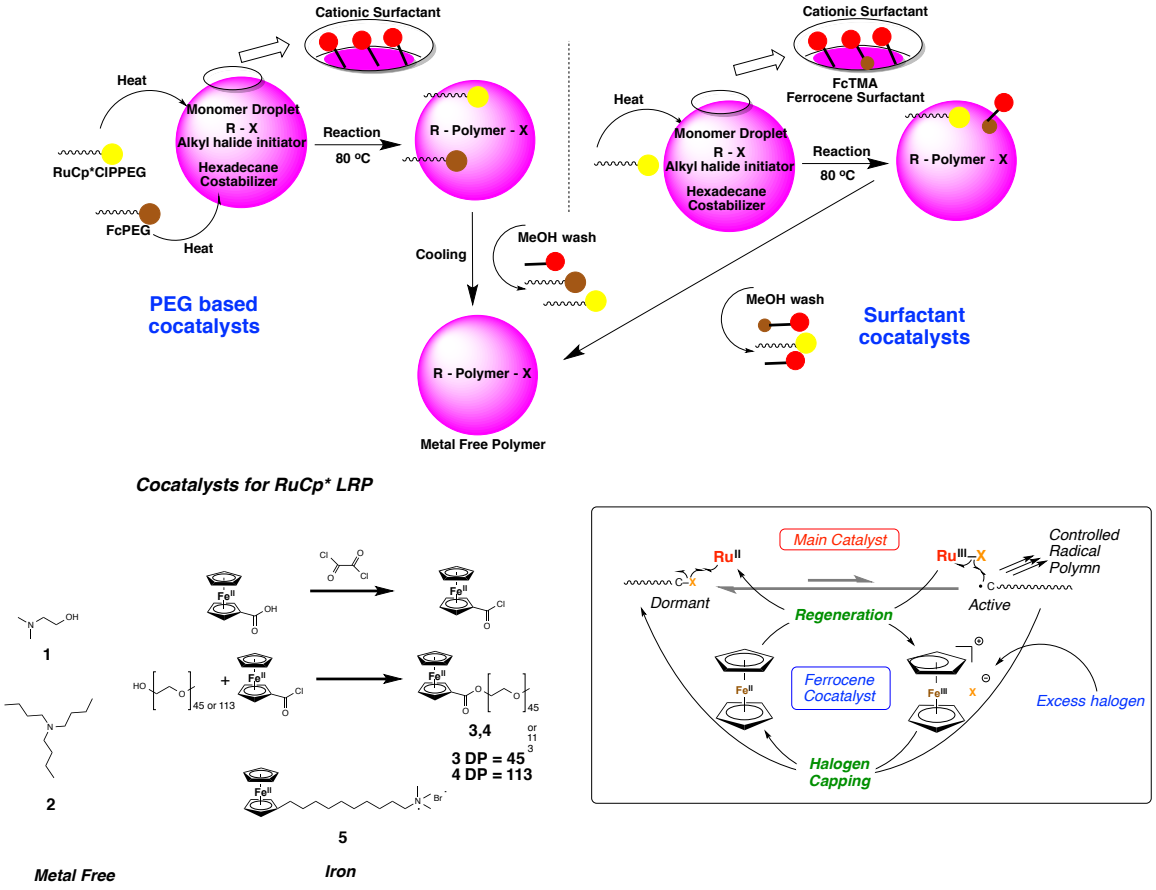

5.4 Experimental

5.4.1 Materials

Butyl methacrylate and benzyl methacrylate (BMA and BzMA, Tokyo Kasei; purity > 99%) were dried overnight over calcium chloride and purified by double distillation under reduced pressure over calcium hydride before use. Potassium carbonate (K_2CO_3, Wako, purity > 99.5%) was degassed by vacuum–argon purge cycles before use. Hexadecyltrimethylammonium bromide (CTAB, Sigma-Aldrich; BioXtra purity ≥99%,), hexadecyltrimethylammonium chloride (CTAC,

Sigma-Aldrich; BioXtra purity ≥99%), ferrocene monocarboxylic acid (ferrocene carboxylic acid, MP Biomedicals), oxalyl chloride (Sigma Aldrich; Reagentplus purity ≥99%), 11-Ferrocenyltrimethylundecylammonium bromide (Ferrocnyl TMA, Dojindo Laboratories, purity >95%), poly(ethylene glycol) methyl ether (average M_n 2000 Da, PEG_{45}, and average M_n 5000 Da, PEG_{113}, Sigma-Aldrich)and hexadecane (Sigma Aldrich, purity >99%,) were used without any purification. Ethyl-2-chloro-2-phenylacetate (ECPA, Aldrich; purity >97%) was distilled under reduced pressure before use. (4-hydroxyphenyl) diphenylphosphine (Sigma-Aldrich; purity > 98%)**,** poly(ethylene glycol) methyl ether tosylate (PEG-tosylate, Sigma-Aldrich; average M_n 5000 Da or M_n 2000 Da) and $[RuCp^*Cl]_4$ [chloro(pentamethylcyclopentadienyl) ruthenium(II) tetramer, Aldrich] were used as received, and were handled in a glove box under a moisture- and oxygen-free argon atmosphere (H_2O < 1 ppm, O_2 < 1 ppm). 1,2,3,4-tetrahydro-naphthalene (tetralin, Kisida Chemical; purity > 98%), internal standards in NMR conversion analysis was dried over calcium chloride overnight and distilled twice over calcium hydride. Triethylamine (Et_3N, TCI; purity >98%), Tributylamine (n-Bu_3N, TCI; purity >98%), and 2-dimethylaminoethanol (DMAE, Sigma-Aldrich; purity >99.5%) were purged with argon before use. Water (Wako Chemicals; distilled) was bubbled with dry nitrogen for 30 mins before use.

5.4.2 Synthesis of PPEG45 and PPEG113

As described previously.[14] The PEG_{113}-phosphine ligand used for the temperature sensitive catalyst RuClCp*(PPEG) used in the solution and miniemulsion polymerizations was synthesized as follows: 0.200 g (0.719 mmol) (4-hydroxyphenyl)diphenylphosphine, 3.269 g (0.68 mmol) of poly(ethylene glycol) methyl ether tosylate (average M_n 5,000 Da), and 0.136 g (0.965 mmol) of potassium carbonate were added to 10 mL of DMF and reacted at 80°C for 72 h. The solution was very viscous, and was therefore diluted with methanol prior to being precipitated by cooling and the addition of ether. The polymer was solubilized in chloroform to filter off the salt and was

precipitated by cooling and the addition of ether and hexane. The same molar rations were used for the synthesis of $PPEG_{45}$ but used poly(ethylene glycol) methyl ether tosylate (average M_n 2,000 Da).

5.4.3 Synthesis of FcPEG2000 (3)

Oxyalyl chloride (2.0 mL, 23 mmol) was added to a suspension of ferrocene monocarboxylic acid (1.00 g, 4.35 mmol) suspended in 20 mL of CH_2Cl_2 and was allowed to stir at room temperature for 2.5 hours at which point the reaction solution was evaporated under reduced pressure and immediately dissolved in CH_2Cl_2. This solution was added drop-wise to a solution of poly(ethelyene glycol) methyl ether M_n 2000 Da (6.0 g, 3.0 mmol) and triethylamine (1.1 mL, 8 mmol) in CH_2Cl_2 at 0 °C and then stirred overnight at room temperature to yield the crude FcPEG2000, **3**. This solution was dried under reduced pressure and then washed with water extracted with CH_2Cl_2 and then the organic layer was dried with Mg_2SO_4 and evaporated to a small volume of liquid. The final product was obtained by 3 successive reprecipitations of crude product in 0 °C diethylether. Finally the product was dried in vacuum at room temperature over night to afford the final product **3**.

5.4.4 Synthesis of FcPEG5000 (4)

Synthesis of **4** used the same procedure as for the synthesis **3** but with poly(ethelyene glycol) methyl ether M_n 5000 Da.

5.4.5 Miniemulsion polymerization

The RuCp*Cl(PPEG5000) catalyst was synthesized by the addition of 1.0 mg (0.0009 mmol) of RuClCp* tetramer with 38.1 mg (0.007 mmol) of the PEG-phosphine catalyst (M_n 5000 Da) in 1.25 ml of toluene and heated at 80°C for 1 h to form the active catalyst. The toluene was removed under vacuum after this aging process and refilled with Ar. Under an inert atmosphere 7.5 mL of deionized water containing 0.0435 g (0.12 mmol) of CTAB was added 1.2 mL (7.1 mmol) of BMA, 0.1 mL of tetraline (internal standard for monomer conversion by ^{1}H NMR), 0.072 mL of hexadecane (HD), 38.1 mg (0.007 mmol) of FcPEG, **4**, and 0.014 mg (0.078 mmol, 500 mM in toluene) of the initiator ECPA were mixed and then added to the water phase containing surfactant and catalyst at 0°C and was stirred vigorously. Under stirring at 0°C the mixture was ultrasonicated for 3 mins at 50% output and 50% duty while under a flowing argon blanket. The polymerization took place in either sealed glass tubes or in an air free Schlenk flask. Aliquots were periodically taken and measured by GC conversion and GPC for molecular weight data. DLS measurements were taken for particle size analysis.

5.4.6 Characterization

The molecular weight distributions of the polymers were measured by gel permeation chromatography (GPC) with THF as an eluent on three polystyrene gel columns (Shodex KF-803; pore size, 20-1000 A; 8.0 mm i.d. × 30 cm; flow rate, 1.0 mL min) connected to a DU-H2000 pump, a 74S-RI refractive index detector, and a 41-UV ultraviolet detector (all from Shodex). The columns were calibrated against 13 standard poly(MMA) samples (Polymer Laboratories; M_n = 500–3840000 Da; M_w/M_n = 1.06–1.22) as well as the monomer. ^{1}H NMR spectra were recorded in $CDCl_3$ or CD_2Cl_2 or DMSO-d6 at 25 °C on a JEOL JNM-LA500 spectrometer operating at 500.16 MHz.

5.5 Results and Discussion

5.5.1 Amine Cocatalysts

To improve the catalysis of RuCp*Cl(PPEG) in miniemulsion, while still having easily produced metal-free polymers, I used amine cocatalysts. It is known that water acts as an activator for Ru catalyzed LRP.[20] Polymerizations in suspension have shown rate enhancements compared to solution polymerizations and often don't require any cocatalysts when water is used. With RuCp*Cl(PPEG) in miniemulsion the polymerization slowed after 15 h and nearly 80% conversion, which is significantly faster than polymerizations in solution or bulk with similar catalysts,[21] though it may have not reached completion due to an accumulation of deactivator or because of partitioning of the catalyst to the water phase.

I assessed the differences between two amine co-catalysts of varying hydrophilicity in the LRP of BMA mediated by RuCp*Cl($PPEG_{113}$) and initiated by ECPA in miniemulsion. As seen in Scheme 4, 2-dimethylaminoethanol (**1**) was chosen as it would likely orient at the surface of the droplets because of the more hydrophilic hydroxyl group, while tributylamine (**2)** is more hydrophobic and would more preferentially reside in the droplets.

The polymerizations were run with the same catalyst concentrations (1 catalyst per 20 chains) and targeted degree of polymerizations (DP = 100). In both polymerizations, conversions reached approximately 80% (**1**, 78%, 6.75 h; **2**, 84%, 6.75 h) conversion in under 7 h, though higher conversions could be reached. Using cocatalyst **1,** the polymerization was able to reach high conversions (98%) after 36 h indicating that high conversions are possible using these co-catalysts. The more hydrophobic co-catalyst, **2**, reached 95% conversion in approximately 20 h. There is no discernable difference between the rates using either co-catalyst indicating that at these concentrations, partitioning of the cocatalyst to the water phase is not a major factor, but it

does show that the rates are improved with respect to the cocatalyst-free polymerizations as it may act as a reducing agent.[22]

Comparing the molecular weight evolution in Figure 16 for these polymerizations, we can see that with both co-catalysts the polymerizations show evidence of livingness. The M_n values increased linearly with respect to conversion for both following a very similar curve. In both these polymerizations the M_w/M_n values were relatively high, at approximately 1.5, and they increase as conversion increases. The measured M_n values were also similarly above the theoretical expected values for this polymerization. This may be due to the catalyst solubility in the monomer droplet at the reaction temperature causing incomplete initiator efficiency. This aspect is looked into greater detail in a below with the FcTMA surfactant-cocatalyst.

The GPCs traces of each polymerization (Figure 17) also show that the molecular weight distribution shifts to higher molecular weights with increasing conversion. A small uncontrolled high molecular weight peak is seen using cocatalyst **1** though it is kept at approximately 1% of total polymer high conversions and likely occurs during the sonication stage as the halide initiator and the catalyst in the activator state are both present during the high energy sonication. This peak does not shift as conversion changes and decreases in relative amount compared to the living polymer, indicating that it is formed at the early stages of the polymerization, and possibly during sonication. Though the M_w/M_n values are fairly high (~1.5) for both polymerizations, the livingness is clearly seen in the GPC traces (Figure 17 – A and B) of the washed samples shifting to higher molecular weights. With less than 10 ppm of residual Ru as measured by ICP-AES an improvement in the catalysis while still removing over 95% of the residual metal in the final polymer.

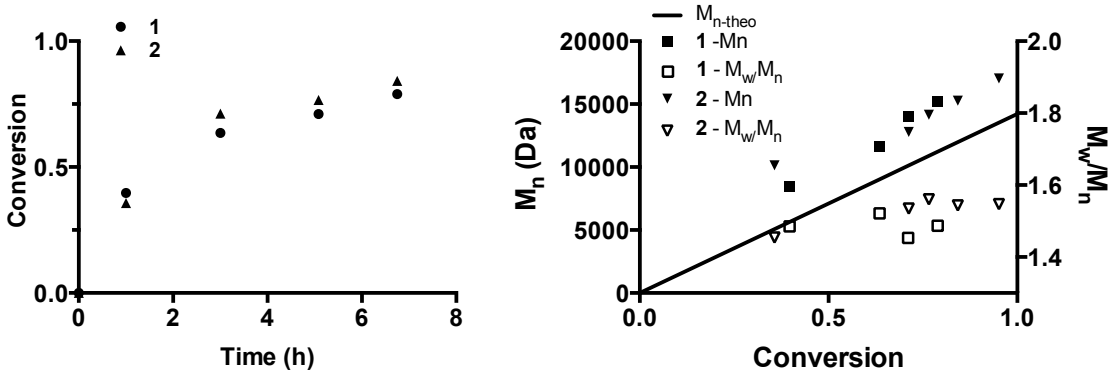

Figure 16. Conversion data for the miniemulsion polymerizations of BMA catalyzed by RuCp*Cl(PPEG$_{113}$) with amine cocatalyst 1 or 2 stabilized by either CTAB: [BMA]$_0$:[ECPA]$_0$:[Ru Catalyst]$_0$ /[amine]$_0$/[surfactant] = 100/1/0.05/0. 5/1.6 with [surfactant]/[hexadecane] = 4.3/5.2 wt% vs BMA at 80 °C. On the right is the GPC data for the same polymerizations.

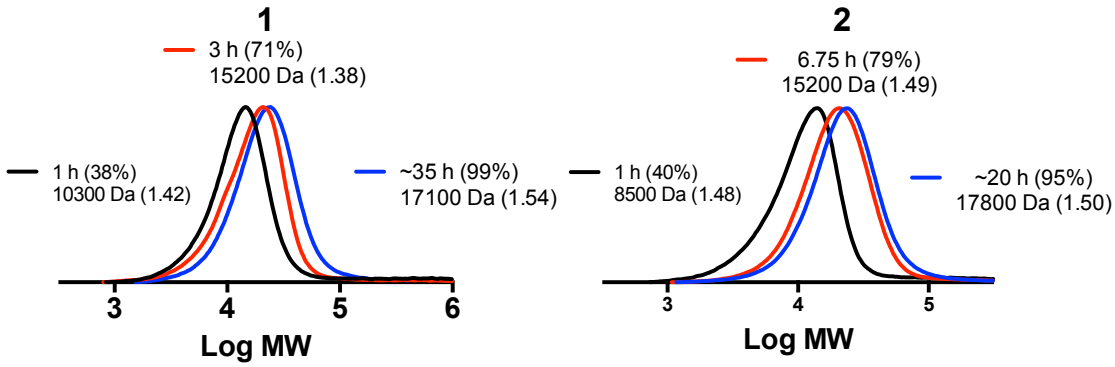

Figure 17. GPC traces for the BMA polymerizations in Figure 16 cocatalyzed with amine coactalyst 1 or 2.

5.5.2 FcPEG co-catalysts

Ferrocene has been shown to give significant improvements though it is difficult to remove from the final product as shown from our previous study in miniemulsion. We investigated a solution

by using PEGylated $FeCp_2$ derivatives as removable cocatalysts as seen in Scheme 4. These cocatalysts were synthesized, first by using ferrocene monocarboxylic acid and oxalyl chloride to form an acid chloride, which was then mixed with monomethylated PEG to form the FcPEG of either approximately 2000 Da (DP = 45, **3**) or of 5000 Da (DP = 113, **4**). Previously, using NOE NMR we demonstrated on the nanoscale that PPEG could effectively be shuttled into or out of the droplet and out by simply raising or lowering the temperature.[14] It is likely that simply changing the end group on such a large polymer will only have minor effects on the shuttling ability. We tested for a cloud point of both the $PPEG_{113}$ and RuCp*Cl$PPEG_{113}$ but it was not detected up to 95 °C. FePEG-**4**, also did not exhibit a cloud below 95 °C indicating that a cloud point was not reached, at reaction temperatures. From previous NOE NMR results, we could see the PPEG ligand in contact with the BMA monomer at 80 °C, which could be aided by the high surface area of a miniemulsion. This shows that there is still partitioning into the droplets/particles allowing the polymerization to proceed and could indicate that the catalyst resides closer to the surface rather than buried in the center of the droplet. However experimentally determining the exact location would be difficult. It is expected that the FePEG cocatalysts could be easily removed in the same manner the RuCp*Cl(PPEG) catalyst as shown below.

Using both FcPEG cocatalysts **3** and **4**, in a catalytic amounts (same molar ratio as the main catalyst: 1 cocatalyst eq per 20 chains), both BMA and BzMA were polymerized with RuCp*Cl$PPEG_{113}$ or RuCp*Cl$PPEG_{45}$ respectively. The shorter $PPEG_{45}$ ligand was used with BzMA as the longer PPEG ligand could not mediate the LRP of BzMA in miniemulsion. (Appendix B).

The polymerization of BMA mediated by RuCp*Cl$PPEG_{113}$ and cocatalyzed with equal equivalents of **3** or **4** both show rate enhancement over the non-cocatalyzed polymerizations, with

both FcPEGs reaching over 90% conversion in approximately 8 h (Figure 18) versus 80% conversion in 15 h. Both of these cocatalysts allowed for living polymerizations to proceed, with the M_n values increasing with conversion and the GPC traces showing shifts to higher molecular weights (Figure 19), although with relatively high M_w/M_n values (~1.5 – 1.6). With the FcPEG being employed, the final products could be washed with methanol producing colorless polymer with 5.2 ppm and 0.90 ppm of residual ruthenium and iron in the final product using cocatalyst **3,** respectively and 7.0 ppm of ruthenium and 0.92 ppm of iron using cocatalyst **4.** When $FeCp_2$ was used, the washed polymer contained more than 100 ppm in the final product measured by ICP-AES. This also shows that only catalytic amounts of iron cocatalysts are required for significant improvements in the polymerization of BMA in miniemulsion.

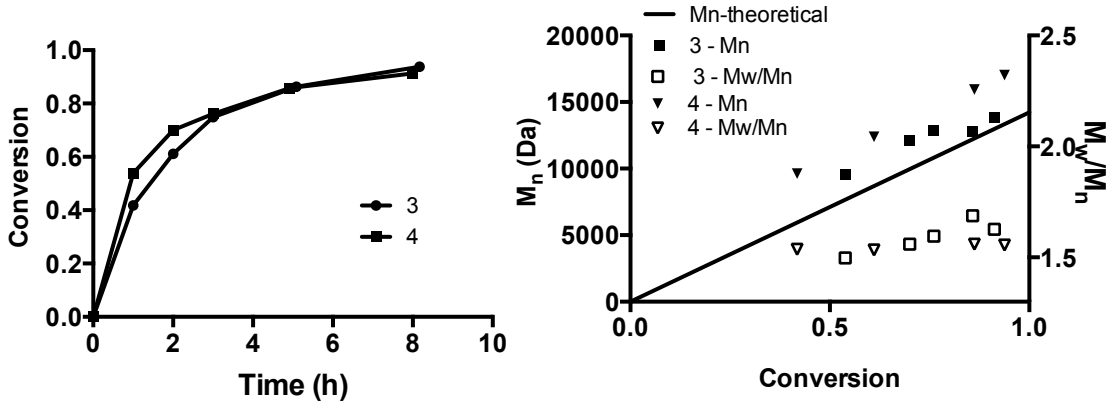

Figure 18. Conversion data for the miniemulsion polymerizations of BMA catalyzed by RuCp*Cl($PPEG_{113}$) with FcPEG cocatalyst 3 or 4 stabilized by CTAB: $[BMA]_0:[ECPA]_0:[Ru\ Catalyst]_0/[FcPEG]_0/[surfactant]$ = 100/1/0.05/0. 05/1.6 with [surfactant]/[hexadecane] = 4.3/5.2 wt% vs BMA at 80 °C. Lines are shown to guide the eye. On the right is the GPC data for the same polymerizations.

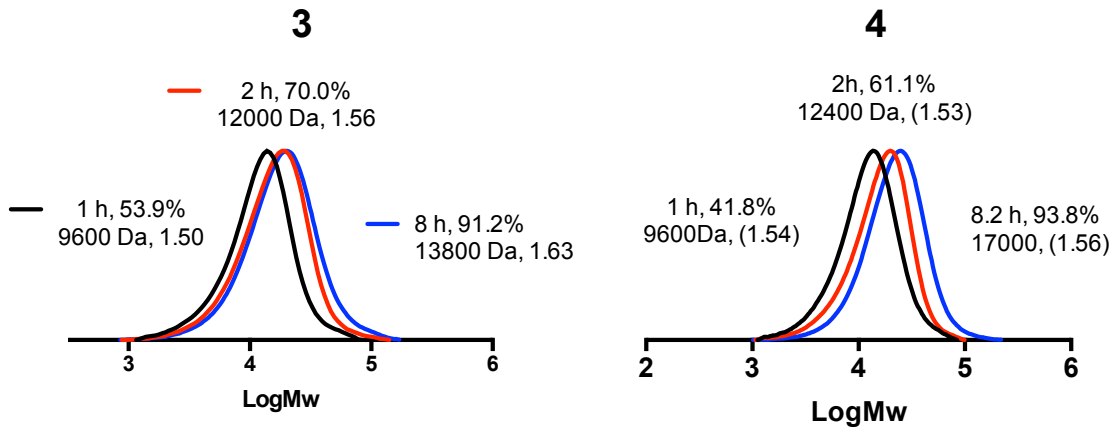

Figure 19 GPC traces for the BMA polymerizations in Figure 18 cocatalyzed with FcPEG cocatalyst 3 or 4.

The polymerization of BzMA mediated by RuCp*ClPPEG$_{45}$ and cocatalyzed by either **3** or **4** showed slightly faster rates than those of BMA with over 95 % conversion reached in 3 to 5 hours as seen in Figure 20. Using either of these catalysts with the ruthenium main catalyst yielded well controlled LRPs with rates comparable with the previous work using the same main catalyst and significantly higher $FeCp_2$ cocatalyst loading (RuCp* : $FeCp_2$ = 1/ 10 vs RuCp* : FePPEG = 1/1). In these polymerizations the dispersities were between 1.2 – 1.3, and the GPC traces (Figure 21) show a clean shift in the molecular weight distribution up to high conversions.

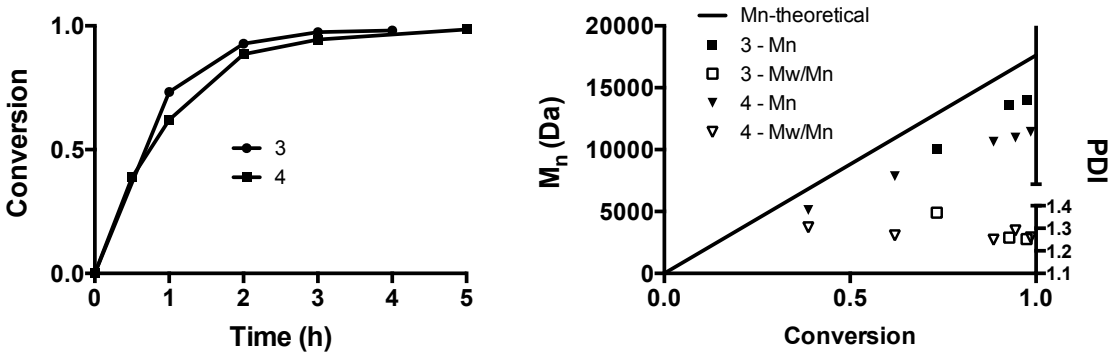

Figure 20 Conversion data for the miniemulsion polymerizations of BzMA catalyzed by RuCp*Cl(PPEG$_{45}$) with FcPEG cocatalyst 3 or 4 stabilized by CTAB: [BzMA]$_0$:[ECPA]$_0$:[Ru Catalyst]$_0$ /[FcPEG]$_0$/[surfactant] = 100/1/0.05/0. 05/1.6 with [surfactant]/[hexadecane] = 4.3/5.2 wt% vs BMA at 80 °C. Lines are shown to guide the eye. On the right is the GPC data for the same polymerizations.

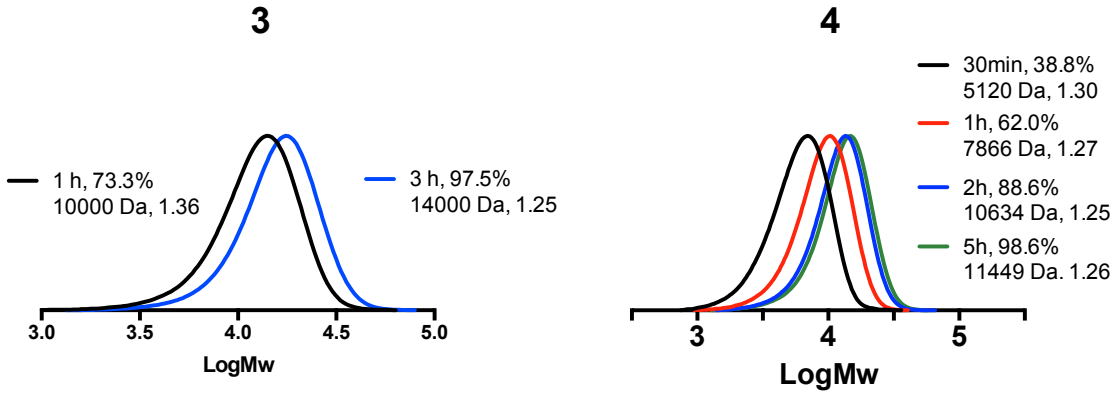

Figure 21 GPC traces for the BzMA polymerizations in Figure 20 cocatalyzed either amine coactalyst 3 or 4.

5.5.3 Ferrocene Surfactant

As the FcPEG displayed high activity even at catalytic amounts (equal amounts as the ruthenium catalyst, 1 equivalent to 20 chains), we decided on a $FeCp_2$ derivative surfactant (FcTMA, **5**) in conjunction with the surfactant CTAB to stabilize the polymerization and provide a function of a

cocatalyst at the surface of the particle and ideally allow for facile removal. We also used this opportunity to polymerize a number of monomers of varying hydrophobicity allowing us to better understand the effect of partitioning of the catalyst in these miniemulsions. A set of polymerizations were performed to determine the effect of the monomer hydrophobicity on the progression of polymerization, in terms of rate and molecular weight evolution, for a polymerization catalyzed by RuCp*Cl$PPEG_{45}$ and a target DP of 100. Results are shown in Figure 22.

Partitioning of the catalyst between the droplets/particles and the water phase is a well-known challenge in ATRP miniemulsion polymerization with copper catalysts. Very hydrophobic ligands are utilized to keep the catalyst in the droplets.[23] Even with these ligands it is known that the Cu(I) and Cu(II) species can still partition into the water phase at different amounts with the deactivator species, Cu(II), partitioning into the water to a greater extent than Cu(I). It is well known that in the early stages of the polymerization, the partitioning can have a large effect on increasing the polymerization rate and increasing bimolecular termination,[24] often requiring large catalyst loading to allow the polymerization to reach appreciable conversions. Different techniques have been used to solve this problem in miniemulsion and emulsion including using tetradentate ligands,[25] using seeded emulsions which traps catalyst in the microemulsion before more monomer is added,[11] or by using a PEG based surfactant ligand which is used to capture free metal salt to prevent it desorbing from the droplets and particles.[12]

Previously (Chapter 4) we have shown that the RuCp*Cl($PPEG_{113}$) can catalyze a living radical polymerization at 60 °C in the presence of $FeCp_2$ and even to small degree at 40 °C, indicating that even at lower temperatures significantly below the cloud point of the catalyst, some catalyst chains can reach the droplets to allow the polymerization to proceed. It is well known that PEG

and PEG derivatives go through a phase transition and as the temperature increases, the PEG chain becomes more hydrophobic. This increase in temperature likely changes the partition coefficient and the absolute concentration in the oil phase even though the cloud point has not been reached.

From the most hydrophilic to hydrophobic (MMA, BMA, BzMA and 2-EHMA), four monomers were polymerized. As the hydrophobicity of the monomer increased, the polymerization rate increased. BzMA and 2-EHMA polymerized significantly faster than BMA or MMA, which have significantly higher water solubility as seen in Figure 22. Similarly, the polymerizations of the more hydrophobic monomers produce M_n values significantly closer to their theoretically predicted values for a living radical polymerization compared to BMA and MMA. Although corrections for the absolute molecular weights were not done, PMMA standards were used. As all of the polymers used were methacrylates the M_n values calculated for the other monomers are not expected to change significantly, while the PMMA M_n values were clearly the furthest from the calculated theoretical values (Figure 22). Because the catalyst must be present in the droplet to induce a living radical polymerization, the partitioning of the catalyst between the droplet and water phases is critical in determining the outcome of the polymerization, influencing initiation efficiency, rate and livingness. Since the catalyst is likely more soluble in more hydrophilic monomers, it is possible that due to larger partitioning of monomer outside of a droplet will also lead to less catalyst present at the site of the polymerization. As the monomer hydrophobicity is increased more monomer is confined to the droplets and therefore more catalyst will be present as well allowing for a faster polymerization. All of these polymerizations yielded controlled LRPs, with efficient removal of both Ru and Fe by precipitation, which also indicates that through a smart catalyst design (possibly by adding a short hydrophobic section) we can increase the fraction of catalyst present in the droplets and particles, thereby improving the polymerization of

more hydrophilic monomers (with respect to initiator efficiency, $M_{n\text{-}exp}/M_{n\text{-}theo}$) while still having a catalyst that is easily removable.

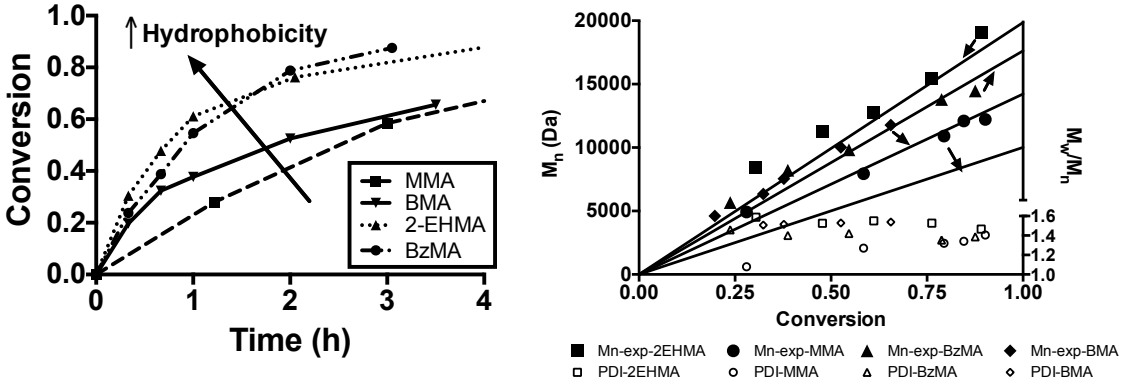

Figure 22. Conversion data for the miniemulsion polymerizations of various monomers catalyzed by RuCp*Cl($PPEG_{45}$) with FcTMA surfactant cocatalyst, 5, stabilized by CTAB: $[monomer]_0$:$[ECPA]_0$:$[Ru\ Catalyst]_0$ /$[FcPEG]_0$/[surfactant] = 100/1/0.05/0. 05/1.6 with [surfactant]/[hexadecane] = 4.3/5.2 wt% vs BMA at 80 °C. On the right is the GPC data for the same polymerizations.

5.6 Conclusions

We have used various cocatalysts for RuCp*Cl(PPEG) catalysts to improve the rate and conversions of BMA and BzMA polymerizations in miniemulsion, while allowing for over 95% reduction of metal residue in the final products, which is an important aspect in making metal mediated LRP more attractive to industry. Both amine cocatalysts and PEGylated ferrocene derivatives FePEG were shown to significantly improve the polymerizations, allowing for over 90% conversion while having less than 10 ppm of Ru or Fe in the final products. Using FcTMA we have elucidated that hydrophobicity and catalyst/ monomer partitioning likely play a key role

in the initiator efficiency of the polymerizations due to the heterogeneous nature of the polymerization.

5.7 References

(1) Kato, M.; Kamigaito, M.; Sawamoto, M.; Higashimura, T. *Macromolecules* **1995**, *28*, 1721–1723.

(2) Wang, J.; Matyjaszewski, K. *J. Am. Chem. Soc.* **1995**, *117*, 5614–5615.

(3) Matyjaszewski, K.; Xia, J. *Chem. Rev.* **2001**, *101*, 2921–2990.

(4) Ouchi, M.; Terashima, T.; Sawamoto, M. *Chem. Rev.* **2009**, *109*, 4963–5050.

(5) Monteiro, M. J.; Cunningham, M. F. *Macromolecules* **2012**, *45*, 4939–4957.

(6) Zetterlund, P. B.; Kagawa, Y.; Okubo, M. *Chem. Rev.* **2008**, *108*, 3747–3794.

(7) Cunningham, M. F. *Prog. Polym. Sci.* **2008**, *33*, 365–398.

(8) Min, K.; Matyjaszewski, K. *Cent. Eur. J. Chem.* **2009**, *7*, 657–674.

(9) Simms, R. W.; Cunningham, M. F. *J. Polym. Sci. Part A Polym. Chem.* **2006**, *44*, 1628–1634.

(10) Elsen, A. M.; Burdyńska, J.; Park, S.; Matyjaszewski, K. *Macromolecules* **2012**, *45*, 7356–7363.

(11) Min, K.; Gao, H.; Matyjaszewski, K. *J. Am. Chem. Soc.* **2006**, *128*, 10521–10526.

(12) Wei, Y.; Jia, Y.; Wang, W.; Li, B.; Zhu, S. *Macromolecules* **2014**, *47*, 7701–7706.

(13) Shiping, P.; Wang, S. W.; Zhu, S. *Polym. Chem.* **2015**, *6*, 2837–2843.

(14) Bultz, E.; Ouchi, M.; Nishizawa, K.; Cunningham, M. F.; Sawamoto, M. *ACS Macro Lett.* **2015**, 628–631.

(15) Ando, T.; Kato, M.; Kamigaito, M.; Sawamoto, M. *Macromolecules* **1996**, *29*, 1070–1072.

(16) Ando, T.; Kamigaito, M.; Sawamoto, M. *Macromolecules* **2000**, *33*, 6732–6737.

(17) Hamasaki, S.; Kamigaito, M.; Sawamoto, M. *Macromolecules* **2002**, *35*, 2934–2940.

(18) Fujimura, K.; Ouchi, M.; Sawamoto, M. *ACS Macro Lett.* **2012**, *1*, 321–323.

(19) Wu, J.-S.; Toda, K.; Tanaka, A.; Sanemasa, I. *Bull. Chem. Soc. Jpn.* **1998**, *71*, 1615–1618.

(20) Nishikawa, T.; Kamigaito, M.; Sawamoto, M. *Macromolecules* **1999**, *32*, 2204–2209.

(21) Toshihide, Y.; Yasuhiro, W.; Tsuyoshi, A.; Masami, K.; Mitsuo, S. *Control. Radic. Polym.* **2006**, *944*, 2–14.

(22) Kwak, Y.; Matyjaszewski, K. *Polym. Int.* **2009**, *58*, 242–247.

(23) Elsen, A. M.; Burdyńska, J.; Park, S.; Matyjaszewski, K. *ACS Macro Lett.* **2013**, *2*, 822–825.

(24) Kagawa, Y.; Zetterlund, P. B.; Minami, H.; Okubo, M. *Macromolecules* **2007**, *40*, 3062–3069.

(25) Elsen, A. M.; Burdyńska, J.; Park, S.; Matyjaszewski, K. *Macromolecules* **2012**, *45*, 7356–7363.

Chapter 6

Reverse and AGET ATRP polymerization of BMA with Iron(III)/EHA_6TREN

6.1 Preface

Initially I had begun research to identify iron catalyst complexes that would be stable in miniemulsion polymerization, and used various ligands that had been successful in miniemulsion polymerization with copper metal salts. Unfortunately there are few water stable iron catalyst complexes but the ligand EHA_6TREN had provided some promising results in bulk and solution polymerization. This chapter presents the work using $FeBr_3$ complexed with EHA_6TREN to mediate reverse ATRP with a radical initiator, or AGET ATRP with an alkyl halide initiator and different reducing agents. This work is being prepared for submission as a manuscript.

6.2 Abstract

A new iron/ligand complex has been identified that can induce a living radical polymerization. Tris(2-bis(3-(2-ethylhexoxy)-3-oxopropyl)aminoethyl)amine (EHA_6TREN), complexed in situ with $FeBr_3$ in bulk (butyl methacrylate, BMA)) or in solution (BMA with anisole) and polymerized with either a thermal radical initiator (azobisisobutyronitrile, AIBN) or an alkyl halide (ethyl α-bromoisobutyrate, EBiB) and a variety of green reducing agents, yields a living radical polymerization. M_n values increase linearly with increasing conversion and the molecular weight distributions shift cleanly to higher molecular weight values with minimal tailing at the low molecular weight end of the distribution, indicating good livingness. Iron as an ATRP

catalyst is desired for low toxicity and high abundance compared to other metal catalysts such as copper or ruthenium.

6.3 Introduction

Atom Transfer Radical Polymerization (ATRP) is a controlled/living radical polymerization technique that allows one to design a polymer with precise composition, molecular weight, narrow molecular weight distributions, end-group functionality and architecture.[1] To achieve this result the active radical concentration is minimized, ideally making the rate of bimolecular termination and chain transfer reactions negligible.[2] ATRP uses a transition metal to reversibly abstract a halogen from an alkyl bromide forming an active radical and increasing the oxidation state of the transition metal catalyst. Many transition metal species have been investigated including Cu,[3] Ru,[4] Fe,[5,6] and Ni,[7]. Among these copper has received the most attention for its versatility, high activity and the fastest rates of polymerization although reports of ATRP using iron catalysts have increased recently due to its low toxicity, biocompatibility and low cost compared to the other metals making iron an attractive catalyst choice.

The ATRP polymerization is controlled by an equilibrium between an active radical and a dormant alkyl halide as seen in **Error! Reference source not found.** Here, a transition metal/ligand complex, shown as Fe^{II}/L_n, in the lower oxidation state (e.g. Cu(I)) can abstract an halogen from an alkyl halide (R-X) through a one electron redox reaction forming an active alkyl radical (R•), resulting in the formation of the catalyst in the higher oxidation state with the abstracted halogen ($X\text{-}Fe^{III}/L_n$, or Cu(II) in the case of copper) . The active alkyl radical can react with monomer (M) briefly before the reverse (deactivation) reaction occurs and the growing polymer is capped as an alkyl halide. This process exists in a dynamic equilibrium ($K_{ATRP} = k_{act}/k_{deact}$), which determines the active radical population. The value of K_{ATRP} is small meaning

that the growing polymer is primarily in the deactivated state and the active radical concentration is kept much lower than in free radical polymerization. This minimizes the effect of bimolecular termination reactions, allowing for the living characteristics of an ATRP polymerization, which include lower dispersities (Đ or M_w/M_n), high end-group functionalities and control of polymer topology. ATRP allows one to precisely tailor molecular weights while allowing further chemistry to be performed on the polymer. ATRP enables the synthesis of exact architectures including block copolymers, which cannot be synthesized by free radical polymerization.

Scheme 5. The ATRP mechanism with an Fe(II)/Fe(III) catalyst.

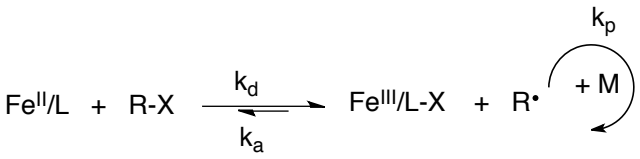

Aside from 'normal' ATRP, an ATRP polymerization can be initiated with the catalyst in the deactivator state (Fe(III)) in conjunction with a thermal initiator that forms a radical and abstracts a halogen from the catalyst to initiate the process known as 'reverse' ATRP.[8] Another process, "activators generated by electron transfer" (AGET) also begins with a catalyst in the deactivator state (Fe(III)) and an alkyl halide initiator; addition of a reducing agent reduces the deactivator to the activator state (Fe(II)) and allows for the ATRP proceeds to then commence like a normal ATRP process. Common reducing agents for Fe ATRP include tin ethylhexanoate,[9] ascorbic acid,[10] or metallic Fe(0).[11]

The ligand is important for the control and activity of an ATRP polymerization, as it determines the solubility of the transition metal catalyst in the reaction medium as well as tuning the redox

potential and activity of the catalyst. ATRP ligands used with iron catalysts have included nitrogen containing molecules,[5] as well as phosphines.[12]

Scheme 6. EHA_6TREN ligand structure.

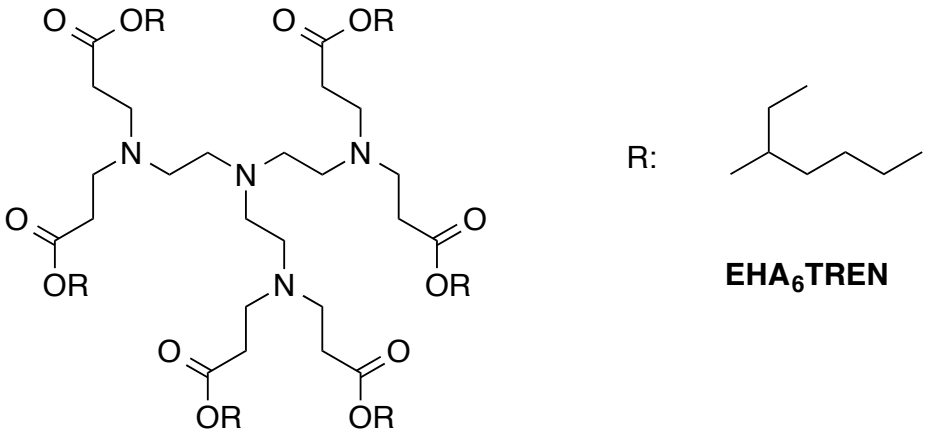

Nitrogen based ligands generally form catalyst complexes that have marginal solubility in the bulk monomer, making scale-up of an ATRP process difficult. Tris(2-bis(3-(2-ethylhexoxy)-3-oxopropyl)aminoethyl)amine (EHA_6TREN), shown in Scheme 6, is fully soluble in acrylates and methacrylates and has previously been employed in copper mediated ATRP for polymerizations using reverse ATRP in miniemulsion,[13,14] allowing for the living radical polymerization of butyl methacrylate and methyl methacrylate. Developing iron catalysts for living radical polymerization is important as these catalysts are considered to be less toxic than copper or ruthenium. Iron is also significantly more abundant than other catalysts meaning that the using these catalysts industrially would allow for lower operating costs. Herein we report the use of a highly soluble EHA_6TREN/ iron (III) complex, which can mediate the polymerization of butyl methacrylate by AGET or reverse ATRP. Using iron catalysts with safe reducing agents like metallic iron or FDA approved reducing agents such as ascorbic acid, a successful living radical

polymerization was achieved, and using oil soluble tin(II) ethylhexanoate also showed promising results.

6.4 Experimental

6.4.1 Materials

All chemicals were purchased from Sigma Aldrich unless otherwise noted. Butyl methacrylate (BMA, 99%) and butyl acrylate (BA, >99%) were passed through a prepacked column for removing hydroquinone and monomethyl ether hydroquinone prior to use. Styrene (ReagentPlus®, 99.9%) was passed through a prepacked column for removing tert-butylcatechol prior to use. Iron (III) bromide ($FeBr_3$, 98%), ethyl α-bromoisobutyrate (EBiB, 98%), tin(II) 2-ethylhexanoate (~95%), ascorbic acid (reagent grade) and iron powder (Fe, >99%) were used as received. 2,2′-Azobis(2-methylbutyronitrile) (VAZO 67, 98%) was recrystallized from methanol. Tris(2-bis(3-(2-ethylhexoxy)-3-oxopropyl)aminoethyl)amine (EHA_6TREN) was synthesized according to literature techniques.[15,16]

6.4.2 General polymerization procedures

6.4.2.1 Bulk polymerization of BMA

In a typical bulk polymerization 52.0 mg (0.18 mmol) of $FeBr_3$, 231 mg (0.185 mmol) of EHA_6TREN and 10.0 g (70.3 mmol) of BMA was added to a round bottom flask and allowed to mix until the solution became a clear, homogeneous, brown solution. To this mixture 13.0 mg (0.08 mmol) of VAZO 67 was added to the flask and the reaction mixture was bubbled with nitrogen for 30 min prior to the flask being immersed in an oil bath at 90°C. Samples for conversion and molecular weight analysis were taken periodically by a deoxygenated syringe and were allowed to dry under forced air evaporation.

6.4.3 Characterization

Sample conversion was determined by gravimetry. Gel permeation chromatography (GPC) was used to determine the molecular weight distribution of the polymer samples. Samples were prepared by dissolving 30 mg of dried polymer in 3 mL of THF. The dissolved samples were then passed through a column packed with basic alumina to remove any remaining copper, before being filtered through a nylon filter (0.2 μm pore size). The GPC was equipped with a Waters 2960 separation module containing four Styragel columns of pore sizes 100, 500, 10^3, 10^4 Å, coupled with a Waters 410 differential refractive index (RI) detector (930 nm) operating at 40 °C. THF was used as eluent and the flow rate was set to 1.0 mL min^{-1}. The detector was calibrated with eight narrow polystyrene standards ranging from 347 to 355 000 g mol^{-1}.

6.5 Results and Discussion

6.5.1 Reverse ATRP

6.5.1.1 Bulk Polymerization

Reverse ATRP employs the use of a thermal initiator to reduce the iron catalyst in the deactivator state. Here the results of reverse ATRP in bulk and solution are discussed. The bulk polymerization of butyl methacrylate (BMA) was conducted using 2,2′-azobis(2-methylbutyronitrile) (VAZO67) and $FeBr_3$ with EHA_6TREN as the ligand. The catalyst-ligand complex is formed in situ and is completely soluble at relatively high catalyst loading. Figure 23 displays the results for the bulk polymerization of $[BMA]_0$: $[FeBr_3]_0$:$[EHA_6TREN]$:[VAZO67] in the ratio of 400:1:1.05:0.45. Figure 23-A shows that the linear normalized conversion plot provides a k_{app} of 0.132 h^{-1}, reaching 59% conversion in 9 h.

The evolution of the molecular weight (M_n) versus conversion produces a linear trend, as expected for a living radical polymerization (Figure 23-B). In this polymerization the dispersity

(Đ, M_w/M_n) increases slightly throughout the polymerization but are stays below a value of 1.3, well below the theoretical minimum of 1.5 for a free radical polymerization. The molecular weights were slightly above the theoretical values, which were estimated by assuming 100% initiator efficiency, indicating that not all the radicals arising from thermal decomposition initiator become chains. The GPC traces for this polymerization are shown in Figure 24 the molecular weight distribution clearly shifts to higher molecular weight as the reaction proceeds. As conversion increased some low molecular weight tailing can be seen, which indicates that low amounts of termination products were formed, although the overall shift in the distributions indicates most of the chains were living.

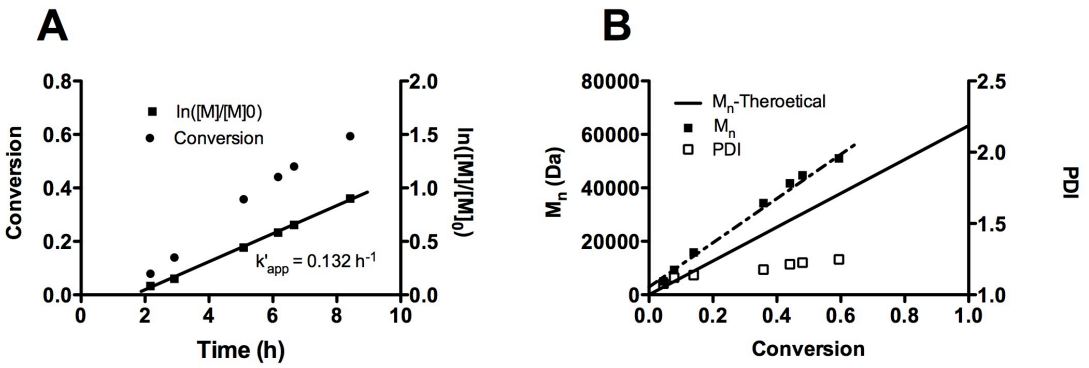

Figure 23. The normalized conversion and M_n vs Conversion plot for the reverse ATRP polymerization of BMA in bulk mediated by EHA_6TREN.

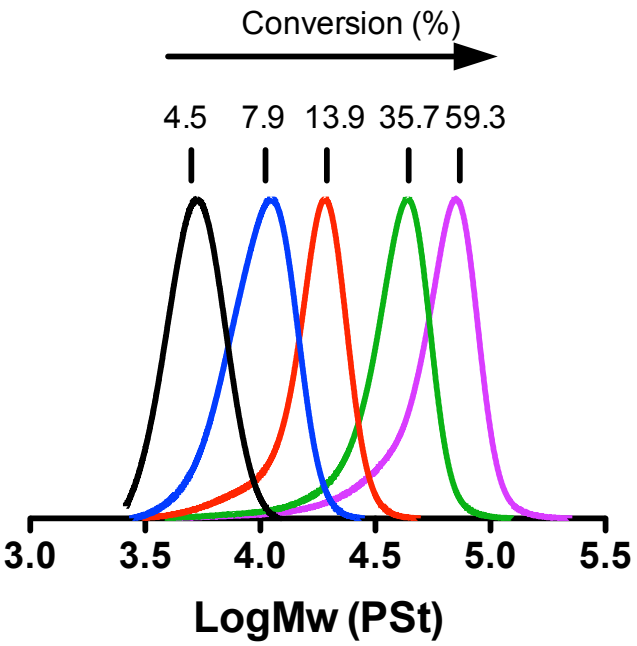

Figure 24. Normalized GPC traces for polymerization 1 of bulk BMA.

Table 1. Results for the reverse ATRP polymerization of BMA run at 50% wt anisole

Entry	[BMA]:[M-2]:[$FeBr_3$/EHA_6TREN]:[VAZO 67]	Time (h)	Conv (%)	$M_{n\,-theo;\ f=1}$	$M_{n\,-exp}$	PDI
1	400 : 0 : 1 : 0.45	8	50	34000	32500	1.35
2	400 : 0 : 1 : 0.8	6	90	34700	35600	1.41
3	200 : 0 : 1 : 0.8	3	91	17500	24600	1.39
4	292 : 108 BA : 1 : 0.45	9	12	-	-	-
5	275 : 125 St : 1 : 0.45	48	~0.5	-	-	-

6.5.1.2 Solution Polymerizations

Polymerizations of BMA and copolymerizations of BMA with either styrene or butyl acrylate were run at 50% wt in anisole with varying ratios of monomer to catalyst and initiator as shown in Table 1. As in the bulk polymerization of BMA mediated by $FeBr_3$/EHA_6TREN and initiated

by VAZO 67, the M_n increased linearly with respect to conversion when homopolymerizations of BMA were performed.

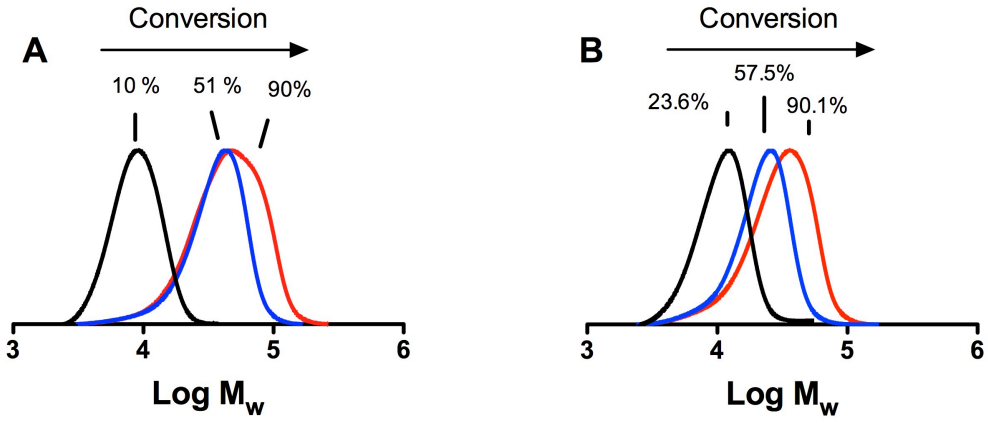

Figure 25. GPC traces from polymerization entry 2 and 3 in A and B respectively. The final molecular weight data is shown in Table 1.

In polymerization **2** the amount of radical initiator was increased by a factor of 1.77 with respect to polymerization **1.** The final conversion reached 90% in 6 h, significantly faster and higher than in polymerization **1**, as the radical concentration was significantly higher and more Fe(III) was reduced to the activating Fe(II). This increase in radical initiator concentration also decreases the M_n as the expected degree of polymerization also decreases by a factor of 1.77 for an equivalent conversion. There was an increase g of the Đ as the conversion increases, to values higher than in polymerization **1**, likely due to the decreased amounts of Fe(III) in the system. The GPC traces from this polymerization seen in Figure 25-A show that there is a clear shift in molecular weight from 10% conversion to approximately 50% conversion though above this value the distribution broadens and does not move at the low end of the trace, indicating livingness is decreasing at higher conversions.

In polymerization **3**, the ratio of initiator to monomer was increased again while the catalyst to initiator ratio was kept constant. Here, the polymerization reached conversions above 90% in less than 3 h with lower molecular weights. The higher rate and final conversion reached was due to the increase in total radical concentration with respect to polymerization **1** and **2** and the larger amount of Fe(II) activator produced by the higher ratio of radical to initiator compared to polymerization **1**. The GPC traces of polymerization **3** seen in Figure 3-B show a clear shift to higher molecular weights at low conversion (between 10% and 57.5% conversion) and at higher conversion some tailing is seen although this is deceased significantly compared to polymerization **2**, with the significant fraction of the distribution shifting to higher molecular weights. The difference in observed behavior between polymerization **3** and **2** could be the difference in total concentration of catalyst present in polymerization **3** (double that of polymerization **2**) even though the ratio of initiator to catalyst was kept constant between these two runs. This higher concentration of catalyst in the reaction solution likely accounts for the better livingness observed in polymerization **3**.

When a 75 wt% BMA copolymerization was performed (as seen in entry 4 and 5, with the molar ratios shown in Table 1) with either BA or styrene, the polymerizations reached only very low final conversions, indicating that the catalyst cannot effectively abstract the halogen from styrene or butyl acrylate end groups, and suggesting that the $FeBr_3$/EHA_6TREN catalyst is only active with methacrylate monomers.

6.5.2 AGET ATRP

Scheme 7. AGET ATRP for the polymerization of BMA

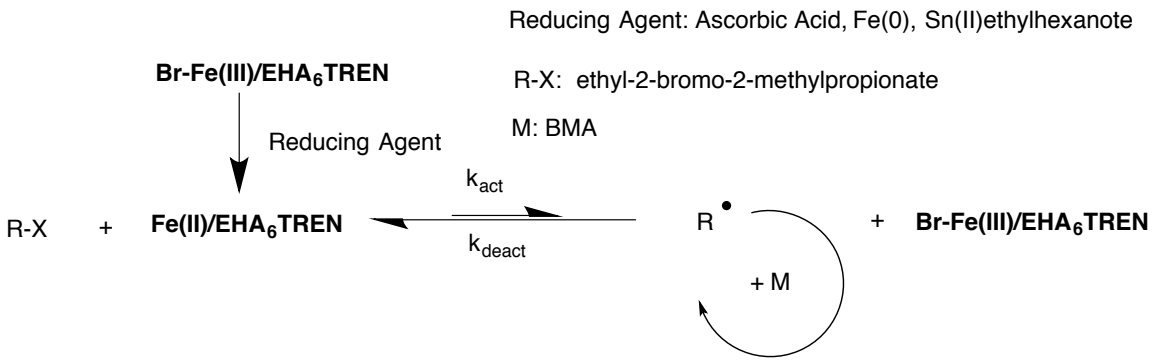

In the next set of experiments the polymerization of BMA in the presence of $FeBr_3$ was initiated by the alkyl halide initiator ethyl α-bromoisobutyrate (EBiB), a common ATRP initiator used in normal, AGET and ARGET polymerizations. The use of alkyl halide initiators allows for the α-end functionalization of a polymer, which can be used for further polymer modifications. For this reason we attempted polymerizations using three different reducing agents to see if the $FeBr_3$/EHA_6TREN catalyst complex could effectively polymerize BMA through an AGET ATRP process. The use of AGET ATRP (Scheme 7), rather than reverse ATRP with a thermal radical initiator, can also allow for the synthesis of pure block copolymers without the synthesis of a side product (homopolymer) initiated by the radical initiator.

Tin(II) ethylhexanoate is commonly used in organic soluble polymerizations as a reducing agent for ATRP and when used with $FeBr_3$/EHA_6TREN for a BMA polymerization, in 50 wt% anisole, a smooth conversion profile is seen for up to the 6 h and approximately 65% conversion. The GPC traces from this polymerization indicate that a living polymerization occurred as the M_n increases from approximately 17000 Da to 25800 Da, the M_w/M_n stays at approximately 1.3, and the entire molecular weight distribution shifts to higher molecular weight (Figure 5).

Using iron powder, Fe(0), in similar conditions, induced a slower polymerization initially although after 29 h (not shown on the conversion plot) almost full quantitative conversion of BMA was seen. The slow polymerization using Fe(0) compared to tin(II) ethylhexanoate is likely due to the heterogeneous nature of this reducing agent, while tin(II) ethylhexanoate is full soluble in BMA/anisole mixtures. The molecular weight distributions when using Fe(0) as the reducing agent show a clear shift to higher molecular weights although at the highest conversions there is a broadening of at the high end of the distribution likely caused by chain-chain coupling.

Like tin(II) ethylhexanoate, ascorbic acid is another FDA approved reducing agent. This naturally occurring carbohydrate (also known as vitamin C) is water-soluble and is commonly used in aqueous AGET or ARGET ATRP or in dispersed phase emulsion ATRP as a reducing agent. In BMA/ anisole, ascorbic acid is not readily soluble which likely accounting for the slow polymerization, as the reducing agent reacts heterogeneously, compared to the tin(II) ethylhexanoate which is readily soluble at these polymerization conditions. Although a slower polymerization occurred, ascorbic acid as a reducing agent induced a living radical polymerization as seen in the GPC traces with the polymer shifting to higher molecular weights with increasing conversion. After 8.5 h, 52% conversion was reached with a M_n of 24000 and M_w/M_n value of 1.44, slightly higher than the polymerization using the tin(II) ethylhexanoate as a reducing agent. There seems to be some tailing of the distribution at the molecular weight end, likely indicating that some dead chains are accumulating during the course of the polymerization, which is often seen for non-ideal catalysts in ATRP polymerizations.

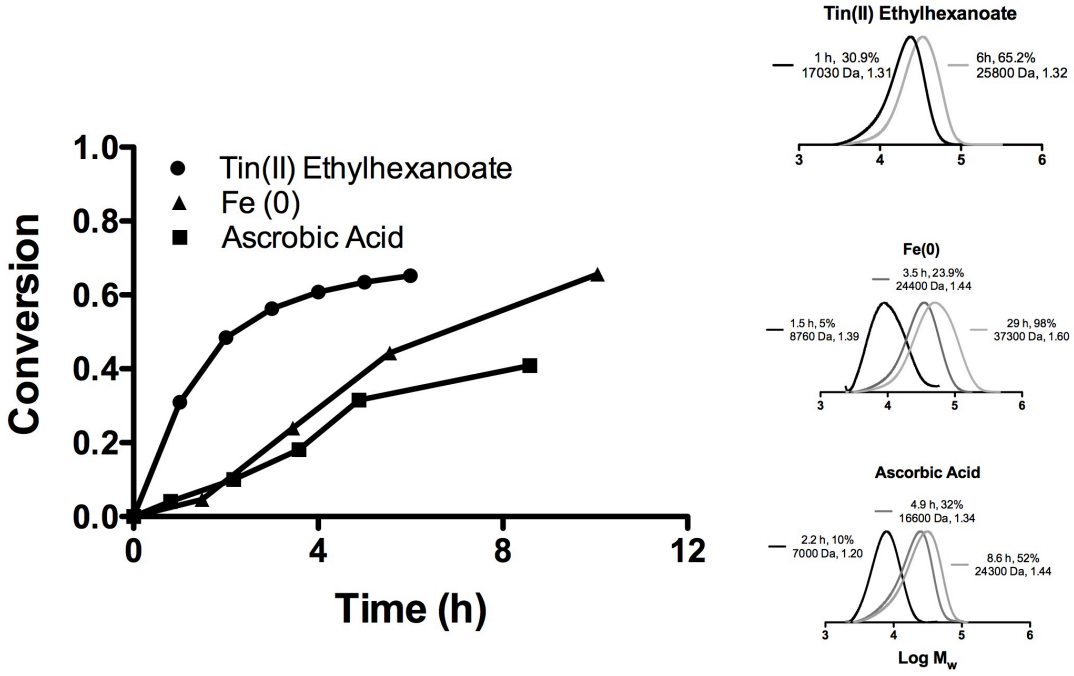

Figure 26. AGET ATRP initiated by EBib with Fe(III) reduced by either tin(II) ethylhexanoate, iron powder or ascorbic acid.

6.6 Conclusions

In summary we have shown that the $FeBr_3/EHA_6TREN$ catalyst complex, formed in situ, can induce a living radical polymerization, initiated by either a thermal radical initiator or an alkyl halide in the presence of a reducing agent to form the active Fe(II) species. Because of iron's low toxicity and abundance, its use in living radical polymerizations is important for making ATRP more attractive to industry. Iron may not need to be removed to the same degree as other catalysts from the final polymer products as it is considered safer than other heavy metal catalysts making iron ATRP a preferable choice for making advanced materials.

The EHA_6TREN ligand, most known for its complexation with copper salts and used in emulsion polymerization, formed a completely soluble catalyst complex in bulk BMA or BMA /anisole solutions and showed polymerization with fast rates, achieving 65% conversion in as little as 6 h. Research with this ligand/catalyst combination should be continued to ideally find a water stable iron catalyst for ATRP polymerization in emulsion or miniemulsion, allowing for VOC free polymerizations.

6.7 References

(1) Ouchi, M.; Terashima, T.; Sawamoto, M. *Chemical Reviews* **2009**, *109*, 4963–5050.

(2) Braunecker, W. a.; Matyjaszewski, K. *Progress in Polymer Science* **2007**, *32*, 93–146.

(3) Wang, J.-S.; Matyjaszewski, K. *Journal of the American Chemical Society* **1995**, *117*, 5614–5615.

(4) Kato, M.; Kamigaito, M.; Sawamoto, M.; Higashimura, T. *Macromolecules* **1995**, *28*, 1721–1723.

(5) Matyjaszewski, K.; Wei, M.; Xia, J.; McDermott, N. E. *Macromolecules* **1997**, *30*, 8161–8164.

(6) Ando, T.; Kamigaito, M.; Sawamoto, M. *Macromolecules* **1997**, *30*, 4507–4510.

(7) Granel, C.; Dubois, P.; Jérôme, R.; Teyssié, P. *Macromolecules* **1996**, *29*, 8576–8582.

(8) Xia, J.; Matyjaszewski, K. *Macromolecules* **1997**, *30*, 7692–7696.

(9) Luo, R.; Sen, A. *Macromolecules* **2008**, *41*, 4514–4518.

(10) Tao, M.; Zhang, L.; Jiang, H.; Zhang, Z.; Zhu, J. 1–8.

(11) Qin, J.; Cheng, Z.; Zhang, L.; Zhang, Z.; Zhu, J.; Zhu, X. *Macromolecular Chemistry and Physics* **2011**, *212*, 999–1006.

(12) Di Lena, F.; Matyjaszewski, K. *Progress in Polymer Science* **2010**, *35*, 959–1021.

(13) Li, M.; Matyjaszewski, K. *Macromolecules* **2003**, *36*, 6028–6035.

(14) Simms, R. W.; Cunningham, M. F. *Journal of Polymer Science Part A: Polymer Chemistry* **2006**, *44*, 1628–1634.

(15) Klee, J. E.; Neidhart, F.; Flammersheim, H.-J.; Mülhaupt, R. *Macromolecular Chemistry and Physics* **1999**, *200*, 517–523.

(16) Zeng, F.; Shen, Y.; Zhu, S.; Pelton, R. *Macromolecules* **2000**, *33*, 1628–1635.

Chapter 7

Summary and Conclusions

In this thesis metal mediated living radical polymerizations were studied using thermoresponsive polymer-bound ruthenium catalysts and iron cocatalysts in miniemulsion. Iron catalyzed polymerizations with a hydrophobic ligand were also run in bulk and solution with a ligand previously designed for copper mediated ATRP in miniemulsion.

Using a thermoresponsive ruthenium PEG catalyst RuCp*ClPPEG$_{113}$ we showed that at elevated temperatures the catalyst would transfer phases from the aqueous to organic phase. In a BMA containing miniemulsion using 1D NOE NMR we showed that a NOE peak exists at 80 °C caused by the PPEG ligand and the BMA in close proximity to each other (< 5 Å) indicating that the catalyst had been shuttled into the droplets. After cooling to room temperature the 1D NOE NMR showed no interaction between the PPEG ligand and the BMA monomer in miniemulsion suggesting that the catalyst had been successfully shuttled out of the droplets. Using the RuCp*ClPPEG$_{113}$ catalyst we showed the polymerization occurred much faster than a standard RuCp*Cl(PPh$_3$)$_2$ likely because the large PEG chain attached to the triphenyl phosphine caused enough steric hindrance so that only one ligand could effectively bind to the metal center. Both catalysts could induce a living radical polymerization, demonstrated by increasing M_n with conversion and shifting of the entire molecular weight distribution to higher values. Over 98% metal residue in the final polymer synthesized using the RuCp*ClPPEG$_{113}$ could be removed by washing with methanol or simple precipitation.

The above polymerization could only reach 80% conversion so the use of a cocatalyst ferrocene (FeCp$_2$) in miniemulsion was investigated. This cocatalyst is believed to add a second catalytic

cycle that acts to reduce the Ru(III) species to Ru(II); the Fe(III) species that is formed rapidly degrades to reform $FeCp_2$ and caps an active radical species. Initially using $FeCp_2$ we found a rate enhancement and significantly higher conversions could be reached (> 90%, < 8 h). Upon investigation it was found that this cocatalyst is stable in water only when excess halogen was present. The use of a non-ionic surfactant to stabilize the miniemulsion produced a non-living polymerization, although the addition of NaCl to the water phase allowed a living radical polymerization to proceed to almost complete conversion, likely because $FeCp_2^+Cl^-$ at the particle interface would result in loss of the charged species to the water phase. Addition of NaCl ensured that there was enough halogen present to allow the second catalytic cycle to occur effectively in the droplets/particles. Cationic surfactants with chlorine or bromine counter ions were shown to have a clear effect on the polymerization rate, and addition of a chlorine surfactant provided polymers with that were exclusively end capped with chlorine.

Since ferrocene was hydrophobic and could not completely be removed by precipitation like the main ruthenium catalyst, various other cocatalysts were used in miniemulsion including amine cocatalysts, which allowed BMA polymerizations to reach high conversions in under 10 h, and ferrocene derivatives that were either thermoresponsive and shuttling as with the main catalyst, or surfactants containing ferrocene that would reside at the surface of the droplets/particles. With all of these cocatalysts, conversions over 90 % could be reached in under 10 h, with low catalyst and cocatalyst loading (~ 1 catalyst per 20 chains). Furthermore, catalyst could be easily removed to allow for colourless final products to be synthesized easily.

Finally, we have identified a new iron/ligand complex that can successfully polymerize butyl methacrylate with reasonable polymerization rates.

Chapter 8

Recommendations for Future Work

To better understand the use of thermoresponsive catalysts in miniemulsion, further studies should be completed. Catalyst tuning can be done to add short hydrophobic moieties. This may act more like a surfactant but could allow the polymerization with improved initiator efficiencies in miniemulsion. Since we found that the more hydrophobic monomers could be initiated more efficiently we expect that tuning the ligand with an increased hydrophobic section may keep the catalyst more strongly located in the droplets for more effective polymerization. This can be done if better control and mostly like lower dispersities are required.

Using water-soluble initiators, extremely hydrophobic initiators or inisurfmers could also provide some insight into the reaction conditions before and during the phase transition of the catalyst. Since only two different initiators were used to initiate the polymerizations the effect of changing the initiator solubility may change the properties of the final polymers. For example, with a more hydrophilic monomer, a more hydrophobic initiator can be used, which could allow more initiator to be present in the droplets, as it will partition significantly less into the water phase. Conversely, using a water-soluble initiator would allow the initiation to occur more like a reverse ATRP or free radical polymerization and could provide valuable information for setting up emulsion polymerizations without the use of sonication as both the initiator and the catalyst would reside in the aqueous phase at the initial stage of the polymerization.

Attempts to remove the catalyst from the particles by dialysis were attempted but were unsuccessful and therefore further studies should be undertaken to determine exactly where the

catalyst is post-polymerization. Following the work by Zhu et al.[1] for determining catalyst leakage, stronger centrifugation conditions could be used to determine if the thermoresponsive catalyst is located in the water phase, or at the particle interface, or buried in the particle. It is possible (maybe likely) the catalyst is distributed between all three locations. Also, if extremely tight molecular weight distributions are not required then it may be possible to use significantly more water-soluble catalysts and where the polymerizations could occur at the droplet interphase, allowing for more easily removed catalysts.

Ruthenium is not an ideal catalyst to use on the industrial scale so synthesizing copper catalysts with thermoresponsive behaviors for miniemulsion would be ideal as well as one can start with copper in the deactivator state, compared with ruthenium which can only be formed as an activator. Ruthenium also is a toxic heavy metal so nearly complete removal from the final materials is required to make these polymerizations suitable for industry. RuCp* catalysts require phosphine ligands and these ligand as well as the metal center can be oxidized easily, meaning that exact concentrations of the active catalyst are not known, as well as potentially poisoning significant amounts of catalyst before the polymerization even begins. Since the nitrogen based ligands for copper will not be oxidized, a Cu(II) catalyst can be prepared. Using this form of a copper catalyst one can raise the temperature, allowing the catalyst to enter the droplets before adding the reducing agent or radical initiator. This may solve some of the issues of the extremely broad molecular weight distributions seen in Appendix B as the catalyst has time to uniformly enter the reaction site before the polymerization begins. Conversely, initiating the polymerization at low temperature could provide some insight in to the aqueous phase kinetics at low conversions and low temperatures.

Since miniemulsion has not found widespread use in industry, the next important role would be to find the conditions at which thermoresponsive catalysts can effective mediate a living radical polymerization in emulsion, in *ab initio* emulsion polymerization or in seeded emulsion polymerization. This was investigated briefly with limited success. Miniemulsions require high shear devices to form the submicron droplets and final particles, and also require the use of a costabilizer, which can act as a plasticizer in the final products. For some end-uses this will not be ideal. If these water-soluble catalysts can be used in emulsion it would alleviate these two issues as emulsion polymerization does not require the sonication or microfluidzer to form the droplets, simplifying industrialization, which would allow for polymerizations without the need of a costabilizer.

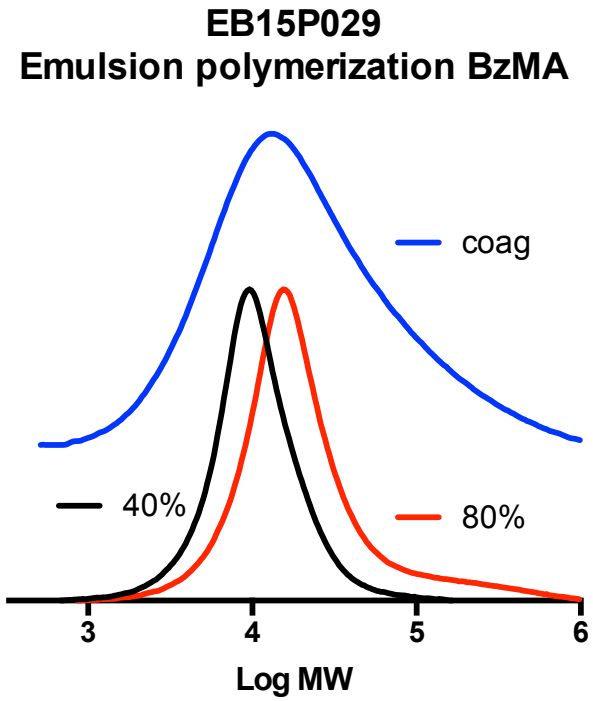

Figure 27. GPC traces for the ab initio emulsion polymerization with RuCp*PPEG$_{45}$ initiated by ECPA with FcTMA surfactant cocatalyst, 5, stabilized by CTAB:

$[monomer]_0$:$[ECPA]_0$:$[Ru\ Catalyst]_0$ /$[FcPEG]_0$/[surfactant] = 100/1/0.05/0. 05/1.6 with [surfactant] 4.3 wt% vs BzMA at 80 °C. Polymerizations were run at solids content of 15 wt%.

Attempts were made at both ab initio and seeded emulsion polymerizations however they suffered from significant colloidal instability (~20 - 50 % coagulum), although there were some signs of successful living polymerization. Figure 27 shows the GPC trace of an *ab initio* emulsion polymerization of BzMA catalyzed by $RuCp^*ClPPEG_{45}$. Between 40% conversion and 80% conversion the suspended particles showed reasonable livingness with molecular weight distributions shifting to higher values, although the coagulum was shown to have a very broad molecular weight distribution by comparison. The particle size grew from 127 nm to 189 nm (vol fraction) indicating that the emulsion process was successful to a limited degree. This indicates that there could be conditions that allow an *ab initio* emulsion polymerization to proceed successfully under suitable conditions. The best conditions to run this polymerization in would be to use a water soluble initiator, in conditions where initiation could occur in the water phase and the growing polymers could enter micelles which would become the loci of the polymerization, opposed to oil soluble initiators which would partition between the droplets and the micelles and to a small degree the water phase. This is one likely reason why extremely large quantities of coagulum were obtained in the previous emulsion type polymerizations.

Appendix A

Supplemental Material from Chapter 3 – ACS Macro Letters Supplementary Information

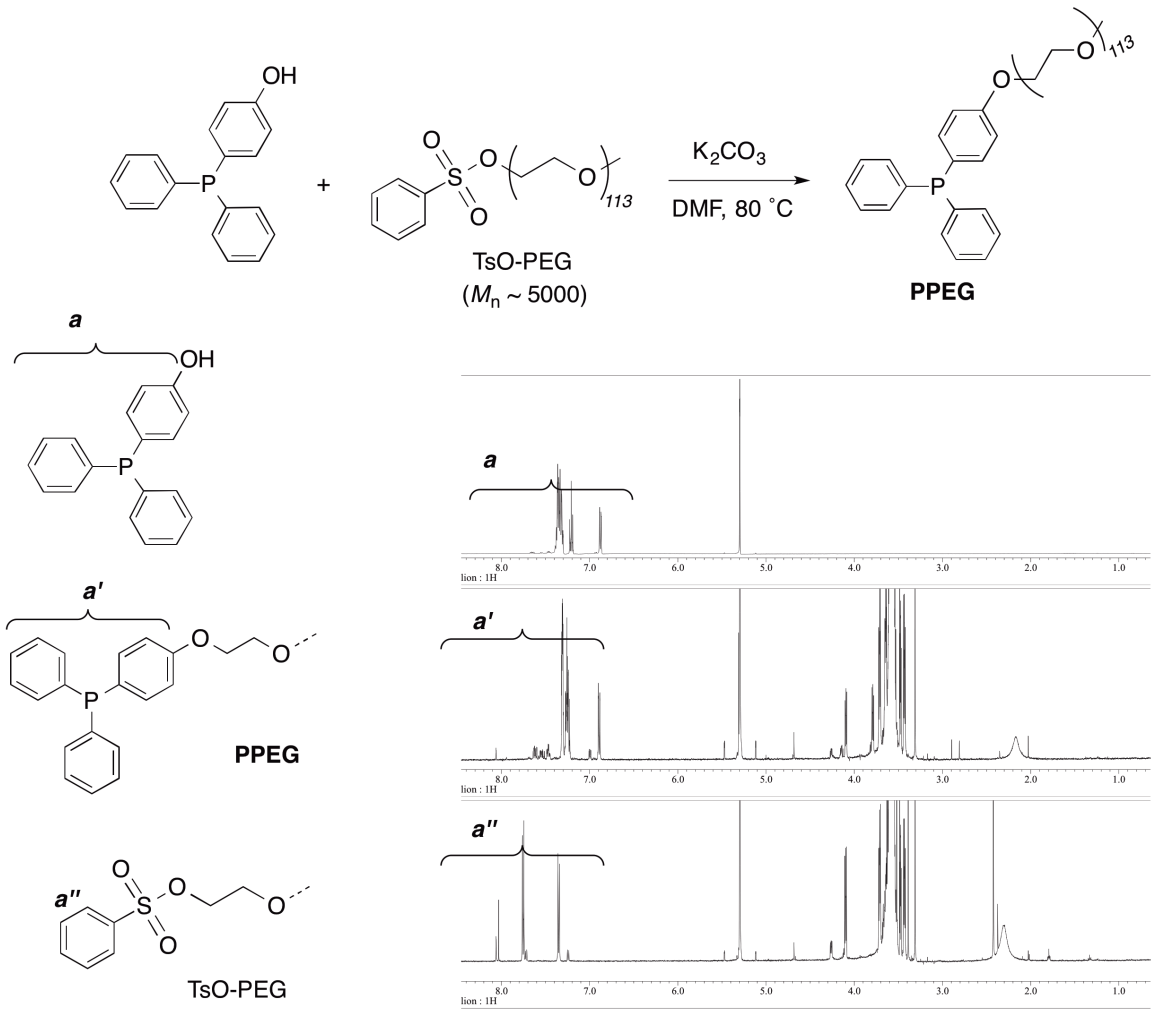

Figure A1-1 – Ligand Synthesis scheme with NMR showing complete conversion of PEG-TsO to PPEG.

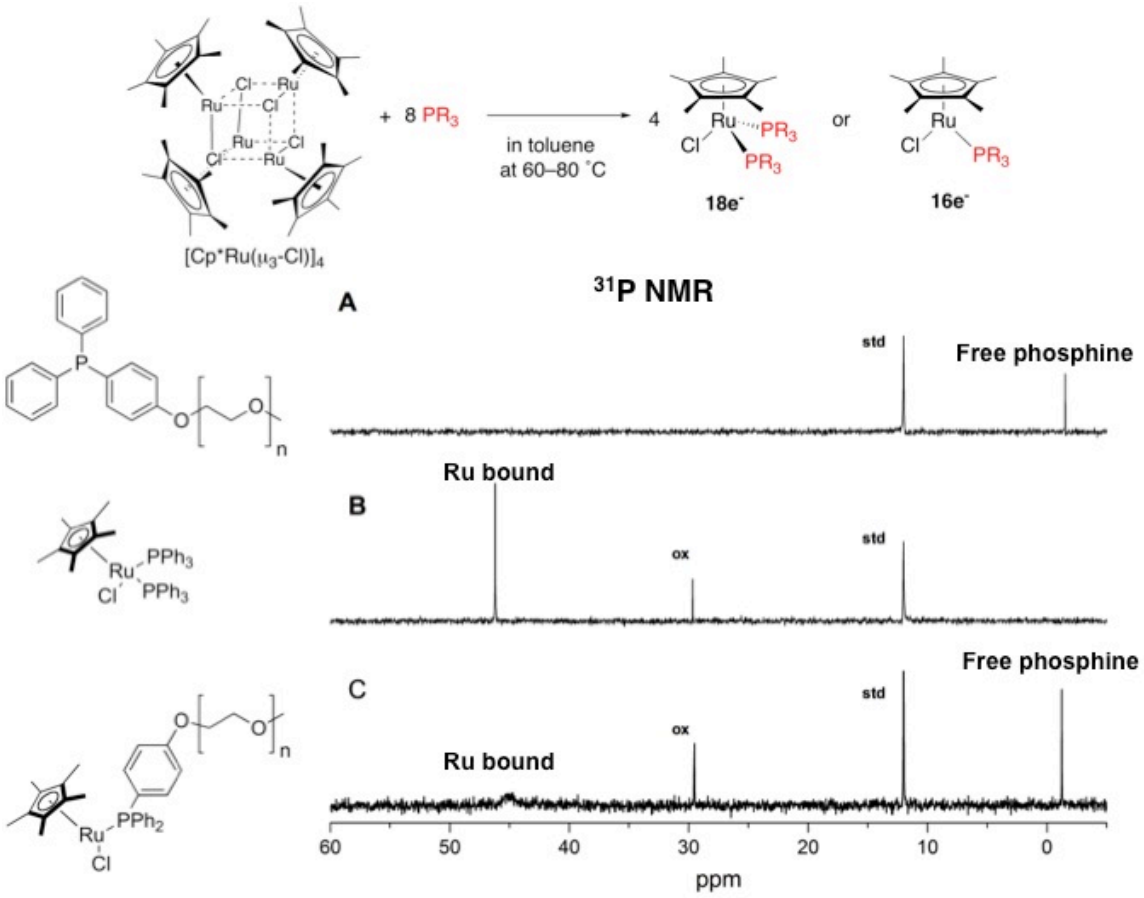

Figure A1-2 - ^{31}P NMR spectra for characterization of PPEG coordination on Cp*Ru complex. Samples were prepared in 10 mg/ml concentrations in toluene-d8. Samples containing ruthenium were prepared with 2 ligand equivalents to 1 ruthenium.

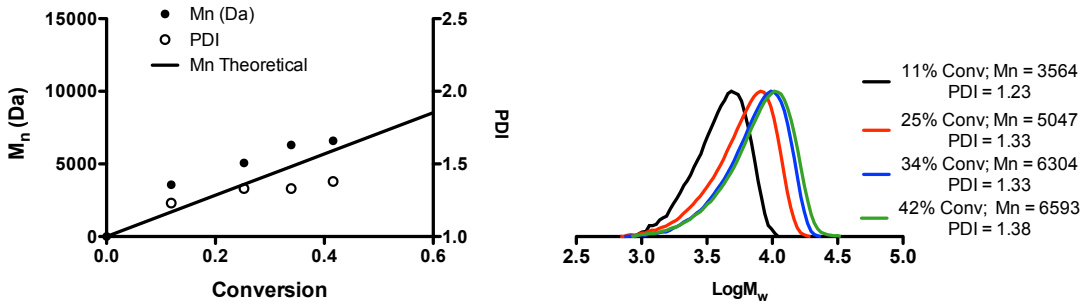

Figure A1-3 – Evolution of M_n and PDI vs conversion plot (left) for the miniemulsion polymerization of BMA with RuCp*Cl(PPh3)2 at 80°C, and the GPC traces of polymers from the obtained latex. Polymerization conditions: [BMA]0:[ECPA]0:[RuCp*Cl(PPh3)2]0 = 4000/40/2 mM in toluene with [CTAB]/[hexadecane] = 4.3/5.2 wt % vs BMA.

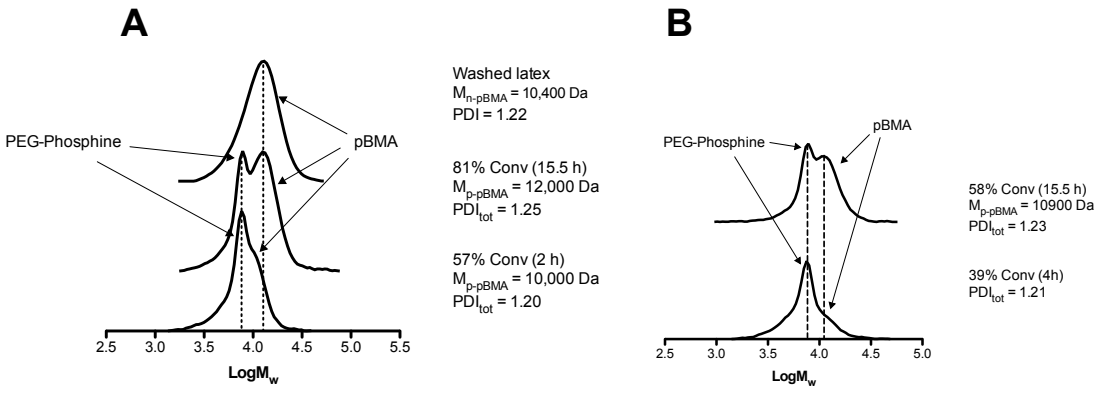

Figure A1-4. GPC traces for the polymerization of BMA at 80°C (A) and 40°C (B) with the thermoresponsive catalyst RuCp*Cl(PPEG), and the catalyst-free sample post-washing. Polymerization conditions: [BMA]0:[ECPA] 0:[[Ru(Cp*)Cl]4]0:[PEG-ligand]0 = 4000/40/0.5/4.0 mM with [CTAB]/[hexadecane] = 4.3/5.2 wt % vs BMA.

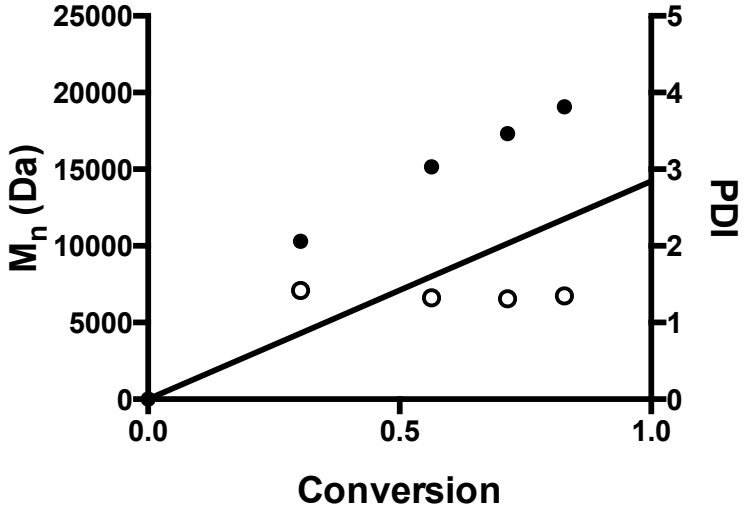

Figure A1-5 Evolution of M_n and PDI vs conversion plot (right) for the miniemulsion polymerization of BMA at 80°C mediated by RuCp*Cl(PPEG). Polymerization conditions: [BMA]0:[ECPA]0:[RuCp*Cl(PPh3)2]0 = 100/1/0.05 with [CTAB]/[hexadecane] = 4.3/5.2 wt % vs BMA.

Appendix B

RuCp* Ligand Design Work with $FeCp_2$ and Catalyst Addition Post-Sonication Experiments

This appendix shows the polymerizations in miniemulsion of BMA or BzMA catalyzed by various ligands complexed to RuCp*. This section shows that the ligand design can affect the catalyst's ability to successfully mediate a miniemulsion Mt-LRP. For example in Figure B1 and Figure B2 we see that $PPEG_3$, a PEG ligand with three short PEG chains (DP =12), can successfully mediate an LRP in miniemulsion in the presence of toluene (BMA = 4 M in toluene) up to 60% conversion in 40 hours. When this is changed to a toluene-free polymerization, the rate is much faster but looking at the GPC traces in Figure B2 we see that the polymerization is not controlled at all, likely due to the catalyst solubility in the droplets or particles at elevated temperatures. When $FeCp_2$ is added to the miniemulsion, the polymerization showed a rate enhancement as expected but also provided signs of livingness with a shift in the molecular weight distributions to high conversions. In this case the solubility of the catalyst was likely marginal in the droplets/ particles but the addition of the ferrocene increased the speed of deactivation allowing for an LRP to be realized.

In Figure B3 we see the conversion profiles and the GPC traces for the BzMA polymerizations in miniemulsion catalyzed either by $RuCp^*ClPPEG_{113}$, $RuCp^*Cl(PPEG_3)_2$, or $RuCp^*Cl(PPh_3)_2$ with or without the addition of $FeCp_2$. The polymerizations all show an increased rate with the addition of ferrocene but using the $PPEG_{113}$ we see that the polymerization was uncontrolled with or without the addition of ferrocene. This likely occurs because the main catalyst is not sufficiently soluble in the droplets/particles that an LRP can occur, even with the increased rate of deactivation by the addition of ferrocene, showing that tuning of the catalyst is required for successful LRP of various monomers.

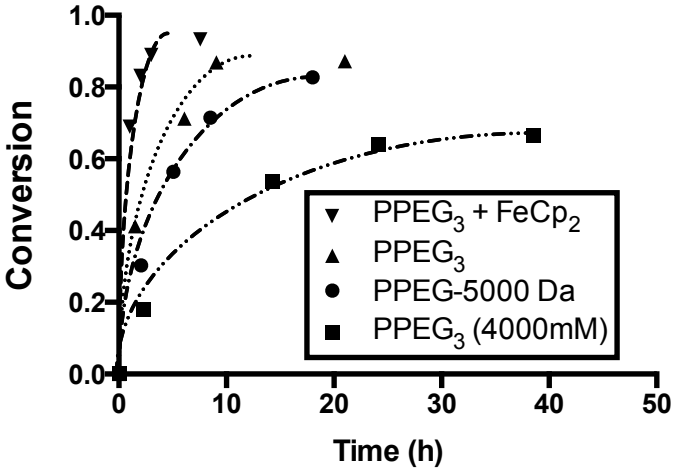

Figure B1. Rate data for the miniemulsion polymerization of BMA catalyzed by RuCp*PPEG shown above for a target DP = 100 and a catalyst to chain ratio of 1:20 at 15% solids wt fraction with [CTAB]/[hexadecane] = 4.3/5.2 wt % vs BMA. When present $FeCp_2$ vs RuCp* = 10/1.

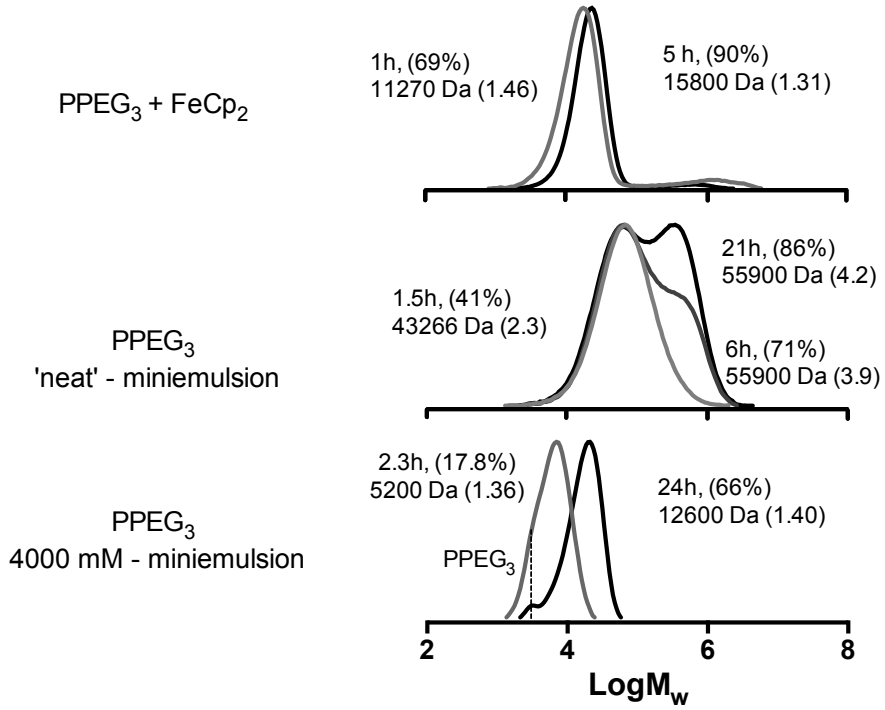

Figure B2. GPC traces for the polymerizations shown in Figure B1 using the $PPEG_3$ ligand in a 4M in toluene polymerization and a toluene free polymerization with or without added ferrocene.

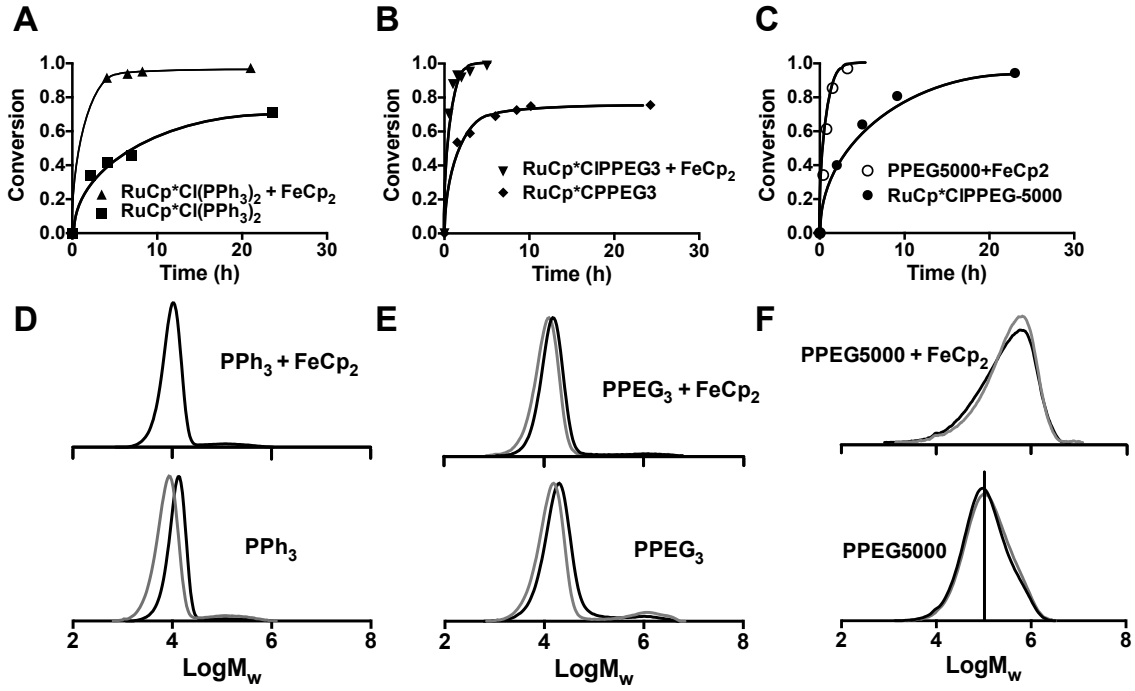

Figure B3. Rate data and GPC traces for the miniemulsion polymerization of BzMA catalyzed by RuCp*PPEG shown above for a target DP = 100 and a catalyst to chain ratio of 1:20 at 15% solids wt fraction with [CTAB]/[hexadecane] = 4.3/5.2 wt % vs BMA with or without $FeCp_2$. When present $FeCp_2$ vs RuCp* = 10/1.

The addition of the catalyst post-sonication to the miniemulsion was explored using either BMA catalyzed RuCp*$ClPPEG_{113}$ or BzMA catalyzed by RuCp*$ClPPEG_{45}$. When adding the catalyst post-sonication with BMA we see a very broad MWD, with dispersity above 3 – 4 but as the polymerization progresses the M_n increases linearly with conversion and the molecular weight distribution shifts cleanly to high molecular weight values compared with the BzMA

polymerization where the M_w/M_n values are significantly lower. It is possible that the RuCp* head group is more soluble in the monomer at lower temperatures, so the head group may already be associating with the droplets compared with the BMA polymerization where this is not occurring. As the polymerization temperature is raised the BzMA polymerization is likely being initiated more evenly as the head groups are distributed around all of the droplets, while in the polymerizations with BMA droplets are initiated less uniformly as the catalyst must migrate to the droplets to initiate the polymerization. Because of the dispersed nature of the polymerization, the initiation likely is spread out over a longer period of time, causing the broad disruption compared to the polymerization of BzMA. This also indicates that the sonication in the presence of the catalyst may bury some of the catalyst in the droplet at the beginning of the polymerization, as the polymerizations in Chapter 3 had significantly narrower distributions compared to the polymerization when the catalyst was added after sonication when using BMA.

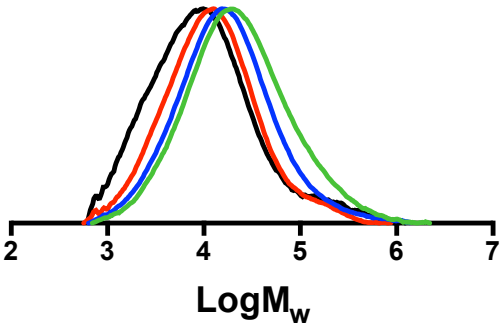

	Time (h)	Conv (%)	M_n (Da)	M_w/M_n
—	0.33	22.2	5050	5.3
—	1	32.4	6750	3.6
—	2	42.8	9100	4.0
—	3	53.5	11600	4.5

Figure B4. Rate data and GPC traces for the miniemulsion polymerization of BMA catalyzed by RuCp*PPEG shown above for a target DP = 100 and a catalyst to chain ratio of 1:20 at 15% solids wt fraction with [CTAB]/[hexadecane] = 4.3/5.2 wt % vs BMA with or without $FeCp_2$. When present $FeCp_2$ vs RuCp* = 10/1. Catalyst added after sonication.

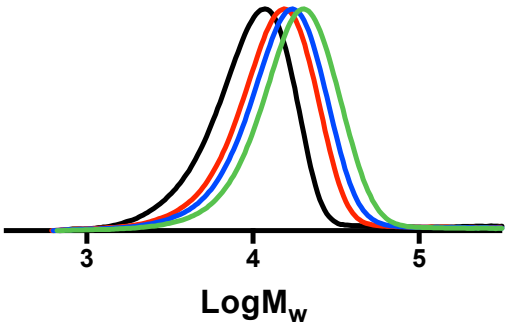

	Time (h)	Conv (%)	M_n (Da)	M_w/M_n
—	0.33	42.7	7700	1.4
—	0.66	62.2	10300	1.4
—	1	73.1	11800	1.4
—	3	94.0	14400	1.4

Figure B5. Rate data and GPC traces for the miniemulsion polymerization of BMA catalyzed by RuCp*PPEG shown above for a target DP = 100 and a catalyst to chain ratio of 1:20 at 15% solids weight fraction with [CTAB]/[hexadecane] = 4.3/5.2 wt % vs BMA with or without $FeCp_2$. When present $FeCp_2$ vs RuCp* = 10/1. Catalyst added after sonication.